Assessing Holocene Climate Variability in the Arctic Ocean

David Morris

MChem, University of Sheffield, 2004

MSc, University of Newcastle-upon-Tyne, 2006

A dissertation presented to the Graduate Faculty

of the University of Virginia in Candidacy for the Degree of

Doctor of Philosophy

Department of Environmental Sciences

University of Virginia

May, 2016

Table of Contents

List of Abbreviations

BC	Barrow Canyon transect
C:N	Carbon:Nitrogen ratio
C3	C3 photosynthetic pathway
C4	C4 photosynthetic pathway
CAM	Crassulacean acid metabolism photosynthetic pathway
dCO_2	Dissolved carbon dioxide
DIC	Dissolved inorganic carbon
ΔR	Regional reservoir correction for $\Delta^{14}C$
EA	Elemental Analysis
EB	East of Barrow Canyon transect
EHS	East of Hanna Shoal transect
GC	Gas chromatography
GC-IRMS	Gas chromatography - isotope ratio mass spectrometry
HOTRAX	Healy-Oden transarctic expedition
HPLC	High performance liquid chromatography
IRMS	Isotope ratio mass spectrometry
JPC	Jumbo piston core
OC	Organic carbon
OEP	Odd:Even predominance
POC	Particulate organic carbon
POM	Particulate organic matter
SBI	Shelf basin interactions
SIMM	Stable isotope mixing model
TCD	Thermal conductivity detector

TOC	Total organic carbon
UCM	Unresolved complex mixture
WHS	West of Hanna Shoal transect

Abstract

The western Arctic Ocean is a unique part of the world's oceans, and is an area undergoing significant climate changes. The effects and possible climate feedbacks of these changes are not yet fully understood. Decreased sea ice cover could lead to increased productivity in the water column, or a reduction in total productivity through the loss of sea ice algal contributions. Climate change could also alter the patterns of terrestrial inputs from rivers and coastal erosion.

In this dissertation, carbon and nitrogen elemental and isotopic compositions from 19 surface sediment samples and 7 cores from 4 shelf to basin transects were analyzed, as well as a longer jumbo piston core and neutral lipid extracts, in order to better understand the balance of organic material inputs in the sediments of the Chukchi and Alaskan Beaufort Seas. Bulk $\delta^{13}C$, $\delta^{15}N$ and compound specific isotope analysis on these samples were performed, and it was found that the bulk of the material was comprised of pelagic material, with distinct contributions from sea ice algae, degraded marine material and terrestrial organic matter.

The C:N ratios for surface sediments were between 5.3 and 11.5 (mean 9.0±1.3). The mean %TOC was 1.2±0.3% and mean %TN was 0.16±0.02%. The highest %TOC contents were observed in the Barrow Canyon transect, likely reflecting heightened overlying productivity. The $\delta^{13}C$ of this preserved material varied from -22.1 to -16.7‰ (mean -19.4±1.3‰). A trend to depletion in ^{13}C and higher C:N in eastern sites was observed. Among the surface samples, $\delta^{15}N$ varied from 4.1 to 7.6‰ (mean 5.7±1.1‰).

The deeper core HLY 090501 provided a sediment record on Holocene timescales. We found that the majority of the organic material was marine, but that much of this marine matter had been reworked and advected to the core location. Mean $\delta^{13}C$ was -23.2‰. We also observed a trend towards more depleted ^{13}C downcore (to -24.9‰),

which is indicative of a stronger terrestrial contribution to the oldest parts of the core, which was consistent with coastal retreat at the end of the last glacial maximum.

Using compound specific isotope analysis on alkane biomarkers, we found evidence of terrestrial material in the sediments. Due to the odd to even predominance in the distribution pattern and $\delta^{13}C$ (mean -31.6‰) of the alkane biomarkers, we concluded that terrestrial material does contribute to the carbon cycle in the Western Arctic Ocean.

An evaluation of the inputs of organic matter to the western Arctic sediment was accomplished using bulk $\delta^{13}C$ and $\delta^{15}N$ values with the novel technique of a Bayesian analysis multi-source mixing model. This model was used to estimate proportional contributions of sea ice algae, water column phytoplankton and terrestrial organic matter. We conclude that water column productivity is the source of between 50 and 70% of the organic carbon buried in this portion of the western Arctic. The remaining 25-35% of carbon is mainly supplied by sea ice algal productivity, with at most 15% of sedimentary carbon derived from terrestrial inputs.

Chapter 1: Introduction

Sea ice is a vital part of the Arctic system, but is currently in decline. Arctic sea ice extent has fallen by 30% since satellite records began in 1979. Since 2002, a series of extreme September sea ice extent minima have occurred, with record minima being seen in 2002, 2005 and then 2007. Some researchers (e.g. Stroeve et al., 2012) now fear that sea ice may reach a critical threshold at which a transition to a seasonally ice free Arctic occurs, perhaps as soon as mid-century (Massonnet et al., 2012). As the Arctic is experiencing these rapid changes, a better understanding of the Arctic system is certainly called for.

Polar marine biogeochemistry is an important part of the Arctic system, and of the global carbon cycle. It is heavily influenced by ice, which plays a significant role in controlling light availability (Fortier et al., 2002), stratification and nutrient supply (Vancoppenolle et al., 2013). Sea ice algae influences pelagic biogeochemistry and food webs once released from the ice, seeding the spring phytoplankton bloom, providing important early grazing material for zooplankton, and exporting organic matter to the benthos (Thomas and Dieckmann, 2003). The spring bloom starts under the ice, and then follows summer sea ice retreat (Perrette et al., 2011). Recent decreases in sea ice extent have been associated with increases in pelagic productivity (Arrigo et al., 2008, Tremblay et al., 2011). And marine ecosystem shifts are occurring in response to changes in sea ice extent (Grebmeier et al., 2006). As sea ice volume and extent continues its rapid decline, the effect that this will have on Arctic marine biogeochemistry is not yet well understood.

In order to better grasp the consequences of future changes, obtaining a fuller understanding of the present, and past, of the Arctic carbon cycle has become urgent. The objective of this dissertation is to better estimate the contributions made to the

marine carbon cycle by terrestrial, pelagic and sea ice sources through the use of C:N, bulk $\delta^{13}C$, $\delta^{15}N$ and compound specific isotope analysis of n-alkanes.

Chapter 2 discusses the sampling and analytical methods used in the rest of the dissertation, including C:N by EA, $\delta^{13}C$, $\delta^{15}N$ and $\delta^{34}S$ by elemental analysis-isotope ratio mass spectrometry (EA-IRMS), the extraction and separation of the neutral organic fraction from the sediments and the analysis of the neutral organic fraction by GC-IRMS.

Chapter 3 presents data from a series of surface samples and cores taken from the Northeastern Chukchi and Western Beaufort seas. Using $\delta^{13}C$ and $\delta^{15}N$ in conjunction with the Bayesian SIMM SIAR (Parnell et al., 2010), it was estimated that the contribution of terrestrial material to the sediments was around 10%, with the bulk of the OC being of pelagic marine origin. This estimate, while relatively high for a coastal sediment, is considerably lower than other studies (e.g. Goñi et al., 2013) that have predicted much higher terrestrial contributions. Our findings highlight the importance of marine productivity to the Chukchi and Beaufort Seas.

Chapter 4 uses the Bayesian SIMMs SIAR and MixSIAR (Stock and Semmens, 2013) to analyze $\delta^{13}C$ and $\delta^{15}N$ from a longer jumbo piston core from the Chukchi Sea. The two models produce very similar results and both estimate high marine contributions over Holocene timescales, even though sea level rose by an estimated 60-70m over the lifetime of the core. The enriched $\delta^{15}N$ indicate the importance of degraded marine material to the sediments (Faux et al., 2011; Magen et al., 2010; Tolosa et al., 2013).

Chapter 5 uses GC-IRMS to investigate the sources of *n*-alkanes found in the sediments. The majority of n-alkanes were clearly terrestrial in origin, with no evidence for a sea ice algal contribution to the short chain alkanes. The sea ice algal biomarker, IP25 (Belt et al., 2007), was also not observed. These findings support the contention that although

there is a terrestrial contribution to the OC of the Western Arctic Ocean, the most significant contribution is from pelagic phytoplankton.

Literature review

The Arctic is unique among the world's oceans in that it is essentially landlocked. Surrounded by continents, its only sources of inflow are the Bering Strait (0.83Sv (Roach et al., 1995; Woodgate and Aagaard, 2005), Barents Sea (2Sv) and Fram Strait (1.5Sv (Rudels et al., 2004)) with outflow via the Canadian Archipelago (0.8Sv (Muenchow et al., 2006)) and western Fram Strait (3.5Sv (Melling, 2000)). Bathymetrically, the Arctic is characterized by large ocean shelves which make up 56% of the total area of the Arctic Ocean and its surrounding seas, as well as 30% of the total global shelf area (Stein and Macdonald, 2004). Owing to their relative shallowness, these epicontinental seas receive a disproportionate amount of terrestrial runoff relative to their volume: 11% of global runoff to 1% of global ocean volume (Shiklomanov, 1998).

One of the motivating factors for this study is the possibility that the Arctic seas act as sinks for organic carbon. 10-1000 million metric tons of Carbon is cycled between different pools on the land, in the atmosphere and in the ocean, as it undergoes chemical transformations. Phytoplankton act as a biological pump, drawing down dissolved inorganic carbon (DIC) from the ocean in photosynthesis. Of the resulting reduced organic carbon compounds, most are consumed and respired. But a small fraction remains, and can be preserved in sediments, acting as a long-term sink for atmospheric CO_2.

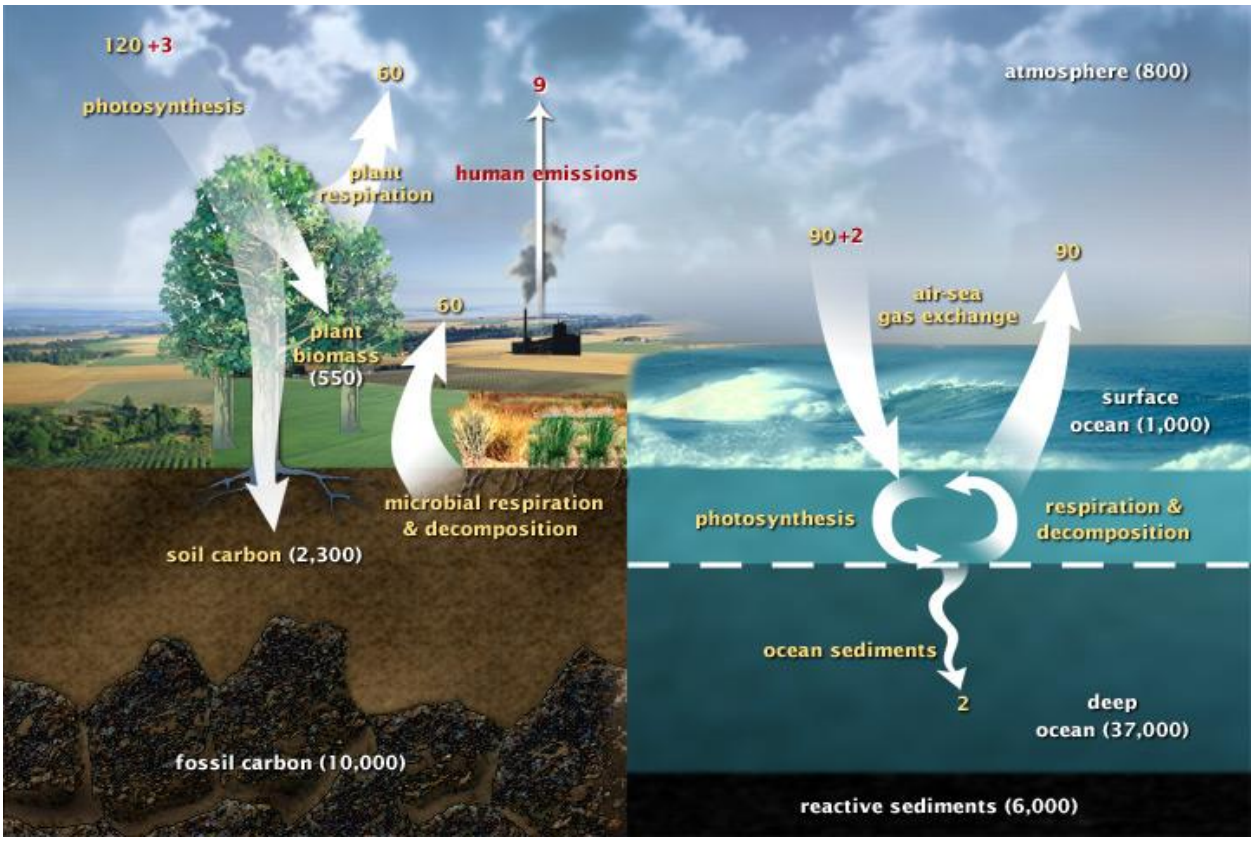

Figure 1 The organic carbon cycle. Yellow and red numbers represent natural and man-made fluxes, respectively. White text represents storage. Reproduced from US DOE. Climate Placemat: Energy-Climate Nexus, US Department of Energy Office of Science. US DOE. Climate Placemat: Energy-Climate Nexus, US Department of Energy Office of Science.

Terrestrial influence on the organic carbon cycle in the Arctic Ocean is thought to be considerable, due to strong links between land and sea. Carbon fixed on land can be transported to the oceans via riverine transport, coastal erosion and atmospheric deposition directly, or after storage in soil carbon or permafrost. This material is typically resistant to microbial degradation, and could potentially be stored in ocean sediments too. Perturbations to the system that affect terrestrial supply, surface marine productivity or sea ice algal productivity therefore have the potential to alter the balance of the carbon cycle in the Chukchi and Beaufort Seas.

The unusually large ocean shelves and high terrestrial inputs have a major impact on the organic carbon cycle in the Arctic. Arctic rivers drain vast expanses of boreal forest and permafrost tundra and peatlands, containing between 1400 and 1850Pg C (McGuire

et al., 2009). The high runoff in the Arctic connects this terrestrial carbon to the ocean, supplying 6x10^{6}tC/yr particulate organic carbon (POC) (Rachold et al., 2004) to the coastal ocean. Carbon is also fixed and recycled through marine productivity. Much of the Arctic has very low rates of primary production (250Mta^{-1} POC, 329Mta^{-1} total organic carbon (TOC) (Sakshaug, 2004)), but shelf areas can support much higher productivity given sufficient nutrients (e.g. 720-840gm^{-2}a^{-1}C (Springer and McRoy, 1993) in the Chukchi and Bering Seas). A small proportion of this marine and terrestrial is then buried; one of the few ways that organic carbon can be sequestered, long-term (Bauer et al., 2013).

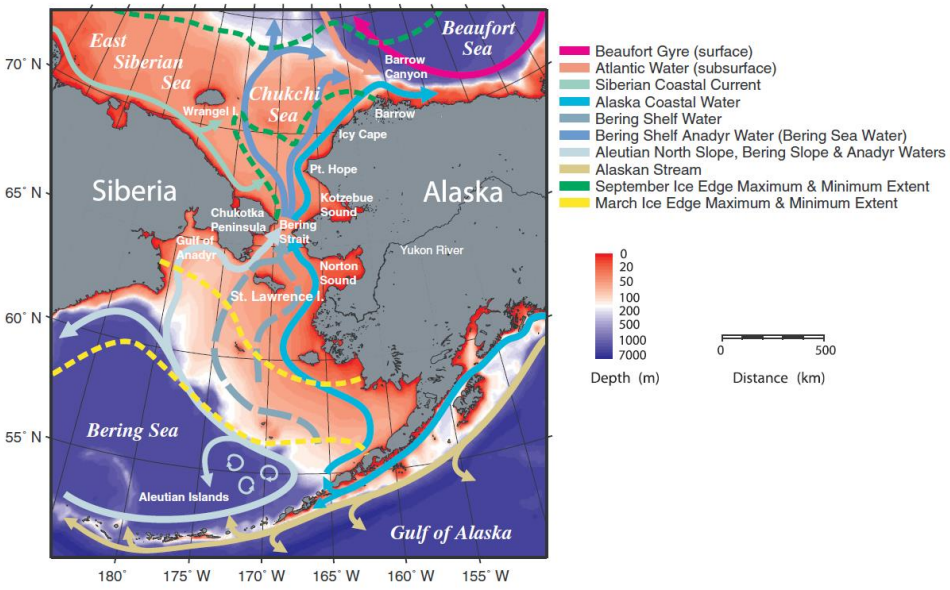

Fig. 1. Schematic of water mass type and sea ice extent in the northern Bering, Chukchi, eastern East Siberian and western Beaufort Seas (modified from map provided by Tom Weingartner and Seth Danielson, University of Alaska Fairbanks).

Given recent changes in sea ice cover (Johannessen et al., 1999; Perovich and Richter-Menge, 2009), changes in river discharge (Peterson et al., 2002; McClelland et al., 2006), increasing coastal erosion (Mars and Houseknecht, 2007; Vonk et al., 2012) and changes in carbon storage in permafrost soils (Gorham, 1991; Hugelius et al., 2013; Vonk et al., 2013; Schreiner et al., 2014), understanding the present status of the Arctic carbon cycle

is crucial to predicting the response of the carbon cycle to climate forcings, especially the role presently played by sea ice.

While sea ice is not unique to the Arctic, it is one of the most critical physical phenomena in the Arctic and its marginal seas, since it influences so many physical processes. At its maximum extent, Arctic sea ice covers nearly 3% of the earth's surface ($15x10^6$ km^2) (Dieckmann and Hellmer, 2003), constituting one of the largest biomes on the planet. Owing to the high albedo of sea ice, it reflects a large amount of incoming shortwave radiation, lowering surface temperatures. As a strong insulator, and as a physical barrier, it decreases exchange between the ocean and atmosphere as well as mitigating the effects of waves and winds. Sea ice is also critical habitat for ice-adapted fauna such as polar bears, walrus and ringed seals (Schnack-Schiel, 2003).

Sea ice also affects the carbon cycle. It limits productivity by attenuating light penetration of the ocean surface (Fortier et al., 2002; Hill et al., 2005), but it also provides a habitat for sea ice algae and brine formation during ice growth can remobilize nutrients from the water column. Loss of sea ice cover also alters the timing and intensity of the spring bloom (Stabeno et al., 2001). The recent discovery of shade adapted, under ice phytoplankton blooms (Arrigo et al., 2012) illustrates both the importance of sea ice, and how little we know about it.

Sea ice is also linked to the terrestrial component of the organic carbon cycle. The major sources of terrestrial organic carbon (OC) to the Arctic Ocean are rivers and coastal erosion. Rivers link the carbon cycle and the hydrologic cycle, and are the most significant source of terrestrial OC. Arctic rivers, including the Lena, Ob and Yenisei in the Eurasian Arctic, and the Mackenzie and Yukon in the North American Arctic, discharge 3300km^3 per year, and transport around $6x10^6$ t POC per year (Rachold et al., 2004). Sea ice provides an additional mechanism for transporting this terrestrial

material from the coasts onto the shelf, slope and basin (Eicken et al., 2005). This terrestrial material can either be entrained in the sea ice during sea ice formation, or be deposited on top of ice floes during the spring flood.

Coastal erosion is a less significant source of OC than riverine inputs, but it can be locally important. Much of the Arctic coastline consists of carbon rich soils (Tarnocai et al., 2009), in yedoma deposits and exposed, low-lying bluffs. The average rate of coastal retreat is 0.5m/yr (Lantuit et al., 2012), and coastal erosion is thought to supply up to $6.7x10^6$ t/yr TOC (Stein, 2008). The presence of landfast ice reduces coastal erosion by shielding the coast from storms (Legendre et al., 1992; Reimnitz and Are, 2000; O'Brien et al., 2006; Are et al., 2008).

Our study focuses on the Chukchi and Beaufort Seas. The Chukchi Sea has a broad, flat shelf with an average depth of 50m and is covered in sea ice from November to May (Walsh et al., 2005). During the summer months, the sea is highly productive, with primary production as high as 720-840$gm^{-2}a^{-1}C$ (Springer and McRoy, 1993), supporting fisheries and a significant benthic ecosystem. Inflow from the Bering Sea consists of two main water masses separated by a sharp hydrographic front: nutrient-rich Anadyr water in the west and nutrient-poor Alaskan Coastal Water in the east. Phytoplankton primary productivity east of the front is generally considerably lower (50-70$gm^{-2}a^{-1}C$) (Grebmeier et al., 1995; Hansell et al., 1993) than to the west (400$gm^{-2}a^{-1}C$) (Walsh and Dieterle, 1994).

Terrestrial carbon is supplied to the Eastern Chukchi by the Yukon River, which exports $2x10^{11}m^3$ fresh water and 2.02Mta^{-1} TOC (Guo and Macdonald, 2006) annually, as well as by numerous smaller rivers. Erosion of the organic carbon-rich peats and exposed bluffs (Jorgenson and Brown, 2005) found along the Chukchi and Beaufort Seas is another major mechanism by which terrestrial organic carbon can be supplied to the

Arctic Ocean, with the coastline storing perhaps 0.07MtTOCm^{-1} (Dou et al., 2010). However, coastal erosion in the Alaskan Chukchi has not yet been well-constrained; based upon erosion rates from the Russian Chukchi coast, Grigoriev et al. (2004) estimated an input of 0.4Mta^{-1} TOC for the Alaskan Chukchi coast.

Analytical approaches

Conditions in the Arctic appear to be suited to high terrestrial OC inputs to the sediment. Seasonal sea ice cover enables transport of coastal materials offshore (Eicken et al., 2005). High and increasing, rates of coastal erosion, also contributes to the terrestrial OC input. In contrast, marine primary productivity is generally low (250Mta^{-1} POC, 329Mta^{-1} total organic carbon (TOC) (Sakshaug, 2004)), so it is not surprising that numerous studies have reported significant terrestrial influence on the oceanic carbon cycle in the Arctic (Macdonald et al., 1998; Goñi, 2000; Belicka et al., 2004; Stein and Macdonald, 2004; Goñi et al., 2005; Tesi et al., 2014), but questions remain as to the extent of the terrestrial contribution.

Unraveling the carbon cycle in the Arctic will therefore require quantifying terrestrial and marine contributions to sediments of the shelves, basins and slopes of the Arctic and its marginal seas. A number of organic geochemical proxies can be used to distinguish the chemical signatures of allochthonous (terrestrial) and autochthonous (marine) material deposited and preserved in ocean sediments. The contributions made by each to the final mixture can then be estimated.

Carbon:Nitrogen

Carbon:Nitrogen (C:N) can be obtained through elemental analysis (EA). Due to the structural carbohydrates that they produce, terrestrial higher plants contain considerable amounts of C, and have C:N >15. Marine phytoplankton do not synthesize

these, and consequently contain relatively more N. Typical marine C:N are around 6, although certain conditions (e.g. nutrient limitation) can result in higher marine C:N up to around 10 in polynyas and sea ice (Bauerfeind et al., 1997; Søreide et al., 2010).

Stable carbon and nitrogen isotopes

Stable carbon isotopes are another valuable proxy. Here, differences in carbon isotope composition between marine and terrestrial organic matter stem from differences in the carbon pools and photosynthetic pathways that are used to fix carbon in photosynthesis. Marine phytoplankton draw on dissolved CO_2 (dCO_2) for photosynthesis, which is relatively ^{13}C enriched compared with the atmospheric CO_2 that is drawn from by land plants. Within terrestrial plants, there are also three photosynthetic pathways, C_3, C_4 and CAM, which also discriminate against ^{13}C to different extents. However, C_4 and CAM plants are not found within Arctic ecosystems which means that the terrestrial component can be relatively tightly constrained to around -27‰. The range is much broader for the marine component, from -16.7‰ to -30.4‰ (Stein, 2008), since it not only encompasses sea ice algae and pelagic algae, but also incorporates factors such as the high dCO_2 due to low surface temperatures, community composition, cell growth rate and cell size.

Since the sediment reflects a mixture of inputs, once the $\delta^{13}C$ of the sources and mixture are known, one can use a linear mixing model to determine the contribution made by each source.

$$\delta^{13}C_{Mix} = fraction_{Terrestrial} * \delta^{13}C_{Terrestrial} + fraction_{Marine} * \delta^{13}C_{Marine}$$

This approach has been fruitfully applied in many contexts (e.g. (Gearing et al., 1977)). But the presence of a third, isotopically distinct end member in the form of sea ice algae, and the difficulty of constraining the marine end member, complicates the use of two end membered mixing models in the Arctic. While careful attention to regional and

seasonal trends can yield in a more robust marine end member, a three end-membered mixing model would still be underdetermined without a second isotope.

$\delta^{15}N$ can also help us to distinguish between marine and terrestrial organic matter, as well as conveying information about nutrient utilization and recycling. Combining carbon and nitrogen isotopes provides additional information about sources and cycling, strengthening interpretation and C:N and $\delta^{13}C$.

Bayesian stable isotope mixing models (SIMMs) are an alternative to linear mixing models (Parnell et al., 2013). These models generate probability distributions for each potential source that incorporate uncertainty in the end members. These models are commonly used to estimate the contributions made by multiple food sources to diet in isotope ecology. Bayesian mixing models are underdetermined when the number of potential sources (n) exceeds the number of isotopes (n+1). This is common in complex ecosystems, but ecologist have nevertheless successfully used these models to study diet in undetermined systems (Inger et al., Stock and Semmens, 2013). Our system is simpler, with three sources and two isotopes, and is well suited to the model. We believe this is the first time these tools have been applied to sedimentary organic matter.

n-Alkanes and compound specific isotope analysis

As well as leaving fingerprints in the bulk sedimentary material, plants (and animals) can leave molecular fossils, or biomarkers, in sediments which can be identified through gas chromatography (GC). The presence, absence and distribution of these compounds can be used to identify sources such as higher plants, classes of algae etc., as well as estimate the relative contributions of these sources to the whole.

n-Alkanes have been widely used as proxies for higher plants. When higher plant material is present, a strong odd to even predominance (OEP) is observed for the C_{23} to

C_{34} homologues, with a maximum distribution at C_{27}, C_{29} or C_{31}. By contrast, marine phytoplankton are typically associated with shorter chain alkanes, such as C_{15}, C_{17} and C_{19}. Petrogenic sources can also supply alkanes, which can be distinguished by low OEP and a distinct hump in the GC trace due to unresolved complex mixture.

In order to resolve ambiguities in alkanes, $\delta^{13}C$ for specific compounds can be obtained using gas chromatography in conjunction with isotope ratio mass spectrometry (GC-IRMS). GC-IRMS provides an extra layer of information that can be used to confirm sources for specific markers or indicate mixed or misidentified sources.

In the following chapters, I will use these tools from the organic geochemistry toolbox to further our understanding of the relative contributions of sea ice algae, pelagic phytoplankton and terrestrial material to the marine carbon cycle of the Western Arctic Ocean.

Are, F., Reimnitz, E., Grigoriev, M., Hubberten, H., Rachold, V., 2008. The Influence of Cryogenic Processes on the Erosional Arctic Shoreface. J. Coast. Res. 24, 110–121. doi:10.2112/05-0573.1

Arrigo, K.R., Perovich, D.K., Pickart, R.S., Brown, Z.W., van Dijken, G.L., Lowry, K.E., Mills, M.M., Palmer, M.A., Balch, W.M., Bahr, F., Bates, N.R., Benitez-Nelson, C., Bowler, B., Brownlee, E., Ehn, J.K., Frey, K.E., Garley, R., Laney, S.R., Lubelczyk, L., Mathis, J., Matsuoka, A., Mitchell, B.G., Moore, G.W.K., Ortega-Retuerta, E., Pal, S., Polashenski, C.M., Reynolds, R.A., Schieber, B., Sosik, H.M., Stephens, M., Swift, J.H., 2012. Massive Phytoplankton Blooms Under Arctic Sea Ice. Science 16, 409–422. doi:10.1126/science.1215065

Arrigo, K.R., van Dijken, G., Pabi, S., 2008. Impact of a shrinking Arctic ice cover on marine primary production. Geophys. Res. Lett. 35, L19603. doi:10.1029/2008GL035028

Bauer, J.E., Cai, W.-J., Raymond, P. A, Bianchi, T.S., Hopkinson, C.S., Regnier, P.A.G., 2013. The changing carbon cycle of the coastal ocean. Nature 504, 61–70. doi:10.1038/nature12857

Bauerfeind, E., Garrity, C., Krumbholz, M., Ramseier, R., Voss, M., 1997. Seasonal variability of sediment trap collections in the Northeast Water polynya. Part 2. Biochemical and microscopic composition of sedimenting matter. J. Mar. Syst. 10, 371–389.

Belicka, L.L., MacDonald, R.W., Yunker, M.B., Harvey, H.R., 2004. The role of depositional regime on carbon transport and preservation in Arctic Ocean sediments. Mar. Chem. 86, 65–88.

Belt, S.T., Rowland, S.J., Poulin, M., Masse, G., Michel, C., Leblanc, B., 2007. A novel chemical fossil of palaeo sea ice : IP 25. Org. Geochem. 38, 16–27. doi:10.1016/j.orggeochem.2006.09.013

Dieckmann, G.S., Hellmer, H.H., n.d. The Importance of Sea Ice: An Overview, in: Sea Ice. Blackwell Science Ltd, Oxford, UK, pp. 1–21. doi:10.1002/9780470757161.ch1

Dou, F., Yu, X., Ping, C., Michaelson, G., Guo, L., Jorgenson, T., 2010. Spatial variation of tundra soil organic carbon along the coastline of northern Alaska. Geoderma 154, 328–335. doi:10.1016/j.geoderma.2009.10.020

Eicken, H., Gradinger, R., Gaylord, A., Mahoney, A., Rigor, I., Melling, H., 2005. Sediment transport by sea ice in the Chukchi and Beaufort Seas: Increasing importance due to changing ice conditions? Deep. Res. 52, 3281–3302. doi:10.1016/j.dsr2.2005.10.006

Faux, J.F., Belicka, L.L., Rodger Harvey, H., 2011. Organic sources and carbon sequestration in Holocene shelf sediments from the western Arctic Ocean. Cont. Shelf Res. 31, 1169–1179. doi:10.1016/j.csr.2011.04.001

Fortier, M., Fortier, L., Michel, C., Legendre, L., 2002. Climatic and biological forcing of the vertical flux of biogenic particles under seasonal Arctic sea ice. Mar. Ecol. Prog. Ser. 225, 1–16.

Gearing, P., Plucker, F., Parker, P.L., 1977. Organic carbon stable isotope ratios of continental margin sediments. Mar. Chem. 5, 251–266.

Goñi, M., 2000. Distribution and sources of organic biomarkers in arctic sediments from the Mackenzie River and Beaufort Shelf. Mar. Chem. 71, 23–51. doi:10.1016/S0304-4203(00)00037-2

Goñi, M. A., O'Connor, A.E., Kuzyk, Z.Z., Yunker, M.B., Gobeil, C., MacDonald, R.W., 2013. Distribution and sources of organic matter in surface marine sediments across the North American Arctic margin. J. Geophys. Res. Ocean. 118, 4017–4035. doi:10.1002/jgrc.20286

Goñi, M.A., Yunker, M.B., MacDonald, R.W., Eglinton, T.I., 2005. The supply and

preservation of ancient and modern components of organic carbon in the Canadian Beaufort Shelf of the Arctic Ocean. Mar. Chem. 93, 53 – 73. doi:10.1016/j.marchem.2004.08.001

Gorham, E., 1991. Northern Peatlands: Role in the Carbon Cycle and Probable Responses to Climatic Warming. Ecol. Appl. 1, 182–195.

Grebmeier, J.M., Overland, J.E., Moore, S.E., Farley, E. V, Carmack, E.C., Cooper, L.W., Frey, K.E., Helle, J.H., McLaughlin, F.A., McNutt, S.L., 2006. A major ecosystem shift in the northern Bering Sea. Science 311, 1461–1464. doi:10.1126/science.1121365

Grebmeier, J.M., Smith, W.O., Conover, R.J., 1995. Biological Processes on Arctic Continental Shelves: Ice-Ocean-Biotic Interactions, in: Arctic Oceanography: Marginal Ice Zones and Continental Shelves. American Geophysical Union, Washington, DC, pp. 231–262.

Grigoriev, M.N., Rachold, V., Hubberten, H.W., Schirrmeister, L., 2004. Organic carbon input to the Arctic Seas through coastal erosion, in: Stein, R., Macdonald, R. (Eds.), The Organic Carbon Cycle in the Arctic Ocean. Springer, Heidelberg, pp. 41–45.

Guo, L., MacDonald, R.W., 2006. Source and transport of terrigenous organic matter in the upper Yukon River: Evidence from isotope ($\delta^{13}C$, $\Delta^{14}C$, and $\delta^{15}N$) composition of dissolved, colloidal, and particulate phases. Global Biogeochem. Cycles 20, n/a–n/a. doi:10.1029/2005GB002593

Hansell, D., Whitledge, T., Goering, J., 1993. Patterns of nitrate utilization and new production over the Bering-Chukchi shelf. Cont. Shelf Res. 13, 601–627. doi:10.1016/0278-4343(93)90096-G

Hill, V., Cota, G., Stockwell, D., 2005. Spring and summer phytoplankton communities in the Chukchi and Eastern Beaufort Seas. Deep. Res. II 52, 3369–3385.

Hugelius, G., Bockheim, J.G., Camill, P., Elberling, B., Grosse, G., Harden, J.W., Johnson, K., Jorgenson, T., Koven, C.D., Kuhry, P., Michaelson, G., Mishra, U., Palmtag, J., Ping, C.-L., O'Donnell, J., Schirrmeister, L., Schuur, E.A.G., Sheng, Y., Smith, L.C., Strauss, J., Yu, Z., 2013. A new data set for estimating organic carbon storage to 3 m depth in soils of the northern circumpolar permafrost region. Earth Syst. Sci. Data 5, 393–402. doi:10.5194/essd-5-393-2013

Inger, R., Jackson, A., Parnell, A., Bearhop, S., n.d. SIAR V4 (Stable Isotope Analysis in R) An Ecologist ' s Guide. Matrix.

Johannessen, O.M., 1999. Satellite Evidence for an Arctic Sea Ice Cover in Transformation. Science (80-.). 286, 1937–1939. doi:10.1126/science.286.5446.1937

Jorgenson, M., Brown, J., 2005. Classification of the Alaskan Beaufort Sea Coast and

estimation of carbon and sediment inputs from coastal erosion. Geo-Marine Lett. 25, 69–80. doi:10.1007/s00367-004-0188-8

Lantuit, H., Overduin, P.P., Couture, N., Wetterich, S., Aré, F., Atkinson, D., Brown, J., Cherkashov, G., Drozdov, D., Donald Forbes, L., Graves-Gaylord, A., Grigoriev, M., Hubberten, H.W., Jordan, J., Jorgenson, T., Ødegård, R.S., Ogorodov, S., Pollard, W.H., Rachold, V., Sedenko, S., Solomon, S., Steenhuisen, F., Streletskaya, I., Vasiliev, A., 2012. The Arctic Coastal Dynamics Database: A New Classification Scheme and Statistics on Arctic Permafrost Coastlines. Estuaries and Coasts 35, 383–400. doi:10.1007/s12237-010-9362-6

Legendre, L., Ackley, S., Dieckmann, G., Gulliksen, B., Horner, R., Hoshiai, T., Melnikov, I., Reeburgh, W., Spindler, M., Sullivan, C., 1992. Ecology of sea ice biota. Polar Biol. 12, 429–444. doi:10.1007/BF00243114

MacDonald, R.W., Solomon, S.M., Cranston, R.E., Welch, H.E., Yunker, M.B., Gobeil, C., 1998. A sediment and organic carbon budget for the Canadian Beaufort Shelf. Mar. Geol. 144, 255–273.

Magen, C., Chaillou, G., Crowe, S.A., Mucci, A., Sundby, B., Gao, A., Makabe, R., Sasaki, H., 2010. Origin and fate of particulate organic matter in the southern Beaufort Sea - Amundsen Gulf region, Canadian Arctic. Estuar. Coast. Shelf Sci. 86, 31–41. doi:10.1016/j.ecss.2009.09.009

Mars, J.C., Houseknecht, D.W., 2007. Quantitative remote sensing study indicates doubling of coastal erosion rate in past 50 yr along a segment of the Arctic coast of Alaska. Geology 35, 583–586. doi:10.1130/G23672A.1

Massonnet, F., Fichefet, T., Goosse, H., Bitz, C.M., Philippon-Berthier, G., Holland, M.M., Barriat, P.-Y., 2012. Constraining projections of summer Arctic sea ice. Cryosph. 6, 1383–1394. doi:10.5194/tc-6-1383-2012

McClelland, J.W., Déry, S.J., Peterson, B.J., Holmes, R.M., Wood, E.F., 2006. A pan-arctic evaluation of changes in river discharge during the latter half of the 20th century. Geophys. Res. Lett. 33, L06715. doi:10.1029/2006GL025753

McGuire, A.D., Anderson, L.G., Christensen, T.R., Dallimore, S., Guo, L., Hayes, D.J., Heimann, M., Lorenson, T.D., Macdonald, R.W., Roulet, N., 2009. Sensitivity of the carbon cycle in the Arctic to climate change. Ecol. Monogr. 79, 523–555. doi:10.1890/08-2025.1

Melling, H., 2000. Exchanges of fresh water through the shallow straits of the North American Arctic, in: Lewis, E.L., Jones, E.P., Lemke, P., Prowse, T.D., Wadhams, P. (Eds.), The Freshwater Budget of the Arctic Ocean. Springer, pp. 479–502.

Muenchow, A., Melling, H., Falkner, K., 2006. An Observational Estimate of Volume and Freshwater Flux Leaving the Arctic Ocean through Nares Strait. J. Phys. Oceanogr. 36, 2025–2041.

O'Brien, M.C., MacDonald, R.W., Melling, H., Iseki, K., 2006. Particle fluxes and geochemistry on the Canadian Beaufort Shelf: Implications for sediment transport and deposition. Cont. Shelf Res. 26, 41–81. doi:10.1016/j.csr.2005.09.007

Parnell, A.C., Inger, R., Bearhop, S., Jackson, A.L., 2010. Source partitioning using stable isotopes: coping with too much variation. PLoS One 5, e9672. doi:10.1371/journal.pone.0009672

Parnell, A.C., Phillips, D.L., Bearhop, S., Semmens, B.X., Ward, E.J., Moore, J.W., Jackson, A.L., Grey, J., Kelly, D.J., Inger, R., 2013. Bayesian stable isotope mixing models. Environmetrics 24, 387–399. doi:10.1002/env.2221

Perovich, D.K., Richter-Menge, J.A., 2009. Loss of Sea Ice in the Arctic. Ann. Rev. Mar. Sci. 1, 417–441. doi:10.1146/annurev.marine.010908.163805

Perrette, M., Yool, A., Quartly, G.D., Popova, E.E., 2011. Near-ubiquity of ice-edge blooms in the Arctic. Biogeosciences 8, 515–524. doi:10.5194/bg-8-515-2011

Peterson, B.J., Holmes, R.M., McClelland, J.W., Vörösmarty, C.J., Lammers, R.B., Shiklomanov, A.I., Shiklomanov, I.A., Rahmstorf, S., 2002. Increasing river discharge to the Arctic Ocean. Science 298, 2171–3. doi:10.1126/science.1077445

Rachold, V., Eicken, H., Gordeev, V., Grigoriev, M., Hubberten, H., Lisitzin, A., Shevchenko, V., Schirmeister, L., 2004. Modern Terrigenous Organic Carbon Input to the Arctic Ocean, in: Stein, R., Macdonald, R.W. (Eds.), The Organic Carbon Cycle in the Arctic Ocean. Springer, pp. 33–56.

Reimnitz, E., Are, F.E., 2000. Coastal Bluff and Shoreface Comparison over 34 Years Indicates Large Supply of Erosion Products to Arctic Seas. Polarforschung 68, 231 – 235.

Roach, A.T., Aagaard, K., Pease, C.H., Salo, S.A., Weingartner, T., Pavlov, V., Kulakov, M., 1995. Direct measurements of transport and water properties through the Bering Strait. J. Geophys. Res. 100, 18443–18457. doi:10.1029/95JC01673

Rudels, B., Jones, E.P., Schauer, U., Eriksson, P., 2004. Atlantic sources of the Arctic Ocean surface and halocline waters. Polar Res. 23, 181–208. doi:10.1111/j.1751-8369.2004.tb00007.x

Sakshaug, E., 2004. Primary and Secondary Production in the Arctic Seas, in: Stein, R., MacDonald, R. (Eds.), The Organic Carbon Cycle in the Arctic Ocean. Springer, pp. 57–82.

Schnack-Schiel, S.B., n.d. The Macrobiology of Sea Ice, in: Sea Ice. Blackwell Science Ltd, Oxford, UK, pp. 211–239. doi:10.1002/9780470757161.ch7

Schreiner, K.M., Bianchi, T.S., Rosenheim, B.E., 2014. Evidence for permafrost thaw and transport from an Alaskan North Slope watershed. Geophys. Res. Lett. 41, 3117–3126. doi:10.1002/2014GL059514

Shiklomanov, I.A., 1998. Comprehensive Assessment of the Freshwater Resources of the World: Assessment of Water Reources and Water Availability in the World. Geneva.

Søreide, J.E., Leu, E., Berge, J., Graeve, M., Falk-Petersen, S., 2010. Timing of blooms, algal food quality and Calanus glacialis reproduction and growth in a changing Arctic. Glob. Chang. Biol. no–no. doi:10.1111/j.1365-2486.2010.02175.x

Springer, A., McRoy, C., 1993. The paradox of pelagic food webs in the northern Bering Sea—III. Patterns of primary production. Cont. Shelf Res. 13, 575–599. doi:10.1016/0278-4343(93)90095-F

Stabeno, P.J., Bond, N.A., Kachel, N.B., Salo, S.A., 2001. On the temporal variability of the physical environment over the south-eastern Bering Sea. Fish. Oceanogr. 10, 81–98.

Stein, R., 2008. Arctic Ocean Sediments: Processes, Proxies, and Paleoenvironment, 1st ed. Elsevier B.V., Amsterdam, NL.

Stein, R., MacDonald, R.W., 2004. The organic carbon cycle in the Arctic Ocean. Springer.

Stock, B.C., Semmens, B.X., 2013. MixSIAR GUI User Manual, version 1.0.

Stroeve, J.C., Serreze, M.C., Holland, M.M., Kay, J.E., Malanik, J., Barrett, A.P., 2012. The Arctic's rapidly shrinking sea ice cover: A research synthesis. Clim. Change 110, 1005–1027. doi:10.1007/s10584-011-0101-1

Tarnocai, C., Canadell, J.G., Schuur, E. A. G., Kuhry, P., Mazhitova, G., Zimov, S., 2009. Soil organic carbon pools in the northern circumpolar permafrost region. Global Biogeochem. Cycles 23, n/a–n/a. doi:10.1029/2008GB003327

Tesi, T., Semiletov, I., Hugelius, G., Dudarev, O., Kuhry, P., Gustafsson, Ö., 2014. Composition and fate of terrigenous organic matter along the Arctic land–ocean continuum in East Siberia: Insights from biomarkers and carbon isotopes. Geochim. Cosmochim. Acta 133, 235–256. doi:10.1016/j.gca.2014.02.045

Thomas, D.N., Dieckmann, G.S. (Eds.), 2003. Sea Ice. Blackwell Science Ltd, Oxford, UK. doi:10.1002/9780470757161

Tolosa, I., Fiorini, S., Gasser, B., Martín, J., Miquel, J.C., 2013. Carbon sources in suspended particles and surface sediments from the Beaufort Sea revealed by molecular lipid biomarkers and compound-specific isotope analysis. Biogeosciences 10, 2061–2087. doi:10.5194/bg-10-2061-2013

Tremblay, J.-É., Bélanger, S., Barber, D.G., Asplin, M., Martin, J., Darnis, G., Fortier, L., Gratton, Y., Link, H., Archambault, P., Sallon, A., Michel, C., Williams, W.J., Philippe, B., Gosselin, M., 2011. Climate forcing multiplies biological productivity in the coastal Arctic Ocean. Geophys. Res. Lett. 38, n/a–n/a. doi:10.1029/2011GL048825

Vancoppenolle, M., Meiners, K.M., Michel, C., Bopp, L., Brabant, F., Carnat, G., Delille, B., Lannuzel, D., Madec, G., Moreau, S., Tison, J.L., van der Merwe, P., 2013. Role of sea ice in global biogeochemical cycles: Emerging views and challenges. Quat. Sci. Rev. 79, 207–230. doi:10.1016/j.quascirev.2013.04.011

Vonk, J.E., Mann, P.J., Dowdy, K.L., Davydova, A., Davydov, S.P., Zimov, N., Spencer, R.G.M., Bulygina, E.B., Eglinton, T.I., Holmes, R.M., 2013. Dissolved organic carbon loss from Yedoma permafrost amplified by ice wedge thaw. Environ. Res. Lett. 8, 035023. doi:10.1088/1748-9326/8/3/035023

Vonk, J.E., Sánchez-García, L., van Dongen, B.E., Alling, V., Kosmach, D., Charkin, A., Semiletov, I.P., Dudarev, O. V, Shakhova, N., Roos, P., Eglinton, T.I., Andersson, A., Gustafsson, O., 2012. Activation of old carbon by erosion of coastal and subsea permafrost in Arctic Siberia. Nature 489, 137–40. doi:10.1038/nature11392

Walsh, J., Dieterle, D., Maslowski, W., Grebmeier, J., Whitledge, T., Flint, M., Sukhanova, I., Bates, N., Cota, G., Stockwell, D., 2005. A numerical model of seasonal primary production within the Chukchi/Beaufort Seas. Deep Sea Res. Part II Top. Stud. Oceanogr. 52, 3541–3576. doi:10.1016/j.dsr2.2005.09.009

Walsh, J.J., Dieterle, D.A., 1994. CO_2 cycling in the coastal ocean. I – A numerical analysis of the southeastern Bering Sea with applications to the Chukchi Sea and the northern Gulf of Mexico. Prog. Oceanogr. 34, 335–392. doi:10.1016/0079-6611(94)90019-1

Woodgate, R.A., Aagaard, K., 2005. Revising the Bering Strait freshwater flux into the Arctic Ocean. Geophys. Res. Lett. 32, 3–6. doi:10.1029/2004GL021747

Chapter 2: Methods

Sediment sampling

The study area is composed of portions of the continental shelf, slope and basin of the NE Chukchi Sea and W Beaufort Sea. As part of the Shelf Basins Interactions Program (SBI)(Grebmeier and Harvey, 2005; Grebmeier et al., 2009), samples were selected from four shelf-to-basin transects. Samples from East of Barrow Canyon (EB) were collected between July and August 2002. Those from Barrow Canyon (BC), East of Hanna Shoal (EHS) and West of Hanna Shoal (WHS) were collected during May and June 2002, with the exception of EHS-12 and WHS-12, which were collected in July and August 2004. The sediment cores were taken with a Pouliot box corer with an area of 0.06m^2. The outer edges of the cores were then discarded and the remaining portion was sectioned by 1cm intervals for the first 10cm, and every 2cm thereafter. The subsamples were then stored at -20^{o}C in pre-cleaned plastic or glass I-Chem jars with Teflon lined lids aboard ship until further processing on shore.

Core HLY0501-JPC5 is a 16.7m long Jumbo Piston Core (JPC) taken from the Chukchi slope (72^o 41.4' N, 157^o 31.2' W), at a water depth of 415m (Darby et al., 2009). A trigger core of 2.59m length was also taken and correlated to the piston core using radiocarbon dates and palynological assemblages (McKay, 2009), since piston cores disturb the uppermost sediments during barrel entry. The upper 12.4m of JPC5 and the trigger core consist of a sulfide-rich, olive-gray mud. In JPC5, this is underlain by a 4.33m ice rafted deposit of rich gray to gray brown sandy mud (McKay, 2009).

Radiocarbon dates for JPC5 were obtained using Accelerator Mass Spectrometry (AMS) on six bivalve shells from different core depths. Radiocarbon dates were

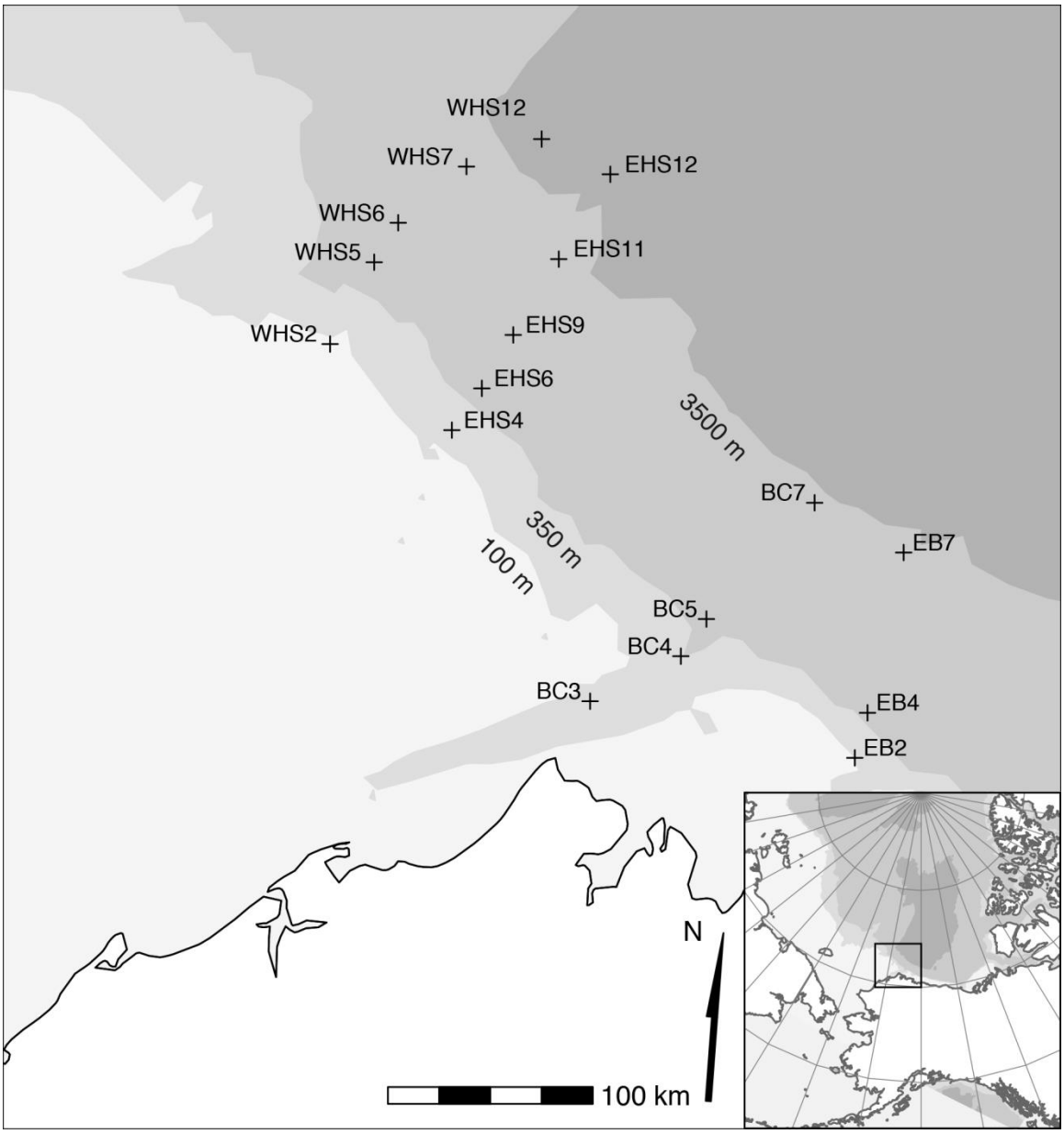

Figure 1: Chukchi Core Locations

then corrected for marine reservoir effects, and stable carbon isotope fluctuations with CALIB 5.0.2. McKay (2008) used a regional reservoir correction (ΔR) of 0 years due to the young, overlying Atlantic water and the surface depth of the sample site, which is below the older Pacific water that lies between 30-200m.

This age model suggested an average sedimentation rate of 156cm/ka. Darby (2009) provides additional sedimentation rate estimates, based on age models of $\Delta R = 0$ years and $\Delta R = 460$ years, to account for uncertainty in the magnitude of the Arctic Ocean reservoir effect. Sedimentation rates for JPC5 were estimated to be between 159 and 161cm/ka with the two models. McKay (2008) estimates the sedimentation rate for the trigger core to be 160.5cm/ka using ^{210}Pb dating. This would imply that the there is a 700 year gap between the bottom of the trigger core and the top of JPC5.

Bulk Isotope Analysis of Sediments Using Elemental Analysis – Isotope Ratio Mass Spectrometry

Bulk sediments were treated with 40% HCl in order to remove inorganic carbon ($CaCO_3$), which would otherwise mask the organic carbon. Samples were then dried overnight in an oven set to 60°C and stored in glass jars. All samples were additionally dried immediately prior to analysis. The samples were then weighed (10-30mg) using a Mettler-Toledo MT5 balance and placed into a tin capsule (Costech, Valencia, CA) in preparation for bulk analysis.

The elemental analysis isotope ration mass spectrometer (EA-IRMS) consisted of an autosampler connected to a Carlo-Erba/Fisons NA1500 NC5 EA and a GV Instruments Optima IRMS (Manchester, UK). Carbon and nitrogen samples were performed with a single combustion, using a dual furnace system with oxidation and reduction furnaces to ensure complete conversion of C and N in the sample to CO_2 and N_2 (Fig 2). The oxidation furnace was held at 1020°C, and contained chromium$_{III}$ oxide (Costech) and silvered cobaltous oxide Co_3O_4/Ag (Costech). The reduction furnace contained reduced copper wire (Costech) and was held at

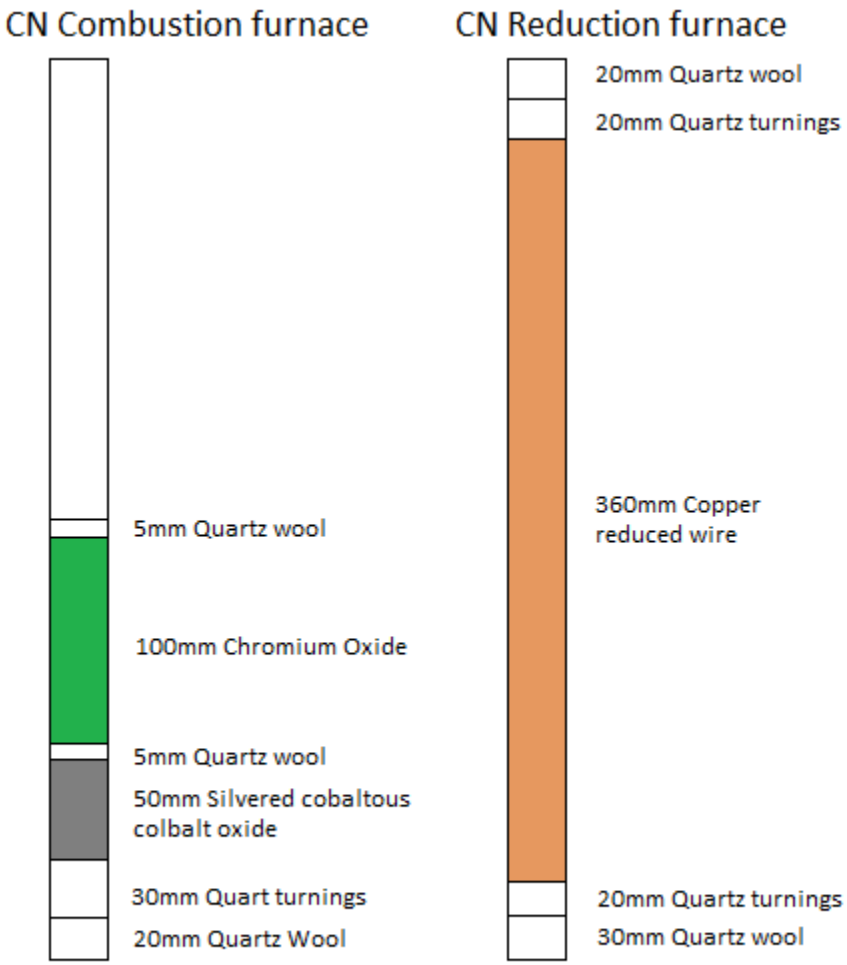

Figure 2: EA Oxidation and Reduction Furnaces

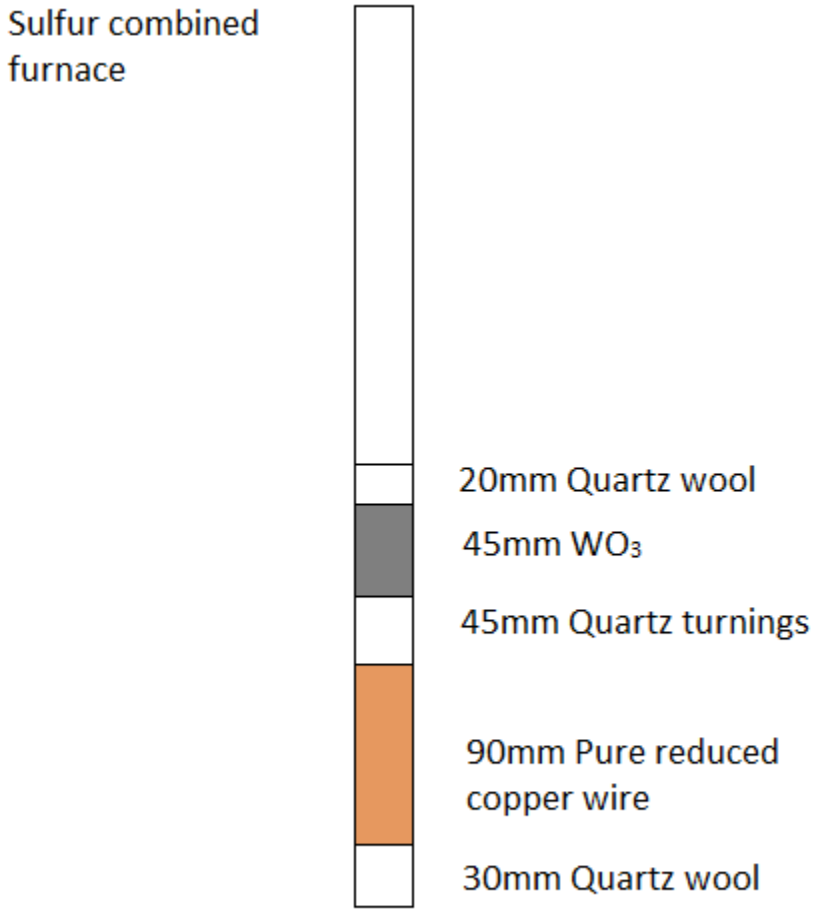

Figure 3: EA Combined Oxidation Reduction Furnace

650°C. A trap containing anhydrous magnesium perchlorate (Costech) stripped water from the outflow. The CO_2 and N_2 were then separated with a Porapak QS 50-80 mesh packed GC column, isothermal at 35°C. Following separation, elemental compositions were obtained with a thermal conductivity detector (TCD). In samples containing typical amounts of carbon (>0.5%), additional He was added with a GV Isochron diluter (GV Instruments, Manchester, UK) to reduce the CO_2 signal before entry to the IRMS.

In the isotope ratio mass spectrometer, molecules are separated by mass and charge. The molecules are first ionized by an electron beam, and then introduced into a flight tube where they are subjected to a magnetic field. Since the lighter ions are deflected more, the initial beam of molecules is thus separated into 3 beams of CO_2 with mass 44, 45 and 46, the intensity of which can be measured with Faraday cups. The signal from the Faraday cups is then converted into a signal in nA, which is then used by the spectrometer's Isodat software. These signals enable the calculation of ratios for the three beams (e.g. for mass 45 to 44 and 46 to 44 for ^{13}C). The ^{13}C is corrected for cross mass overlap to account for contributions from ^{17}O to the mass 45 and 46 beams in the ^{13}C signal, based upon the amount of ^{17}O in the sample (Craig, 1957).

$$\delta^{13}C = 1.0676(\delta_{45}) - 0.0338(\delta^{18}O)$$

Sulfur isotope analysis of the bulk sediments was performed separately, owing to the longer elution time for SO_2 and different operating conditions. Samples were prepared as above, however the furnaces were replaced with a combined oxidation-reduction furnace containing tungsten$_{VI}$ oxide and the temperature was increased to 1050°C, and GC column temperature was increased to 90°C (Fig

3). Elemental composition of sulfur was obtained using the ion beam of the mass spectrometer.

C:N was reported on an atomic basis. Isotope abundances are reported in δ notation as ‰ variations from the relevant standard:

$$\delta_{sample}{}^{N}E\ (‰) = (R_{sample}/R_{standard} - 1) \times 1000$$

where $\delta_{sample}{}^{N}E$ is the isotope composition of the sample with the heavy isotope (N) of the element, E; R is the abundance ratio of the heavy to light isotopes ($^{13}C/^{12}C$, $^{15}N/^{14}N$ or $^{34}S/^{32}S$) of that element. Samples are measured against carbon dioxide, nitrogen and sulfur dioxide laboratory standards which had been calibrated against NBS22, atmospheric N_2 or NBS 127, respectively. Measurement reproducibility is typically better than ±0.2‰ for carbon and nitrogen.

Sediment Extraction for Gas Chromatography

A 1:1 mixture of dichloromethane and methanol was used to extract 5-10g of the wet sediment samples. This was performed in solvent rinsed glass test tubes with Teflon lined caps. The samples were sonicated for 2 minutes at the beginning of the extraction, before being stored overnight at 4°C. Following the extraction, the organic phase was partitioned by the addition of nanopure water and then centrifuged at 1200rpm for 5 minutes. This was repeated 3 times, and all the organic phases were combined and dried by rotary evaporation.

The extracts were spiked with the internal standard, 5a-Cholestane and then saponified with 0.5M KOH in methanol at 30°C for five minutes. The polar and neutral phases were separated by the addition of water and subsequent extraction with a 9:1 mixture of hexane:diethyl ether.

High Performance Liquid Chromatography Separation

The neutral lipid fractions were separated by high performance liquid chromatography (HPLC). A Phenomenex (Torrance, CA) Luna 5μm silica, 100Å 250mm x 4.60mm column was used with Phenomenex silica security guard column (4mm long with an internal diameter of 3.0mm). Samples were eluted with hexane, dichloromethane and methanol at a flow rate of 0.5ml/minute; after an initial isocratic hold of 100% hexane for 10 minutes, the dichloromethane concentration was increased to 20% over 5 minutes. This was followed by a 5 minute gradient to 100% dichloromethane. After this, the percentage of methanol was increased from 0-5% over five minutes and then held at 5% for 23 minutes. The column was then pumped for 10 minutes with 100% hexane in preparation for the next sample at a flow rate of 1ml/min. The alkane fraction of the neutral lipids typically eluted within 0-10 minutes, ketones within 10-20 minutes, followed n-alcohols and sterols between 20-30 minutes.

Gas Chromatography – Isotope Ratio Mass Spectrometry

Gas chromatography – isotope ratio mass spectrometry (GC-IRMS) was performed using an HP 5890 II GC with a 60m x 3.20mm (0.25um internal diameter) DB5 column (J+W Scientific) connected to a GV Instruments (Manchester, UK) Isoprime mass spectrometer (Fig 4). Helium at a flow rate of 1ml/min was used as the carrier gas. Samples were injected splitless, with the entire sample directed into a narrow bore glass inlet sleeve at 280°C. The oven was at an initial temperature of 60°C. After being held at 60°C for one and half minutes, the temperature was increased to 130°C at a rate of 2°C/min. Upon reaching 130°C, a second ramp to 300°C at 4°C/min commenced. The oven was then held at 300°C for 60 minutes, giving a total run time of 138 minutes. A heart-

split valve was used to vent the solvent to the flame ionization detector before being switched to direct gas flow through a ceramic combustion furnace fitted with CuO and nichrome wires at 850°C. Flow from the furnace was supplemented by additional He to carry the GC effluent gases to the IRMS and to provide back pressure for the heart split valve. A cryogenic water trap held at -70°C removed water from the gas flow before introduction to the mass spectrometer. Three pulses of calibrated reference CO_2 were analyzed at the beginning and end of each sample run to enable calculation of isotope ratios relative to the standard and to control signal stability. Additionally, each sample contained a 5a-cholestane as an internal standard, and a deuterated naphthalene standard of known isotopic composition was analyzed daily to monitor instrumental performance. Samples are measured against a carbon dioxide laboratory standard which has been calibrated against the NBS22 standard. Carbon values were corrected for mass overlap with isotopes of oxygen. Measurement reproducibility is typically better than ±0.2‰.

Craig, H., 1957. Isotopic standards for carbon and oxygen and correction factors for mass-spectrometric analysis of carbon dioxide. Geochim. Cosmochim. Acta 12, 133–149. doi:10.1016/0016-7037(57)90024-8

Darby, D. A., Ortiz, J., Polyak, L., Lund, S., Jakobsson, M., Woodgate, R. A., 2009. The role of currents and sea ice in both slowly deposited central Arctic and rapidly deposited Chukchi–Alaskan margin sediments. Glob. Planet. Change 68, 58–72. doi:10.1016/j.gloplacha.2009.02.007

Grebmeier, J.M., Harvey, H.R., Stockwell, D.A., 2009. The Western Arctic Shelf–Basin Interactions (SBI) project, volume II: An overview. Deep Sea Res. Part II Top. Stud. Oceanogr. 56, 1137–1143. doi:10.1016/j.dsr2.2009.03.001

Grebmeier, J.M., arvey, H.R., 2005. The Western Arctic Shelf–Basin Interactions (SBI) project: An overview. Deep Sea Res. Part II Top. Stud. Oceanogr. 52, 3109–3115. doi:10.1016/j.dsr2.2005.10.004

Table 1

Site Name	Station Number	Longitude (W)	Latitude (N)	Depth (m)
EB2	HLY02-03-023	152° 33.2’	71° 27.4’	89
EB4	HLY02-03-021	152° 24.7’	71° 39.0’	498
EB7	HLY02-03-018	151° 59.1’	72° 19.3’	3264
BC3	HLY02-01-037	155° 45.3’	71° 39.0’	183
BC4	HLY02-01-031	154° 49.2’	71° 55.7’	401
BC5	HLY02-01-032	154° 27.8’	72° 04.2’	1317
BC7	HLY02-01-034	154° 29.9’	72° 32.0’	2934
WHS2	HLY02-01-006	160° 34.0’	72° 50.5’	58
WHS5	HLY02-01-009	160° 06.7’	73° 16.8’	1198
WHS6	HLY02-01-010	159° 49.8’	73° 26.7’	1855
WHS7	HLY02-01-011	159° 33.2’	73° 36.7’	2443
WHS12	HLY04-03-051	157° 51.2’	73° 54.1’	3748
EHS4	HLY02-01-019	158° 44.2’	72° 36.3’	86
EHS6	HLY02-01-017	158° 28.5’	72° 51.1’	426
EHS9	HLY02-01-014	158° 08.8’	73° 06.1’	2158
EHS11	HLY02-01-012	157° 31.9’	73° 26.2’	2861
EHS12	HLY04-03-051	156° 45.9’	73° 47.9’	3778
STN1	HLY02-01-001	168° 52.9’	67° 27.2’	52
STN2	HLY02-01-002	167° 28.0’	70° 38.0’	50
JPC5	HLY05-01-05	157° 31.2’	72° 41.4’	415

Table 1: Sample locations

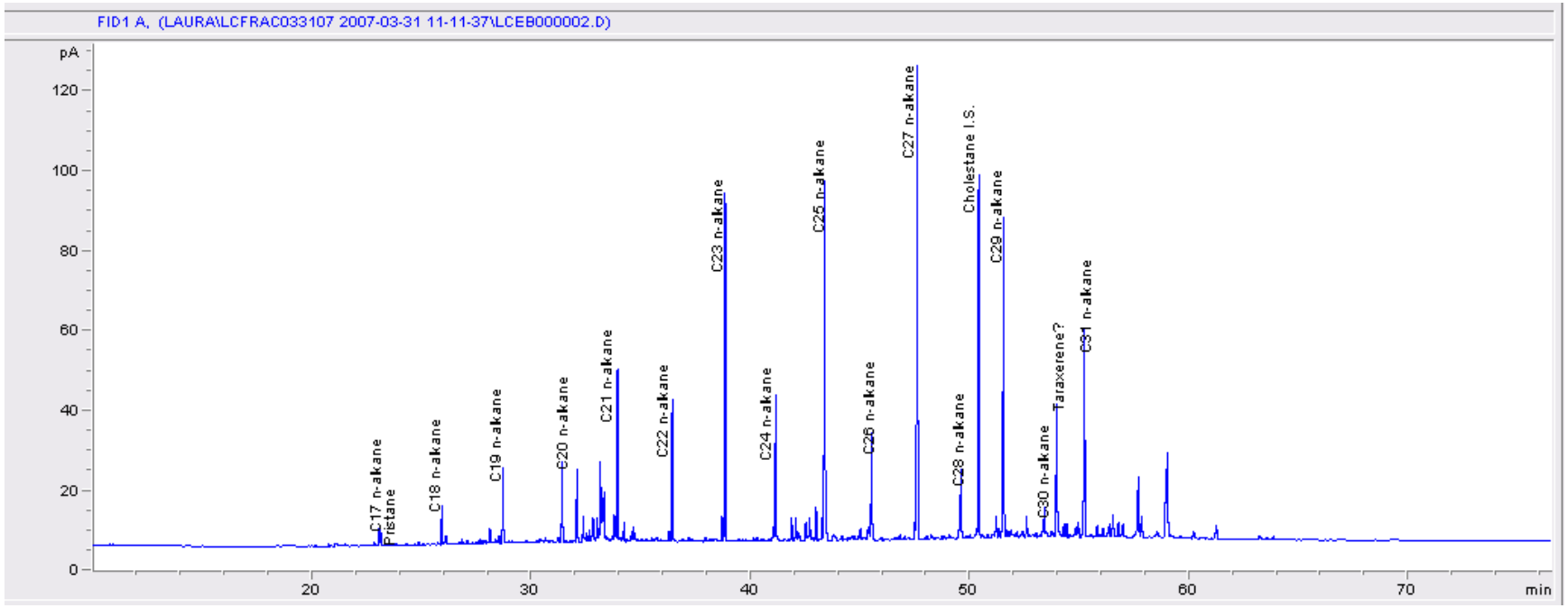

Figure 4: GC-trace for EB4 Hydrocarbon Fraction

Chapter 3: Assessing the importance of terrestrial organic carbon in the Chukchi and Beaufort seas

A version of this chapter has been accepted for publication by Estuarine and Coastal Shelf Science

Introduction

Unraveling the carbon cycle in the Arctic Ocean requires an understanding of the sources and transport of organic carbon in the shelves, slopes and basins of the Arctic Ocean and its marginal seas. The Arctic is unique among the world's oceans in that it is essentially landlocked. Surrounded by continents, its only sources of inflow are the Bering Strait (0.83Sv (Roach et al., 1995; Woodgate and Aagaard, 2005), Barents Sea (2Sv) and Fram Strait (1.5Sv (Rudels et al., 2004)) with outflow via the Canadian Archipelago (0.8Sv (Muenchow et al., 2006)) and western Fram Strait (3.5Sv (Melling, 2000)). Bathymetrically, the Arctic is characterized by large ocean shelves which make up 56% of the total area of the Arctic Ocean and its surrounding seas, as well as 30% of the total global shelf area (Stein and Macdonald, 2004). Owing to their relative shallowness, these epicontinental seas receive a disproportionate amount of terrestrial runoff relative to their volume: 11% of global runoff to 1% of global ocean volume (Shiklomanov, 1998). This runoff supplies $6 Mta^{-1}$ particulate organic carbon (POC) (Rachold et al., 2004). Given that the Arctic also experiences seasonal sea ice cover, which enables transport of coastal materials offshore (Eicken et al., 2005), high rates of coastal erosion, and generally low primary productivity ($250 Mta^{-1}$ POC, $329 Mta^{-1}$ total organic carbon (TOC) (Sakshaug, 2004)), it is not surprising that numerous studies have

reported significant terrestrial influence on the oceanic carbon cycle in the Arctic (Macdonald et al., 1998; Goñi, 2000; Belicka et al., 2004; Stein and Macdonald, 2004; Goñi et al., 2005; Tesi et al., 2014), but questions remain as to the extent of the terrestrial contribution.

High fresh water inputs connect the Arctic carbon cycle to the hydrologic cycle, with heightened discharge increasing the amount of terrestrial matter exported. Terrestrial organic carbon can also be supplied by coastal erosion, which is extensive throughout the Arctic (Rachold et al., 2000; Mars and Houseknecht, 2007). This terrestrial material is then transported by sea ice to the shelf and basin (Eicken et al., 2005). Sea ice also affects other parts of the carbon cycle: it limits productivity by attenuating light penetration of the ocean surface (Fortier et al., 2002; Hill et al., 2005), provides a habitat for sea ice algae (Legendre et al., 1992) and decreases coastal erosion (Reimnitz and Are, 2000; O'Brien et al., 2006; Are et al., 2008). The loss in sea ice cover also alters the timing and intensity of the spring bloom (Stabeno et al., 2001). The recent discovery of shade adapted, under ice phytoplankton blooms (Arrigo et al., 2012) illustrates both the importance of sea ice, and how little we know about it. Given recent changes in sea ice cover (Johannessen et al., 1999; Perovich and Richter-Menge, 2009), changes in river discharge (Peterson et al., 2002; McClelland et al., 2006), increasing coastal erosion (Mars and Houseknecht, 2007; Vonk et al., 2012) and changes in carbon storage in permafrost soils (Gorham, 1991; Hugelius et al., 2013; Vonk et al., 2013; Schreiner et al., 2014), it is crucial to address the carbon cycle in the Arctic and its Holocene history in order to predict the response of the Arctic Ocean to climate change.

The Chukchi Sea has a broad, flat shelf with an average depth of 50m and is covered in sea ice from November to May (Walsh et al., 2005). During the summer months, the sea is highly productive, with primary production as high as 720-840$gm^{-2}a^{-1}C$ (Springer and McRoy, 1993), supporting fisheries and a significant benthic ecosystem. Inflow from the

Bering Sea consists of two main water masses separated by a sharp hydrographic front: nutrient rich Anadyr water in the west and nutrient poor Alaskan Coastal Water in the east. Phytoplankton primary productivity east of the front is generally considerably lower (50-70$gm^{-2}a^{-1}C$) (Grebmeier et al., 1995; Hansell et al., 1993) than to the west (400$gm^{-2}a^{-1}C$) (Walsh and Dieterle, 1994).

Terrestrial carbon is supplied to the Eastern Chukchi by the Yukon River, which exports $2x10^{11}m^3$ fresh water and 2.02Mta^{-1} TOC (Guo and Macdonald, 2006) annually, as well as by numerous smaller rivers. Erosion of the organic carbon-rich peats and exposed bluffs (Jorgenson and Brown, 2005) found along the Chukchi and Beaufort Seas is another major mechanism by which terrestrial organic carbon can be supplied to the Arctic Ocean, with the coastline storing perhaps 0.07$MtTOCm^{-1}$ (Dou et al., 2010). However, coastal erosion in the Alaskan Chukchi has not yet been well-constrained; based upon erosion rates from the Russian Chukchi coast, Grigoriev et al. (2004) estimated an input of 0.4Mta^{-1} TOC for the Alaskan Chukchi coast.

Recent studies in the Beaufort and Chukchi Seas have used $\delta^{13}C$, $\delta^{15}N$, C:N and suites of biomarkers to assess terrestrial inputs to these seas (Goñi, 2000; Naidu, 2000; Fernandes and Sicre, 2000; Goñi et al., 2005, Drenzek et al., 2007). Generally, these studies have suggested that terrestrial organic carbon comprised a minimum of 30% of total organic carbon in Beaufort shelf sediments, with higher proportions of terrestrial material found in the vicinity of the Mackenzie River. Goñi (2000) reported a mean $\delta^{13}C$ of -25.4±0.5‰ for sediments close to the Mackenzie River, which was similar to the mean $\delta^{13}C$ of Mackenzie River sediments (-26.5±0.3‰). Likewise, the shelf sediment C:N of between 12 and 14 was also comparable with river sediments. There is also biomarker evidence for algal and detrital algal contributions to Beaufort sediments and suspended particulate organic matter (Tolosa et al., 2013). In the Chukchi Sea, estimates of terrestrial and marine contributions to the sedimentary bulk carbon from $\delta^{13}C$ have

suggested a more marine system (Naidu, 2000), with bulk sedimentary carbon more $\delta^{13}C$ enriched than in the Beaufort (Dunton et al., 1989). Sediment $\delta^{13}C$ in those studies were around -21‰ and C:N under 10. However, Belicka and Harvey (2009) argued, on the basis of significant terrestrial biomarker concentrations, for the presence of a more ^{13}C enriched marine component such as sea ice algae. This conclusion was supported by evidence of high coastal erosion and potentially high sea ice algal contributions to total primary productivity (Are et al., 2008; Gradinger, 2009). Goñi et al. (2013) also found evidence of degraded terrestrial material in Barrow Canyon sediments.

This study presents bulk $\delta^{13}C$, and $\delta^{15}N$ data from a series of 7 cores and 12 additional core tops taken from the Chukchi and Beaufort Seas. The $\delta^{13}C$ and $\delta^{15}N$ were used to construct a three source Bayesian mixing model to estimate the proportional contributions to the sediments of each source. Although Bayesian modeling has been widely uses by ecologists to determine food web relationships (Parnell et al., 2010), it has not, to our knowledge, been used to resolve sources of organic material to marine sediments. The ability to incorporate additional sources and isotopes into the mixing model is a significant advantage over linear mixing models when dealing with complex systems, such as the Arctic Ocean. Through these analyses, the origins and fate of marine and terrestrial organic matter were investigated in the eastern Chukchi and western Alaskan Beaufort Seas over Holocene timescales, with the ultimate aim of understanding the relative influence of terrestrial and marine sources in the organic carbon cycle in the western Arctic.

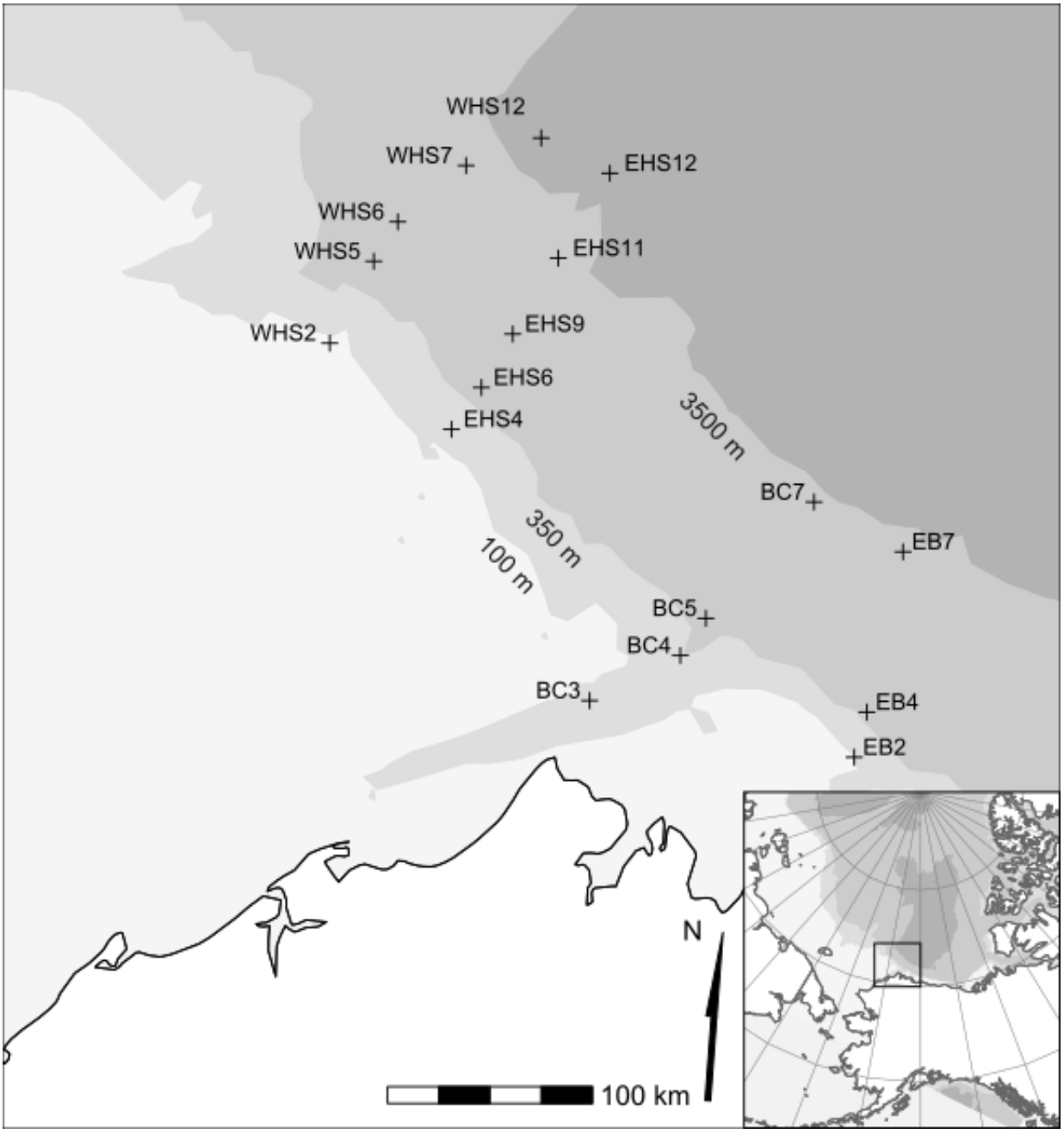

Figure 1: Location chart showing the approximate position of the sample location along four transects. EB: East Barrow; BC: Barrow Canyon; EHS: East Hanna Shoal; WHS: West Hanna Shoal

Experimental Methods

Study area and sediment sampling

The study area is composed of portions of the continental shelf, slope and basin of the north eastern Chukchi Sea and the adjacent western Beaufort Sea (Fig1). These areas fall into the less productive, eastern part of the Chukchi. Phytoplankton primary productivity is generally lower than in the Northern Chukchi at $50gm^{-2}a^{-1}C$ (Macdonald et al., 1987; Carmack et al., 2004), but local productivity can nevertheless be high; for example, heightened primary productivity of $430gm^{-2}a^{-1}C$ has been observed in Barrow Canyon (Hill et al., 2005). Terrestrial inputs from riverine discharge are higher owing to the influence of the Mackenzie River and proximity to the coast. The Mackenzie dominates terrestrial supply to the Beaufort Sea, discharging $3.3x10^{11}m^3a^{-1}$ water and $2.1Mta^{-1}$ POC (Macdonald et al., 1998). In comparison, minor rivers deliver $1.45Mta^{-1}$ sediment and $0.02Mta^{-1}$ POC (Macdonald et al., 1998). Although the Mackenzie is to the east of the Alaskan shelf, ice rafting data (Eicken et al., 2005) and neodymium isotope analyses from the Colville delta (Schreiner et al., 2013) suggest that material from the Mackenzie does reach the Chukchi and Western Beaufort shelves. Coastal erosion supplies $5.6Mta^{-1}$ sediment and between $0.06Mta^{-1}$ and $0.3Mta^{-1}$TOC (Hill et al., 1991, Macdonald et al., 1998). In the Alaskan Beaufort sector the Colville River is the most significant river, discharging $16x10^9m^3a^{-1}$ (Arnborg et al., 1966) and $1.7x10^{-4}Mta^{-1}C$ (Schell, 1983) from its watershed in the Brooks Mountain Range.

As part of the Shelf Basins Interactions Program (SBI), samples were selected from four shelf-to-basin transects. Samples from east of Barrow Canyon (henceforth EB) were collected between July and August 2002. Those from Barrow Canyon (BC), east of Hanna Shoal (EHS) and west of Hanna Shoal (WHS) were collected during May and June 2002, with the exception of EHS-12 and WHS-12, which were collected in July and August 2004. The sediment cores were taken with a Pouliot box corer with an area of $0.06m^2$. The outer edges of the cores were then discarded and the remaining portion was sectioned by 1cm intervals for the first 10cm, and every 2cm thereafter. The

subsamples were then stored aboard ship at -20°C in pre-cleaned plastic or glass I-Chem jars with Teflon lined lids until further processing on shore.

Bulk Sediment Analysis for Carbon and Nitrogen Isotopes and %C, %N

The sediment samples were thawed, homogenized, dried and then treated with 40% HCl in order to remove carbonates. Samples were then oven-dried at 60°C overnight. Isotope analysis of the dried, acidified samples was performed under continuous flow with a Carlo Erba Elemental Analyzer coupled to a Micromass Optima Isotope Ratio Mass Spectrometer (Manchester, UK). Analyses of carbon and nitrogen samples were accomplished with a single combustion, using a dual furnace system consisting of an oxidation furnace at 1020°C and a reduction furnace at 650°C. The resulting gases were chemically dried and separated using gas chromatography before introduction in the mass spectrometer source.

Isotope ratios are reported in δ notation as ‰ variations from the relevant standard:

$$\delta_{sample}{}^{N}E\ (‰) = (R_{sample}/R_{standard} - 1) \times 1000$$

where $\delta_{sample}{}^{N}E$ is the isotope composition of the sample with the heavy isotope (N) of the element, E; R is the abundance ratio of the heavy to light isotopes ($^{13}C/^{12}C$ or $^{15}N/^{14}N$) of that element. Samples are measured against carbon dioxide and nitrogen laboratory standards which had been calibrated against NBS22 and atmospheric N_2, respectively. Carbon values were corrected for mass overlap with isotopes of oxygen. Measurement reproducibility is typically better than ±0.2‰ for carbon and nitrogen. $\delta^{15}N$ was essentially unchanged for a subsample of unacidified sediments. Elemental compositions for carbon and nitrogen were obtained using a thermal conductivity detector. The C:N ratios are calculated on an atomic basis.

Bayesian isotope mixing analysis

Owing to the difficulty of establishing marine end members, as well as the likelihood of a greater than binary end member mixture, a Bayesian approach was preferred over standard mixing models. This approach enabled the estimation of the proportional contribution of sea ice algae, pelagic phytoplankton and terrestrial organic matter as probability distributions. The Bayesian analysis was performed using the software package SIAR (Stable Isotope Analysis in R) (Parnell et al., 2010). We assumed that no isotope discrimination occurred between the source and incorporation into the surface sediment. We also assumed that the end members selected reflected primary production in the water column and sea ice, and terrestrial organic matter for the entire region covered by the study (Table 2). Means and the 25-75th and 5-95th percentiles of the probability distributions were reported for the contribution of each end member.

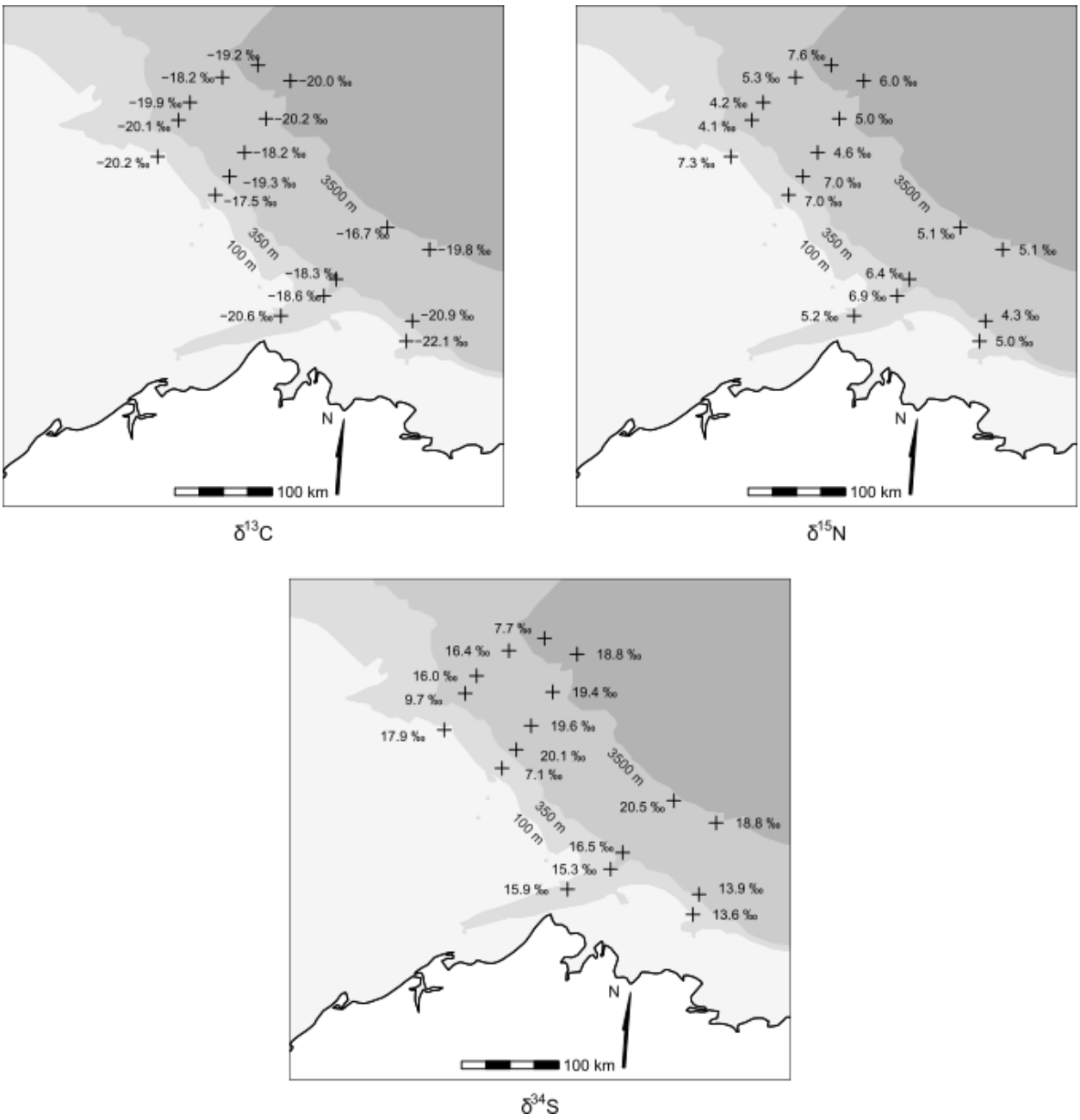

Figure 2: Location chart displaying surface $\delta^{13}C$, $\delta^{15}N$ and $\delta^{34}S$ of sample sites

Results

Surface Sediments

In surface sediments in this study (Table 1, Fig 2), TOC was comparable to other Arctic sediments (Fahl and Stein, 1997) and ranged from 0.67% to 1.87%, with a mean of 1.25%. TOC was generally lower in the Hanna Shoal transects (WHS, EHS) than those around Barrow Canyon (BC, EB), with the WHS transect having the lowest overall carbon content at approximately 1%. The station closest to the shore had the lowest %TOC of each transect except in the case of EHS, where the site located in the Canada Basin had a very low %TOC of 0.67%. Linear regression of TOC/total N was used to estimate the proportion of bound inorganic nitrogen (Schubert, 2001). It was found that the samples contained little bound nitrogen (under 0.01%), except for the EHS12 site, where the bound %N was 0.12% (Schubert, 2001). The %N co-varied closely with TOC. C:N ratios ranged from 7.3 to 11.5, with a mean of 9.1. The EHS12 core top was an exception, with high bound N resulting in an anomalously low C:N ratio of 5.3.

The sediments were generally enriched in ^{13}C when compared to other reported surface sediments from the region (Naidu, 2000; Ruttenberg and Goñi, 1997) ranging from -22.1 to -16.7‰, with a mean of -19.4‰. While consistently ^{13}C enriched, these data are within the bounds of previously reported data (Naidu et al., 1993). A general east – west trend in ^{13}C enrichment was observed in the surface cores, with the EB transect most ^{13}C depleted. The $\delta^{13}C$ of the sediments also tended to be greater in the slope and basin stations and more depleted on the shelf. The Barrow Canyon transect, a region of higher primary productivity, was highly enriched in ^{13}C. The $\delta^{15}N$ ranged from 5.1 to 6.9‰, with a mean of 5.7‰. The two surface sediment samples from the Southern Chukchi (STN locations) fit the general pattern with enriched mean $\delta^{13}C$ (-19.2‰) and mean $\delta^{15}N$ (6.2‰) (Table 1). The C:N ratio for STN1 was 8.8, while for STN2 it was 8.6.

Sediment Cores

Seven locations were analyzed beyond the surface sample, including: EB2, EB4, EB7, EHS4, EHS6, EHS12 and WHS12 (Table 3) [Approximate location of Fig 3-5]. In the EHS4 (Fig 4) and WHS12 (Fig 5) cores, a trend to depletion in ^{13}C was observed down

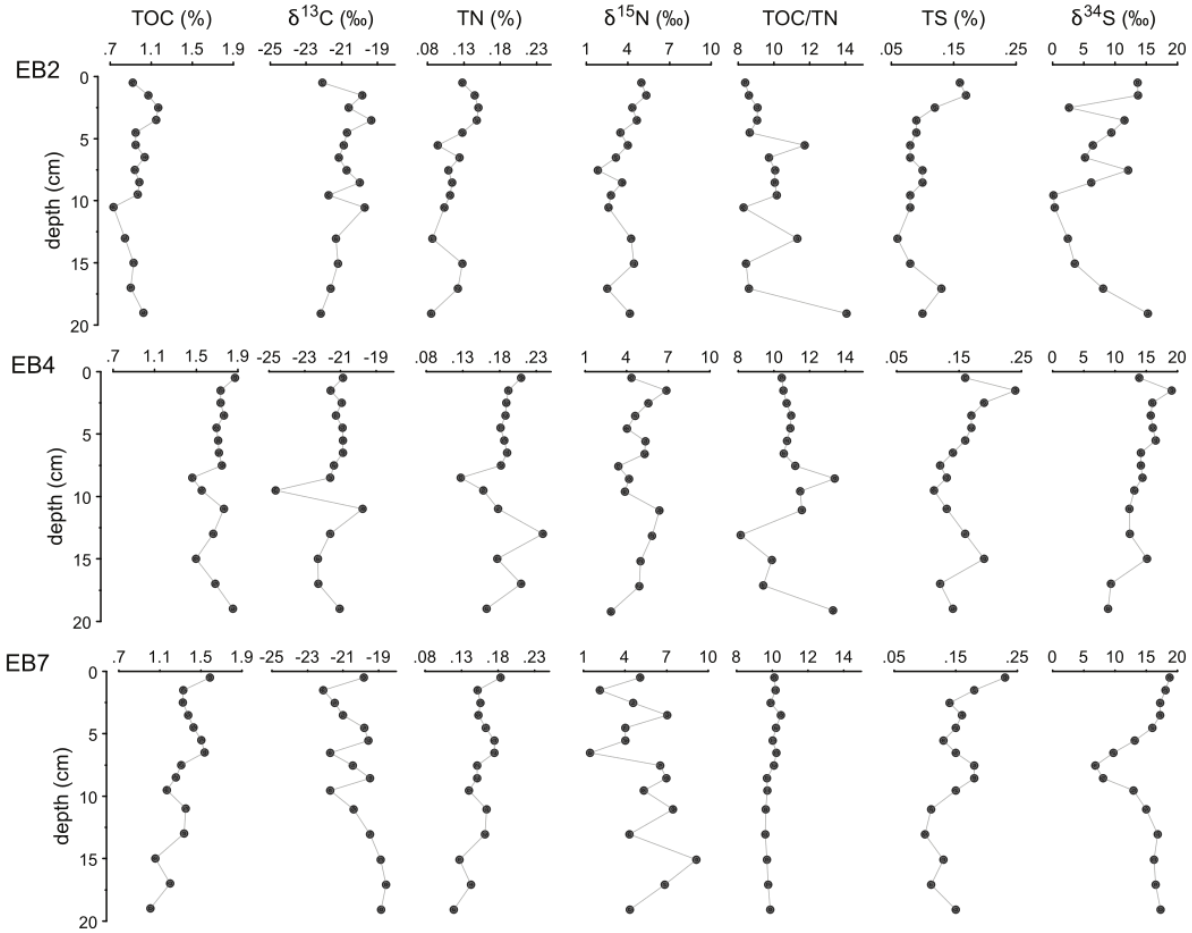

Figure 3: Down core TOC, $\delta^{13}C$, TN, $\delta^{15}N$, TOC/TN (atomic), TS and $\delta^{34}S$ compositions of the East Barrow transect sites, from shelf to basin

core. In EB2 (Fig 3), EB4 (Fig 3), EHS 6 (Fig 4) and EHS12 (Fig 4), little variation exists in $\delta^{13}C$ values downcore. EB7 (Fig 3) was more depleted at the surface than at depth.

Cores EB2 and EB4 (Fig 3) had relatively consistent C:N in the upper 10cm section; typically 9 and 10.5, respectively, while the lower core section showed greater

variability, ranging from 8.1 to 14.1. EB7, EHS4 and EHS6 displayed little downcore variation, with C:N between 9.6 and 10.5, 6.8 and 8.7 and 8.2 and 10.5 respectively. Likewise, the upper 10cm of WHS12 trended from 7.2 at the surface to 8.6. The lower 14cm of the core varied between 3.4 and 8.5, with excursions to higher C:N ratios around 10 in the 16-18cm and 18-20cm samples. Core EHS12 displayed a very distinct trend towards higher C:N ratios downcore, from 5.3 in the surface sediments to 10.8 in the 28-30cm section of the core.

Cores EB2 and EHS4 were more ^{15}N depleted downcore. This depletion was greatest in EHS4, with the 0-1, 1-2 and 2-3cm sections most enriched at 8.0‰, compared with a mean of 4.8‰ for the three lowest sections. The EB2 core changed from 5.0‰ in the surface section to 1.8‰ within the core. EHS12 and WHS12 also reflected this trend to $\delta^{15}N$ depletion in downcore sections. EHS6 had a very consistent $\delta^{15}N$, typically varying between 6.4‰ and 6.9‰ downcore. This more constant signal was punctuated by three excursions to around 8‰. Downcore sections from EB4 and EB7 did not show strong simple trends in $\delta^{15}N$.

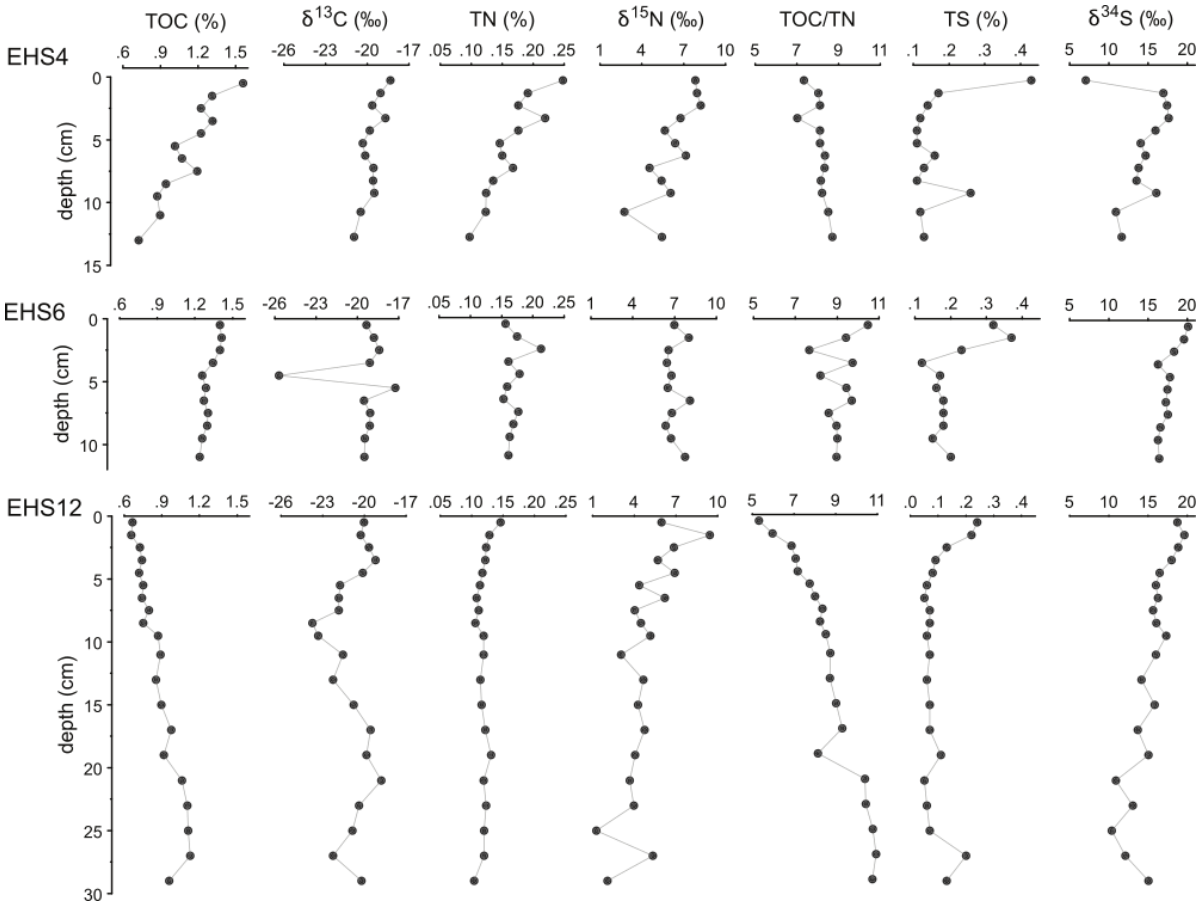

Figure 4: Down core, δ13C, TN, δ15N, TOC/TN (atomic), TS and δ34S compositions of the East Hanna Shoal transect sites, from shelf to basin

In general, the % TOC decreased slowly downcore. EHS4 and WHS12 showed the greatest declines, from 1.56% TOC to 0.72% TOC, and from 0.93% TOC to 0.11% TOC, respectively. In the case of EB2 and EB4, % TOC remained more constant and around 0.92% and 1.70%, respectively. The %N decreased downcore in every core except EHS6, which remained stable around 0.15%, and EHS12, where a decreasing trend in the upper 10cm of the core was followed by a steady %N of 0.12%.

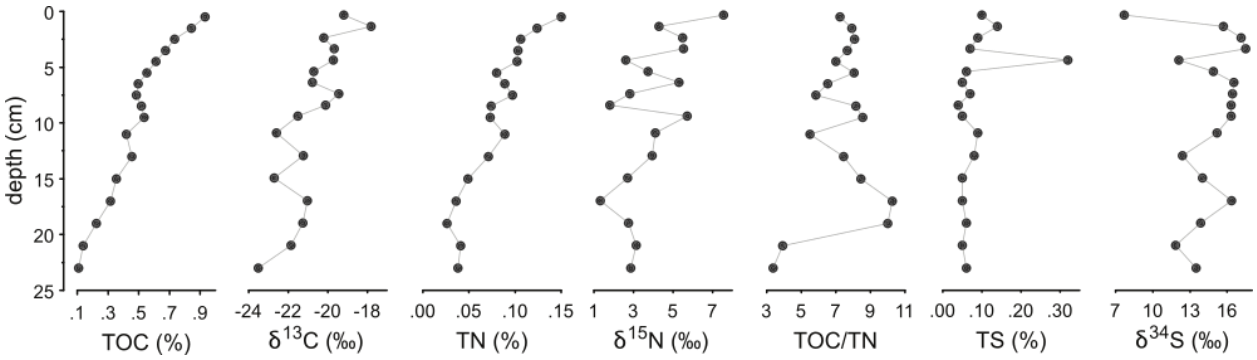

Figure 5: Down core, $\delta^{13}C$, TN, $\delta^{15}N$, TOC/TN (atomic), TS and $\delta^{34}S$ of the West Hanna Shoal transect sites, from shelf to basin

Discussion

In general, surface sediments were more enriched in $\delta^{13}C$ than those reported by previous studies on the Beaufort and Chukchi Seas e.g. (Baskaran and Naidu, 1995; Goñi, 2000; Naidu, 2000), and also more enriched than has been reported in other Arctic sectors e.g. (Fernandes and Sicre, 2000; Gaye et al., 2007). The %C in the surface sediments was between 0.67% and 1.87%, with a trend to decreasing organic carbon content in a westerly direction. The Hanna Shoal samples were consistently poorer in organic carbon than those from Barrow Canyon or from the Southern Chukchi. A likely source of this discrepancy is lower overlying primary productivity in this region due to the lower pre-bloom nitrate concentrations around Hanna Shoal (Bates et al., 2005a).

The ^{13}C enrichment observed could be due to the influence of a third, more enriched end member or low terrestrial contributions. Marine macroalgae (Nilsen et al., 2008) or ice algae (Hobson et al., 1995) are potential sources of enriched carbon; this would imply far greater supply of these materials and a greater role for them in the carbon cycle than has been previously suggested. For example, Gradinger (2009) reported a sea ice algal contribution of 1-2$gCm^{-2}a^{-1}$ to primary productivity, which only amounts to between 0.25% and 0.4% (Grebmeier et al., 2006) of the total phytoplankton productivity in the Chukchi. While intact material from sea ice algal blooms reaches the sea bed

(Gradinger and Bluhm, 2004), and such an end member could address the carbon isotope values observed and balance the terrestrial contributions, it seems likely that sea ice algal productivity could not be sufficiently dominant to shift the total bulk carbon to enriched values in such a decisive manner.

We suggest that a likely explanation is that the carbon isotope signal is not primarily due to a binary mixture of ice algal and terrestrial sources, but rather to additional seasonal and regional changes in the carbon contribution and isotope signature of the local marine water column phytoplankton productivity. The enriched sedimentary $\delta^{13}C$ observed in our samples fits with an east-west trend to depleted ^{13}C in the east that has been previously reported for the Beaufort Sea (Saupe et al., 1989). Furthermore, there is evidence for considerable seasonal variation in algal $\delta^{13}C$. Particulate organic matter (POM) during spring blooms can show significant enrichment in ^{13}C (Cifuentes et al., 1988; Tremblay et al., 2006). The community composition of the bloom may also be important; diatoms are a major component of the spring bloom in the Chukchi and Beaufort Seas (Sukhanova et al., 2009), and have been observed in significant under ice blooms (Arrigo et al., 2012). Diatoms have been reported to be more strongly enriched in ^{13}C than other phytoplankton (Fry and Wainright, 1991). Since water column primary productivity is tightly linked with the benthos and is not remineralized in the upper water column (Grebmeier et al., 1988), this material can then be stored in the sediments. We therefore suggest that the diatom-rich spring bloom is the most likely source of highly enriched ^{13}C in our study area.

Furthermore, other parameters supplied no convincing evidence of high terrestrial inputs. The C:N ratios reported for this area can all be broadly classified as marine, and are similar to previously reported values (Feder et al., 1994). C:N ratios above 12 have been reported for sea ice algae (Gradinger et al., 2009, Leu et al., 2010), and also for water column POM in the Northeast Water polynya (Bauerfeind et al., 1997); the C:N

ratios we report are lower than this. Consequently, we suggest that sites with higher C:N ratios could reflect contributions from low-quality, N-poor algal matter rather than high C:N terrestrial debris.

Nitrogen data further support the marine character of the sites studied. With the $\delta^{15}N$ of local terrestrial material from the Yukon River at 0.8‰±0.5 (Guo and Macdonald, 2006) and $\delta^{15}N$ for phytoplankton of 4.6‰±1.6 (Goering et al., 1990), very few of the surface sediments studied show any sign of high terrestrial nitrogen supply. We propose that the $\delta^{15}N$ signature of the surface sediments reflects the average local NO_3^- concentration and utilization (Altabet et al., 1995). Although sedimentary $\delta^{15}N$ incorporates changes in terrestrial supply, sea ice algal production and advection of POM from other areas, these are likely obscured by the variability of the marine signal.

The NO_3^- concentration of the Chukchi was both spatially and temporally variable in spring 2002. Prior to the bloom, NO_3^- in surface waters ranged from under 0.2μMkg^{-1} in the basin sites (WHS12, EHS12), to 15μMkg^{-1} in the Southern Chukchi (Bates et al., 2005a). NO_3^- concentrations in surface waters were not uniform; the pre-bloom NO_3^- concentration decreased from shelf to basin for the WHS and EHS transects, although the decrease in NO_3^- was not as pronounced in the Barrow Canyon transect. Post-bloom, dissolved NO_3^- was under 0.2μMkg^{-1} at all sites. It follows then, that some of the most enriched sedimentary $\delta^{15}N$ values were observed at shelf sites, such as STN1, STN2, EHS4 and WHS2. The shelves are where the highest productivity, springtime NO_3^- concentrations and the most intense and earliest spring blooms occur. At these locations, heightened NO_3^- utilization may lead to the relatively enriched $\delta^{15}N$ signals in the sediments. Continental slope $\delta^{15}N$ values are generally less enriched, despite lower NO_3^- concentrations, implying that primary productivity is not as intense there (Bates et al., 2005b). The basin sites, WHS12 and EHS12, have higher $\delta^{15}N$ of 7.6‰ and 6.0‰ respectively. These sites are in water depths of 3758m and 3887m respectively and are

not highly productive, which is reflected in the relatively low carbon content of these sites: 0.93% and 0.67% respectively. These sites may be affected by the advection of ^{15}N enriched organic matter from more productive areas. The difference between these two, ostensibly similar, sites could be due to the effects of Hanna Shoal. Currents flow northeast and southeast of Hanna Shoal (Weingartner et al., 2005); WHS12 could receive advected material from the highly productive Bering Sea, whereas EHS12 could be more influenced by the less productive Arctic Coastal Water.

Bayesian Isotope Mixing Model

The central issue for the development of an input budget is the reliability of the marine endmembers, because mixing models could then be used to calculate what proportion of the organic matter stored in Arctic sediments is of terrestrial origin. The marine signal has proven to be highly variable, both spatially and temporally, in $\delta^{13}C$, $\delta^{15}N$ and C:N. For example, C:N ratios above 12 have been reported for sea ice algae (Gradinger et al., 2009, Leu et al., 2010), and also for water column POM in the Northeast Water polynya (Bauerfeind et al., 1997). Gradinger et al., (2009) also observed pre-bloom water column phytoplankton with a $\delta^{13}C$ of around -26‰, which is very close to terrestrial plants. The $\delta^{15}N$ in the sediments can also be dependent on the rate and extent of NO_3^- usage, as well as the $\delta^{15}N$ of the NO_3^- itself (Altabet et al., 1995), leading to great variability in sea ice algal and water column phytoplankton $\delta^{15}N$ signals. Consequently, one can suggest that a portion of the observed variability in the bulk measures of our samples may be attributed to marine productivity.

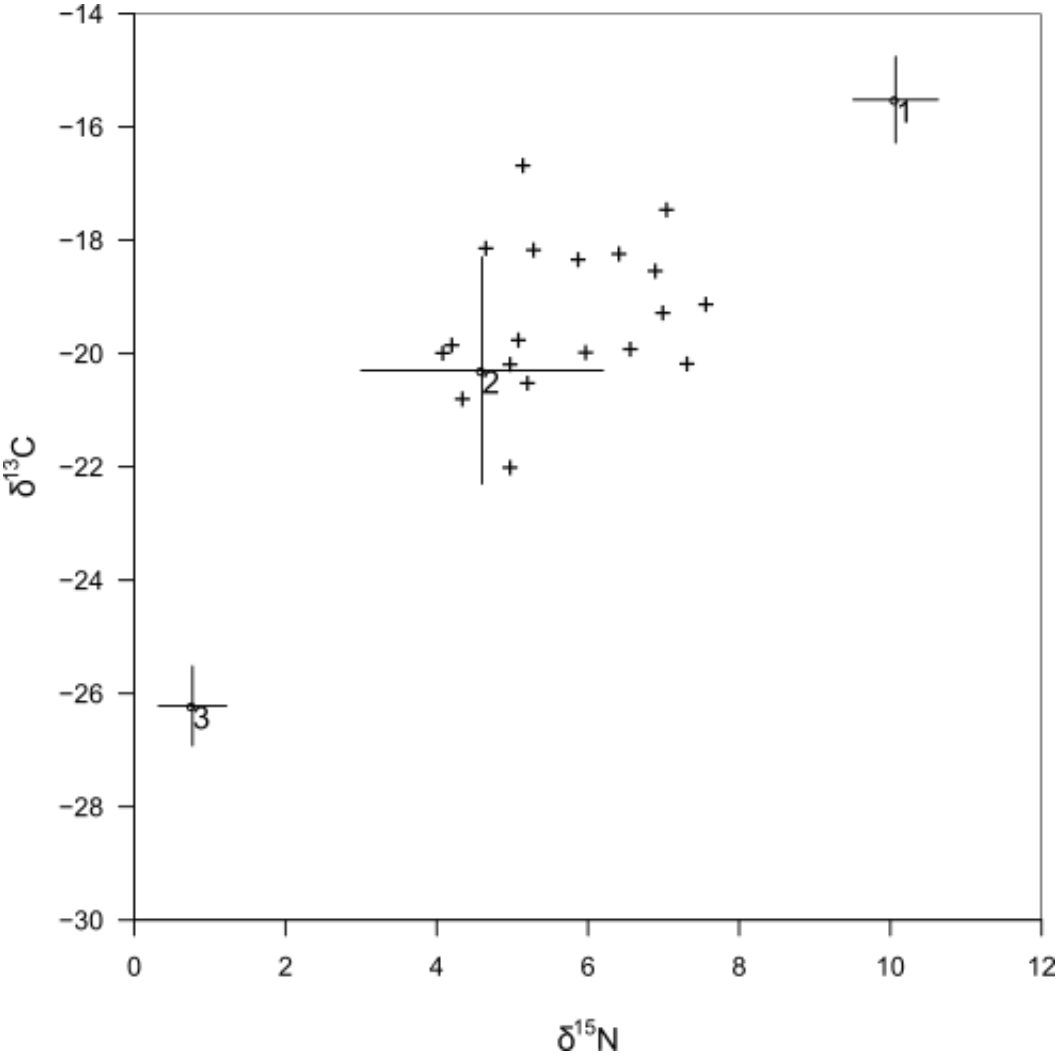

Figure 6: Western Arctic Ocean surface sediment $\delta^{13}C$ and $\delta^{15}N$ composition. Water column phytoplankton (1), Sea ice algae (2) and Terrestrial (3) end member mean $\delta^{13}C$ and $\delta^{15}N$ are plotted, including one standard deviation. + indicates surface sample data

In the Arctic, with known variability in $\delta^{13}C$, $\delta^{15}N$ and C:N ratios, obtaining a reliable estimate of the ratio of terrestrial to marine supply from two endmembered mixing models is difficult. In order to accommodate uncertainty in the endmembers, a Bayesian approach was employed, utilizing the software package SIAR (Stable Isotope Analysis in R) instead of linear mixing models. The Bayesian model incorporates uncertainties in the endmembers into the probability distributions it generates (Table 2). The terrestrial endmember was taken from Yukon River POC (Guo and Macdonald, 2006). The sea ice algal data were taken from Gradinger et al. (2009), with the May bloom data taken as

representative of the bulk of ice algal material deposited to the sediments. The water column phytoplankton $\delta^{13}C$ endmember was set

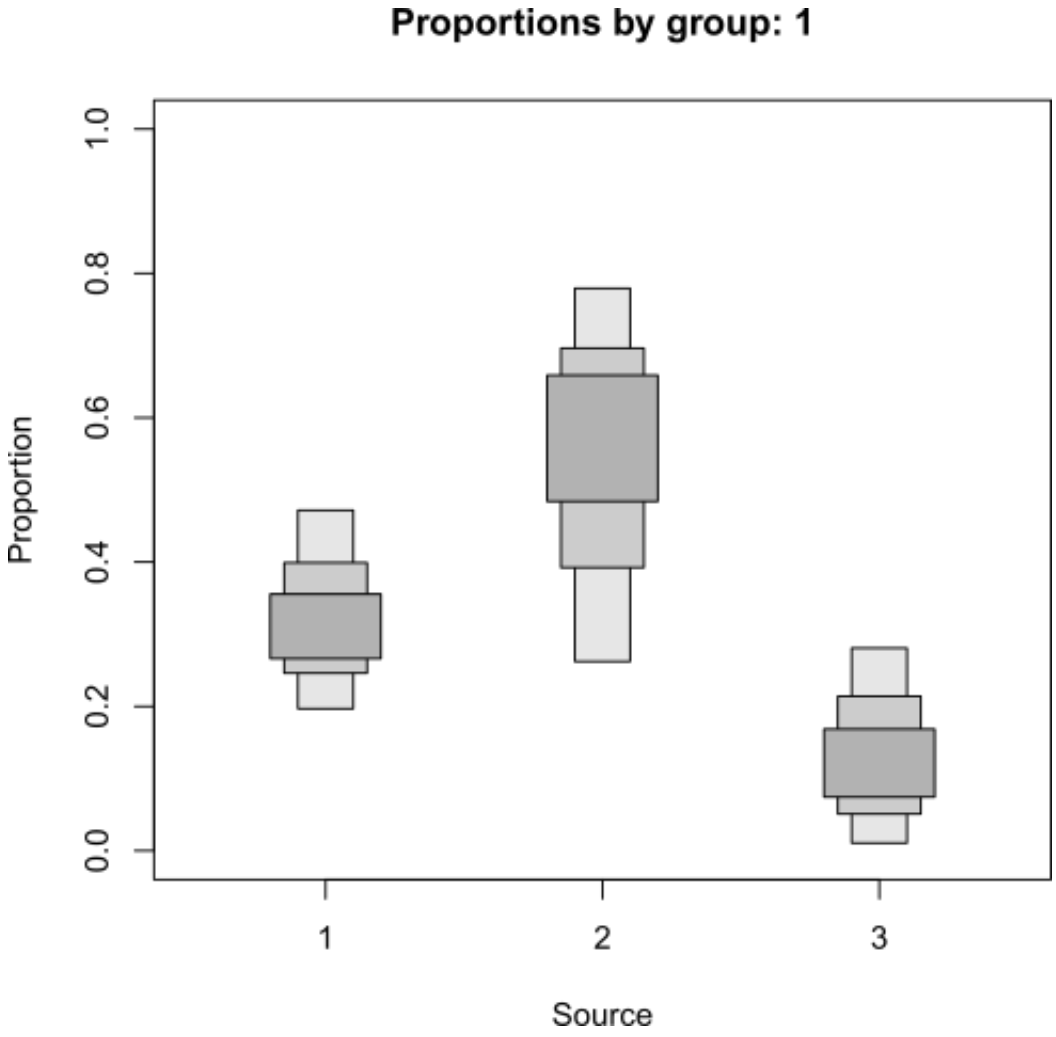

Figure 7: Proportion of surface sediment organic matter by source determined by Bayesian analysis, showing 25, 75 and 95% credibility intervals. 1: Water column phytoplankton; 2: Sea ice algae; 3: Terrestrial

at -20.3±2‰, based upon spring bloom data from Goering et al. (1990). This value is consistent with previous Chukchi studies (Naidu, 2000; Belicka and Harvey, 2009) and with the expected ^{13}C enrichment of diatom-rich spring bloom POM. After performing the Bayesian analysis (Fig 6, Fig 7) on the Chukchi and Beaufort core tops, the probability distribution (95th percentile) for the three organic material sources was that

5-15% of the organic matter buried in the sediments is terrestrial; 25-35% is derived from sea ice algal production and 50-70% is derived from phytoplankton productivity in the water column. The core top samples are plotted with the endmembers in Fig 6. All of the core samples either fall within two standard deviations of the pelagic phytoplankton endmember, or are between it and the sea ice algal endmember. There is no indication of a strong terrestrial contribution unless there is also an equally strong sea ice algal contribution. This solution seems unlikely as it would require much higher sea ice algal productivity and preservation than recent studies (e.g. Gradinger, 2009) have suggested.

Although use of Bayesian methods helps to avoid some of the weaknesses of two endmembered mixing models, these techniques are not without their own problems. First among these difficulties is the lack of a comprehensive isotope data set. Changes to the endmember values or their standard deviations can cause significant shifts in the probability distributions. As more data become available, improved endmember reliability would enable the development of more robust contribution estimates. It is also difficult to separate sources that are relatively similar in the model. Accordingly, the difference between terrestrial and marine sources is more reliable than the difference between sea ice algae and water column algae, as these two components are much closer (in carbon and nitrogen isotopes) to each other than they are to terrestrial organic matter.

Conclusions

Using end members matched to both the region and expected season of deposition, we have attempted to cope with variability in Arctic end members by utilizing a Bayesian model to predict the proportions of organic carbon supplied to the NE Chukchi and W Beaufort by sea ice algae, phytoplankton in the water column and terrestrial sources.

While it is difficult to have end members for simple mixing models that are valid for all regions of the Arctic Ocean, since the water column phytoplankton signal seems to be both regionally and temporally variable, we suggest that, at least for surface sediments, terrestrial inputs are not a major component of the organic matter buried in this region. The low proportion reported based on bulk measurements is in contrast to biomarker estimates. As a result, we suggest that biomarker estimates of terrestrial contributions may be overestimating the influence of terrestrial supply to the carbon cycle of the Arctic Ocean and that the majority of organic carbon buried in the Chukchi and Western Beaufort Seas is autochthonous.

Acknowledgements: This work was supported by the Arctic Natural Sciences Program of the National Science Foundation, grant ARC-0612580. We thank HR Harvey and LL Belicka of the University of Maryland Chesapeake Biological Laboratory for providing bulk sediment samples and Michael Tuite of the University of Virginia for his invaluable assistance.

Altabet, M., Francois, R., Murray, D., Prell, W., 1995. Climate-related variations in denitrification in the Arabian Sea from sediment $^{15}N/^{14}N$ ratios. Nature 373, 506–509.

Are, F., Reimnitz, E., Grigoriev, M., Hubberten, H., Rachold, V., 2008. The Influence of Cryogenic Processes on the Erosional Arctic Shoreface. J. Coast. Res. 24, 110–121. doi:10.2112/05-0573.1

Arnborg, L., Walker, H.J., Peippo, J., 1966. Water Discharge in the Colville River, 1962. Geogr. Ann. Ser. A, Phys. Geogr. 48, 195–210.

Arrigo, K.R., Perovich, D.K., Pickart, R.S., Brown, Z.W., van Dijken, G.L., Lowry, K.E., Mills, M.M., Palmer, M.A., Balch, W.M., Bahr, F., Bates, N.R., Benitez-Nelson, C., Bowler, B., Brownlee, E., Ehn, J.K., Frey, K.E., Garley, R., Laney, S.R., Lubelczyk, L., Mathis, J., Matsuoka, A., Mitchell, B.G., Moore, G.W.K., Ortega-Retuerta, E., Pal, S., Polashenski, C.M., Reynolds, R.A., Schieber, B., Sosik, H.M., Stephens, M., Swift, J.H., 2012. Massive Phytoplankton Blooms Under Arctic Sea Ice. Science 16, 409–422. doi:10.1126/science.1215065

Baskaran, M., Naidu, A.S., 1995. ^{210}Pb-derived chronology and the fluxes of ^{210}Pb and ^{137}Cs isotopes into continental shelf sediments, East Chukchi Sea, Alaskan Arctic. Geochim. Cosmochim. Acta 59, 4435–4448.

Bates, N., Best, M., Hansell, D., 2005a. Spatio-temporal distribution of dissolved inorganic carbon and net community production in the Chukchi and Beaufort Seas. Deep Sea Res. Part II Top. Stud. Oceanogr. 52, 3303–3323. doi:10.1016/j.dsr2.2005.10.005

Bates, N., Hansell, D., Bradley Moran, S., Codispoti, L., 2005b. Seasonal and spatial distribution of particulate organic matter (POM) in the Chukchi and Beaufort Seas. Deep Sea Res. Part II Top. Stud. Oceanogr. 52, 3324–3343. doi:10.1016/j.dsr2.2005.10.003

Bauerfeind, E., Garrity, C., Krumbholz, M., Ramseier, R., Voss, M., 1997. Seasonal variability of sediment trap collections in the Northeast Water polynya. Part 2. Biochemical and microscopic composition of sedimenting matter. J. Mar. Syst. 10, 371–389.

Belicka, L.L., Harvey, H.R., 2009. The sequestration of terrestrial organic carbon in Arctic Ocean sediments: A comparison of methods and implications for regional carbon budgets. Geochim. Cosmochim. Acta 73, 6231–6248. doi:10.1016/j.gca.2009.07.020

Belicka, L.L., MacDonald, R.W., Yunker, M.B., Harvey, H.R., 2004. The role of depositional regime on carbon transport and preservation in Arctic Ocean sediments. Mar. Chem. 86, 65–88.

Carmack, E.C., MacDonald, R.W., Jasper, S., 2004. Phytoplankton productivity on the Canadian Shelf of the Beaufort Sea. Mar. Ecol. Prog. Ser. 277, 37–50.

Cifuentes, A.L.A., Sharp, J.H., Fogel, M.L., Cifuentes, L.A., Fogel, L., 1988. Stable Carbon and Nitrogen Isotope Biogeochemistry in the Delaware Estuary. Limnol. Oceanogr. 33, 1102–1115.

Dou, F., Yu, X., Ping, C., Michaelson, G., Guo, L., Jorgenson, T., 2010. Spatial variation of tundra soil organic carbon along the coastline of northern Alaska. Geoderma 154, 328–335. doi:10.1016/j.geoderma.2009.10.020

Drenzek, N.J., Montluçon, D.B., Yunker, M.B., Macdonald, R.W., Eglinton, T.I., 2007. Constraints on the origin of sedimentary organic carbon in the Beaufort Sea from coupled molecular ^{13}C and ^{14}C measurements. Mar. Chem. 103, 146 – 162. doi:10.1016/j.marchem.2006.06.017

Dunton, K., Saupe, S., Golikov, A., Schell, D., Schonberg, S., 1989. Trophic relationships and isotopic gradients among arctic and subarctic marine fauna. Mar. Ecol. Prog. Ser. 56, 89–97. doi:10.3354/meps056089

Eicken, H., Gradinger, R., Gaylord, A., Mahoney, A., Rigor, I., Melling, H., 2005. Sediment transport by sea ice in the Chukchi and Beaufort Seas: Increasing importance due to changing ice conditions ? Deep. Res. 52, 3281–3302. doi:10.1016/j.dsr2.2005.10.006

Fahl, K., Stein, R., 1997. Modern organic carbon deposition in the Laptev Sea and the adjacent continental slope: surface water productivity vs. terrigenous input. Methods 26, 379–390.

Feder, H.M., Naidu, A.S., Jewett, S.C., Hameedi, J.M., Johnson, W.R., Whitledge, T.E., 1994. The northeastern Chukchi Sea: benthos-environmental interactions. Mar. Ecol. Prog. Ser. 111, 171–190. doi:10.3354/meps111171

Fernandes, M.B., Sicre, M., 2000. The importance of terrestrial organic carbon inputs on Kara Sea shelves as revealed by n-alkanes, OC and $\delta^{13}C$ values. Org. Geochem. 31, 363–374. doi:10.1016/S0146-6380(00)00006-1

Fortier, M., Fortier, L., Michel, C., Legendre, L., 2002. Climatic and biological forcing of the vertical flux of biogenic particles under seasonal Arctic sea ice. Mar. Ecol. Prog. Ser. 225, 1–16.

Fry, B., Wainright, S.C., 1991. Diatom sources of ^{13}C-rich carbon in marine food webs. Mar. Ecol. Prog. Ser. 76, 149–157.

Gaye, B., Fahl, K., Kodina, L., Lahajnar, N., Nagel, B., Unger, D., Gebhardt, A., 2007. Particulate matter fluxes in the southern and central Kara Sea compared to sediments: Bulk fluxes, amino acids, stable carbon and nitrogen isotopes, sterols and fatty acids. Cont. Shelf Res. 27, 2570–2594. doi:10.1016/j.csr.2007.07.003

Goering, J., Alexander, V., Haubenstock, N., 1990. Seasonal variability of stable carbon and nitrogen isotope ratios of organisms in a North Pacific Bay. Estuar. Coast. Shelf Sci. 30, 239–260. doi:10.1016/0272-7714(90)90050-2

Goñi, M.A., 2000. Distribution and sources of organic biomarkers in arctic sediments from the Mackenzie River and Beaufort Shelf. Mar. Chem. 71, 23–51. doi:10.1016/S0304-4203(00)00037-2

Goñi, M.A., O'Connor, A.E., Kuzyk, Z.Z., Yunker, M.B., Gobeil, C., Macdonald, R.W., 2013. Distribution and sources of organic matter in surface marine sediments across the North American Arctic margin. J. Geophys. Res. Ocean. 118, 4017–4035. doi:10.1002/jgrc.20286

Goñi, M.A., Yunker, M.B., Macdonald, R.W., Eglinton, T.I., 2005. The supply and preservation of ancient and modern components of organic carbon in the Canadian Beaufort Shelf of the Arctic Ocean. Mar. Chem. 93, 53 – 73. doi:10.1016/j.marchem.2004.08.001

Gorham, E., 1991. Northern Peatlands: Role in the Carbon Cycle and Probable Responses to Climatic Warming. Ecol. Appl. 1, 182–195.

Gradinger, R., 2009. Sea-ice algae: Major contributors to primary production and algal biomass in the Chukchi and Beaufort Seas during May/June 2002. Deep Sea Res. Part II Top. Stud. Oceanogr. 56, 1201–1212. doi:10.1016/j.dsr2.2008.10.016

Gradinger, R., Bluhm, B., 2004. In-situ observations on the distribution and behavior of amphipods and Arctic cod (Boreogadus saida) under the sea ice of the High Arctic Canada Basin. Polar Biol. 27, 595–603. doi:10.1007/s00300-004-0630-4

Gradinger, R.R., Kaufman, M.R., Bluhm, B.A., 2009. Pivotal role of sea ice sediments in the seasonal development of near-shore Arctic fast ice biota. Mar. Ecol. Prog. Ser. 394, 49–63. doi:10.3354/meps08320

Grebmeier, J., Cooper, L., Feder, H., Sirenko, B., 2006. Ecosystem dynamics of the Pacific-influenced Northern Bering and Chukchi Seas in the Amerasian Arctic. Prog. Oceanogr. 71, 331–361. doi:10.1016/j.pocean.2006.10.001

Grebmeier, J.M., McRoy, C.P., Feder, H.M., 1988. Pelagic-benthic coupling on the shelf of the northern Bering and Chukchi Seas. I. Food supply source and benthic biomass. Mar. Ecol. Prog. Ser. 48, 57–67. doi:10.3354/meps048057

Grebmeier, J.M., Smith, W.O., Conover, R.J., 1995. Biological Processes on Arctic Continental Shelves: Ice-Ocean-Biotic Interactions, in: Arctic Oceanography: Marginal Ice Zones and Continental Shelves. American Geophysical Union, Washington, DC, pp. 231–262.

Grigoriev, M.N., Rachold, V., Hubberten, H.W., Schirrmeister, L., 2004. Organic carbon input to the Arctic Seas through coastal erosion, in: Stein, R., Macdonald, R. (Eds.), The Organic Carbon Cycle in the Arctic Ocean. Springer, Heidelberg, pp. 41–45.

Guo, L., MacDonald, R.W., 2006. Source and transport of terrigenous organic matter in the upper Yukon River: Evidence from isotope ($\delta^{13}C$, $\Delta^{14}C$, and $\delta^{15}N$) composition of dissolved, colloidal, and particulate phases. Global Biogeochem. Cycles 20, n/a–n/a. doi:10.1029/2005GB002593

Hansell, D., Whitledge, T., Goering, J., 1993. Patterns of nitrate utilization and new production over the Bering-Chukchi shelf. Cont. Shelf Res. 13, 601–627. doi:10.1016/0278-4343(93)90096-G

Hill, P., Blasco, S., Harper, J., Fissel, D., 1991. Sedimentation on the Canadian Beaufort Shelf. Cont. Shelf Res. 11, 821–842. doi:10.1016/0278-4343(91)90081-G

Hill, V., Cota, G., Stockwell, D., 2005. Spring and summer phytoplankton communities in the Chukchi and Eastern Beaufort Seas. Deep. Res. II 52, 3369–3385.

Hobson, K.A., Ambrose, W.G., Renaud, P.E., 1995. Sources of primary production, benthic-pelagic coupling, and trophic relationships within the Northeast Water Polynya: insights from $\delta^{13}C$ and $\delta^{15}N$ analysis. Mar. Ecol. Prog. Ser. 128, 1–10. doi:10.3354/meps128001

Hugelius, G., Bockheim, J.G., Camill, P., Elberling, B., Grosse, G., Harden, J.W., Johnson, K., Jorgenson, T., Koven, C.D., Kuhry, P., Michaelson, G., Mishra, U., Palmtag, J., Ping, C.-L., O'Donnell, J., Schirrmeister, L., Schuur, E.A.G., Sheng, Y., Smith, L.C., Strauss, J., Yu, Z., 2013. A new data set for estimating organic carbon storage to 3 m depth in soils of the northern circumpolar permafrost region. Earth Syst. Sci. Data 5, 393–402. doi:10.5194/essd-5-393-2013

Johannessen, O.M., 1999. Satellite Evidence for an Arctic Sea Ice Cover in Transformation. Science (80-.). 286, 1937–1939. doi:10.1126/science.286.5446.1937

Jorgenson, M., Brown, J., 2005. Classification of the Alaskan Beaufort Sea Coast and estimation of carbon and sediment inputs from coastal erosion. Geo-Marine Lett. 25, 69–80. doi:10.1007/s00367-004-0188-8

Legendre, L., Ackley, S., Dieckmann, G., Gulliksen, B., Horner, R., Hoshiai, T., Melnikov, I., Reeburgh, W., Spindler, M., Sullivan, C., 1992. Ecology of sea ice biota. Polar Biol. 12, 429–444. doi:10.1007/BF00243114

Leu, E., Wiktor, J., Søreide, J.E., Berge, J., 2010. Increased irradiance reduces food quality of sea ice algae. Mar. Ecol. Prog. Ser. 411, 49–60. doi:10.3354/meps08647

Macdonald, R.W., Solomon, S.M., Cranston, R.E., Welch, H.E., Yunker, M.B., Gobeil, C., 1998. A sediment and organic carbon budget for the Canadian Beaufort Shelf. Mar. Geol. 144, 255–273.

Macdonald, R.W., Wong, C.S., Erickson, P.E., 1987. The Distribution of Nutrients in the Southeastern Beaufort Sea: Implications for Water Circulation and Primary Production. J. Geophys. Res. 92, 2939–2952. doi:10.1029/JC092iC03p02939

Mars, J.C., Houseknecht, D.W., 2007. Quantitative remote sensing study indicates doubling of coastal erosion rate in past 50 yr along a segment of the Arctic coast of Alaska. Geology 35, 583–586. doi:10.1130/G23672A.1

McClelland, J.W., Déry, S.J., Peterson, B.J., Holmes, R.M., Wood, E.F., 2006. A pan-arctic evaluation of changes in river discharge during the latter half of the 20th century. Geophys. Res. Lett. 33, L06715. doi:10.1029/2006GL025753

Melling, H., 2000. Exchanges of fresh water through the shallow straits of the North American Arctic, in: Lewis, E.L., Jones, E.P., Lemke, P., Prowse, T.D., Wadhams, P. (Eds.), The Freshwater Budget of the Arctic Ocean. Springer, pp. 479–502.

Muenchow, A., Melling, H., Falkner, K., 2006. An Observational Estimate of Volume and Freshwater Flux Leaving the Arctic Ocean through Nares Strait. J. Phys. Oceanogr. 36, 2025–2041.

Naidu, A., Scalan, R., Feder, H., Goering, J., Hameedi, M., Parker, P., Behrens, E., Caughey, M., Jewett, S., 1993. Stable organic carbon isotopes in sediments of the north Bering-south Chukchi seas, Alaskan-Soviet Arctic Shelf. Cont. Shelf Res. 13, 669–691. doi:10.1016/0278-4343(93)90099-J

Naidu, A.S., 2000. Organic carbon isotope ratios ($\delta^{13}C$) of Arctic Amerasian continental shelf sediments. Int. J. Earth Sci. 89, 522–532.

Nilsen, M., Pedersen, T., Nilssen, E.M., Fredriksen, S., 2008. Trophic studies in a high-latitude fjord ecosystem - a comparison of stable isotope analyses ($\delta^{13}C$ and $\delta^{15}N$) and trophic-level estimates from a mass-balance model. Can. J. Fish. Aquat. Sci. 65, 2791–2806. doi:10.1139/F08-180

O'Brien, M.C., Macdonald, R.W., Melling, H., Iseki, K., 2006. Particle fluxes and geochemistry on the Canadian Beaufort Shelf: Implications for sediment transport and deposition. Cont. Shelf Res. 26, 41–81. doi:10.1016/j.csr.2005.09.007

Parnell, A.C., Inger, R., Bearhop, S., Jackson, A.L., 2010. Source partitioning using stable isotopes: coping with too much variation. PLoS One 5, e9672. doi:10.1371/journal.pone.0009672

Perovich, D.K., Richter-Menge, J.A., 2009. Loss of Sea Ice in the Arctic. Ann. Rev. Mar. Sci. 1, 417–441. doi:10.1146/annurev.marine.010908.163805

Peterson, B.J., Holmes, R.M., McClelland, J.W., Vörösmarty, C.J., Lammers, R.B., Shiklomanov, A.I., Shiklomanov, I.A., Rahmstorf, S., 2002. Increasing river discharge to the Arctic Ocean. Science 298, 2171–3. doi:10.1126/science.1077445

Rachold, V., Eicken, H., Gordeev, V., Grigoriev, M., Hubberten, H., Lisitzin, A., Shevchenko, V., Schirmeister, L., 2004. Modern Terrigenous Organic Carbon Input to the Arctic Ocean, in: Stein, R., Macdonald, R.W. (Eds.), The Organic Carbon Cycle in the Arctic Ocean. Springer, pp. 33–56.

Rachold, V., Grigoriev, M.N., Are, F.E., Solomon, S., Reimnitz, E., Kassens, H., Antonow, M., 2000. Coastal erosion vs riverine sediment discharge in the Arctic Shelf seas. Int. J. Earth Sci. 89, 450–460. doi:10.1007/s005310000113

Reimnitz, E., Are, F.E., 2000. Coastal Bluff and Shoreface Comparison over 34 Years Indicates Large Supply of Erosion Products to Arctic Seas. Polarforschung 68, 231 – 235.

Roach, A.T., Aagaard, K., Pease, C.H., Salo, S.A., Weingartner, T., Pavlov, V., Kulakov, M., 1995. Direct measurements of transport and water properties through the Bering Strait. J. Geophys. Res. 100, 18443–18457. doi:10.1029/95JC01673

Rudels, B., Jones, E.P., Schauer, U., Eriksson, P., 2004. Atlantic sources of the Arctic Ocean surface and halocline waters. Polar Res. 23, 181–208. doi:10.1111/j.1751-8369.2004.tb00007.x

Ruttenberg, K.C., Goñi, M., 1997. Phosphorus distribution, C:N:P ratios, and $\delta^{13}C_{oc}$ in arctic, temperate, and tropical coastal sediments: tools for characterizing bulk sedimentary organic matter. Mar. Geol. 139, 123–145.

Sakshaug, E., 2004. Primary and Secondary Production in the Arctic Seas, in: Stein, R., Macdonald, R. (Eds.), The Organic Carbon Cycle in the Arctic Ocean. Springer, pp. 57–82.

Saupe, S.M., Schell, D.M., Griffiths, W.B., 1989. Carbon-isotope ratio gradients in western arctic zooplankton. Mar. Biol. 103, 427–432. doi:10.1007/BF00399574

Schell, D.M., 1983. Carbon-13 and Carbon-14 Abundances in Alaskan Aquatic Organisms: Delayed Production from Peat in Arctic Food Webs. Science (80-.). 219, 1068–71. doi:10.1126/science.219.4588.1068

Schreiner, K.M., Bianchi, T.S., Eglinton, T.I., Allison, M.A., Hanna, A.J.M., 2013. Sources of terrigenous inputs to surface sediments of the Colville River Delta and Simpson's Lagoon, Beaufort Sea, Alaska. J. Geophys. Res. Biogeosciences 118, 808–824. doi:10.1002/jgrg.20065

Schreiner, K.M., Bianchi, T.S., Rosenheim, B.E., 2014. Evidence for permafrost thaw and transport from an Alaskan North Slope watershed. Geophys. Res. Lett. 41, 3117–3126. doi:10.1002/2014GL059514

Schubert, C., 2001. Nitrogen and carbon isotopic composition of marine and terrestrial organic matter in Arctic Ocean sediments: implications for nutrient utilization and organic matter composition. Deep Sea Res. Part I Oceanogr. Res. Pap. 48, 789–810. doi:10.1016/S0967-0637(00)00069-8

Shiklomanov, I.A., 1998. Comprehensive Assessment of the Freshwater Resources of the World: Assessment of Water Reources and Water Availability in the World. Geneva.

Springer, A., McRoy, C., 1993. The paradox of pelagic food webs in the northern Bering Sea—III. Patterns of primary production. Cont. Shelf Res. 13, 575–599. doi:10.1016/0278-4343(93)90095-F

Stabeno, P.J., Bond, N.A., Kachel, N.B., Salo, S.A., 2001. On the temporal variability of the physical environment over the south-eastern Bering Sea. Fish. Oceanogr. 10, 81–98.

Stein, R., Macdonald, R.W., 2004. The organic carbon cycle in the Arctic Ocean. Springer.

Sukhanova, I.N., Flint, M. V, Pautova, L.A., Stockwell, D.A., Grebmeier, J.M., Sergeeva, V.M., 2009. Phytoplankton of the western Arctic in the spring and summer of 2002: Structure and seasonal changes. Deep Sea Res. Part II Top. Stud. Oceanogr. 56, 1223–1236. doi:10.1016/j.dsr2.2008.12.030

Tesi, T., Semiletov, I., Hugelius, G., Dudarev, O., Kuhry, P., Gustafsson, Ö., 2014. Composition and fate of terrigenous organic matter along the Arctic land–ocean continuum in East Siberia: Insights from biomarkers and carbon isotopes. Geochim. Cosmochim. Acta 133, 235–256. doi:10.1016/j.gca.2014.02.045

Tolosa, I., Fiorini, S., Gasser, B., Martín, J., Miquel, J.C., 2013. Carbon sources in suspended particles and surface sediments from the Beaufort Sea revealed by molecular lipid biomarkers and compound-specific isotope analysis. Biogeosciences 10, 2061–2087. doi:10.5194/bg-10-2061-2013

Tremblay, J.-E., Michel, C., Hobson, K.A., Gosselin, M., Price, N.M., 2006. Bloom dynamics in early opening waters of the Arctic Ocean. Limnol. Oceanogr. 51, 900–912.

Vonk, J.E., Mann, P.J., Dowdy, K.L., Davydova, a, Davydov, S.P., Zimov, N., Spencer, R.G.M., Bulygina, E.B., Eglinton, T.I., Holmes, R.M., 2013. Dissolved organic carbon loss from Yedoma permafrost amplified by ice wedge thaw. Environ. Res. Lett. 8, 035023. doi:10.1088/1748-9326/8/3/035023

Vonk, J.E., Sánchez-García, L., van Dongen, B.E., Alling, V., Kosmach, D., Charkin, A, Semiletov, I.P., Dudarev, O. V, Shakhova, N., Roos, P., Eglinton, T.I., Andersson, A, Gustafsson, O., 2012. Activation of old carbon by erosion of coastal and subsea permafrost in Arctic Siberia. Nature 489, 137–40. doi:10.1038/nature11392

Walsh, J., Dieterle, D., Maslowski, W., Grebmeier, J., Whitledge, T., Flint, M., Sukhanova, I., Bates, N., Cota, G., Stockwell, D., 2005. A numerical model of seasonal primary production within the Chukchi/Beaufort Seas. Deep Sea Res. Part II Top. Stud. Oceanogr. 52, 3541–3576. doi:10.1016/j.dsr2.2005.09.009

Walsh, J.J., Dieterle, D.A., 1994. CO_2 cycling in the coastal ocean. I – A numerical analysis of the southeastern Bering Sea with applications to the Chukchi Sea and the northern Gulf of Mexico. Prog. Oceanogr. 34, 335–392. doi:10.1016/0079-6611(94)90019-1

Weingartner, T., Aagaard, K., Woodgate, R., Danielson, S., Sasaki, Y., Cavalieri, D., 2005. Circulation on the north central Chukchi Sea shelf. Deep Sea Res. Part II Top. Stud. Oceanogr. 52, 3150–3174. doi:10.1016/j.dsr2.2005.10.015

Woodgate, R.A., Aagaard, K., 2005. Revising the Bering Strait freshwater flux into the Arctic Ocean. Geophys. Res. Lett. 32, 3–6. doi:10.1029/2004GL021747

site	sample	%TOC	%TN	%S	C:N	δ^{13}C	δ^{15}N	δ^{34}S	Longitude W	Latitude N
EB2	0-1	0.92	0.13	0.16	8.4	-22.1	5.0	13.6	152° 33.2'	71° 27.4'
EB4	0-1	1.87	0.21	0.16	10.5	-20.9	4.3	13.9	152° 24.7'	71° 39.0'
EB7	0-1	1.59	0.18	0.23	10.2	-19.8	5.1	18.8	151° 59.1'	72° 19.3'
BC3	0-1	1.05	0.14	0.21	8.9	-20.6	5.2	15.9	155° 45.3'	71° 39.0'
BC4	0-1	1.63	0.18	0.32	10.7	-18.6	6.9	15.3	154° 49.2'	71° 55.7'
BC5	0-1	1.81	0.18	0.69	11.5	-18.3	6.4	16.5	154° 27.8'	72° 04.2'
BC7	0-1	1.27	0.15	0.30	9.8	-16.7	5.1	20.5	154° 29.9'	72° 32.0'
WHS2	0-1	0.93	0.13	0.50	8.3	-20.2	7.3	17.9	160° 34.0'	72° 50.5'
WHS5	0-1	0.96	0.14	0.23	8.1	-20.1	4.1	9.7	160° 06.7'	73° 16.8'
WHS6	0-1	0.95	0.13	0.74	8.7	-19.9	4.2	16.0	159° 49.8'	73° 26.7'
WHS7	0-1	1.04	0.14	0.19	8.8	-18.2	5.3	16.4	159° 33.2'	73° 36.7'
WHS12	0-1	0.93	0.15	0.10	7.3	-19.2	7.6	7.7	157° 51.2'	73° 54.1'
EHS4	0-1	0.99	0.14	0.45	8.4	-17.5	7.0	7.1	158° 44.2'	72° 36.3'
EHS6	0-1	1.40	0.16	0.32	10.5	-19.3	7.0	20.1	158° 28.5'	72° 51.1'
EHS9	0-1	1.08	0.14	0.71	8.7	-18.2	4.6	19.6	158° 08.8'	73° 06.1'
EHS11	0-1	1.69	0.19	0.20	10.3	-20.2	5.0	19.4	157° 31.9'	73° 26.2'
EHS12	0-1	0.67	0.15	0.24	5.3	-20.0	6.0	18.8	156° 45.9'	73° 47.9'
STN1	0-1	1.14	0.15	0.13	8.8	-20.0	6.6	-5.0	168° 52.9'	67° 27.2'
STN2	0-1	1.31	0.18	0.33	8.6	-18.4	5.9	-5.2	167° 28.0'	70° 38.0'

Table 1: Bulk %TOC, %TN, %S, C:N, δ^{13}C, δ^{15}N, δ^{34}S compositions, and locations for surface sediments

Source	Mean δ^{13}C	Standard Deviation δ^{13}C	Mean δ^{15}N	Standard Deviation δ^{15}N
Ice Algae	-15.5	0.8	10.1	0.6
Pelagic Phytoplankton	-20.3	2.0	4.6	1.6
Terrestrial	-26.2	0.7	0.8	0.5

Table 3: δ^{13}C, δ^{15}N compositions for Ice Algae, Pelagic Phytoplankton and Terrestrial end members

site	sample	%TOC	%TN	%S	C:N	δ^{13}C	δ^{15}N	δ^{34}S
EB2	0-1	0.92	0.13	0.16	8.4	-22.1	5.0	13.6
EB2	1-2	1.07	0.14	0.17	8.6	-19.8	5.3	13.7
EB2	2-3	1.17	0.15	0.12	9.1	-20.6	4.3	2.7
EB2	3-4	1.15	0.15	0.09	9.1	-19.3	4.6	11.5
EB2	4-5	0.95	0.13	0.09	8.6	-20.7	3.5	9.4
EB2	5-6	0.95	0.09	0.08	11.7	-20.9	4.0	6.4
EB2	6-7	1.03	0.12	0.08	9.7	-21.2	3.1	5.2
EB2	7-8	0.94	0.11	0.10	10.1	-20.7	1.8	12.1
EB2	8-9	0.98	0.11	0.10	10.1	-20.0	3.6	6.2
EB2	9-10	0.97	0.11	0.08	10.2	-21.7	2.8	0.1
EB2	10-12	0.73	0.10	0.08	8.3	-19.7	2.6	0.3
EB2	12-14	0.84	0.09	0.06	11.3	-21.3	4.2	2.4
EB2	14-16	0.93	0.13	0.08	8.4	-21.2	4.4	3.5
EB2	16-18	0.90	0.12	0.13	8.6	-21.6	2.5	8.1
EB2	18-20	1.02	0.08	0.10	14.1	-22.2	4.1	15.3
EB4	0-1	1.87	0.21	0.16	10.4	-20.9	4.3	13.9
EB4	1-2	1.73	0.19	0.24	10.5	-21.5	6.9	19.1
EB4	2-3	1.74	0.19	0.19	10.7	-20.9	5.6	16.0
EB4	3-4	1.77	0.19	0.17	11.0	-21.2	4.6	15.8
EB4	4-5	1.69	0.18	0.17	11.0	-20.9	4.0	16.1
EB4	5-6	1.71	0.19	0.16	10.7	-20.9	5.4	16.5
EB4	6-7	1.72	0.19	0.14	10.6	-20.9	5.3	14.2
EB4	7-8	1.75	0.18	0.12	11.2	-21.4	3.4	14.1
EB4	8-9	1.46	0.13	0.13	13.4	-21.6	4.2	14.4
EB4	9-10	1.55	0.16	0.11	11.5	-24.6	3.9	13.1
EB4	10-12	1.76	0.18	0.13	11.6	-19.8	6.4	12.3
EB4	12-14	1.66	0.24	0.16	8.1	-21.6	5.8	12.4
EB4	14-16	1.50	0.18	0.19	9.9	-22.2	5.0	15.1
EB4	16-18	1.68	0.21	0.12	9.4	-22.2	4.9	9.4
EB4	18-20	1.85	0.16	0.14	13.3	-21.0	2.9	8.9
EB7	0-1	1.59	0.18	0.23	10.1	-19.8	5.1	18.8
EB7	1-2	1.33	0.15	0.18	10.3	-22.1	2.2	18.1
EB7	2-3	1.32	0.16	0.14	9.9	-21.5	4.6	17.2
EB7	3-4	1.38	0.15	0.16	10.5	-21.0	7.0	17.2
EB7	4-5	1.43	0.16	0.15	10.2	-19.8	4.0	16.0
EB7	5-6	1.50	0.18	0.13	10.0	-19.6	4.0	13.2
EB7	6-7	1.54	0.18	0.15	10.2	-21.7	1.5	9.7
EB7	7-8	1.31	0.15	0.18	10.1	-20.4	6.5	6.8
EB7	8-9	1.26	0.15	0.18	9.7	-19.5	7.0	8.1
EB7	9-10	1.17	0.14	0.15	9.7	-21.7	5.4	13.0
EB7	10-12	1.35	0.16	0.11	9.6	-20.4	7.4	15.0
EB7	12-14	1.33	0.16	0.10	9.6	-19.5	4.3	16.8
EB7	14-16	1.06	0.13	0.13	9.7	-18.9	9.1	16.3
EB7	16-18	1.20	0.14	0.11	9.8	-18.6	6.9	16.5
EB7	18-20	1.01	0.12	0.15	9.9	-18.9	4.3	17.3
EHS4	0-1	1.56	0.25	0.43	7.3	-18.3	7.8	7.1
EHS4	1-2	1.31	0.19	0.17	8.0	-19.1	8.0	16.9
EHS4	2-3	1.22	0.18	0.14	8.1	-19.6	8.2	17.4
EHS4	3-4	1.32	0.22	0.12	7.0	-18.7	6.8	17.6

site	sample	%TOC	%TN	%S	C:N	δ^{13}C	δ^{15}N	δ^{34}S
EHS4	4-5	1.22	0.18	0.11	8.1	-19.8	5.6	16.0
EHS4	5-6	1.02	0.15	0.11	8.1	-20.3	6.4	14.1
EHS4	6-7	1.07	0.15	0.16	8.3	-20.2	7.2	14.7
EHS4	7-8	1.19	0.17	0.13	8.3	-19.6	4.5	13.8
EHS4	8-9	0.94	0.14	0.11	8.1	-19.6	5.4	13.5
EHS4	9-10	0.87	0.12	0.26	8.2	-19.5	6.1	16.1
EHS4	10-12	0.90	0.12	0.12	8.5	-20.5	2.7	10.9
EHS4	12-14	0.72	0.10	0.13	8.7	-20.9	5.4	11.6
EHS6	0-1	1.40	0.16	0.32	10.5	-19.3	7.0	20.1
EHS6	1-2	1.41	0.18	0.37	9.4	-18.8	8.0	19.6
EHS6	2-3	1.40	0.21	0.23	7.7	-18.4	6.6	18.3
EHS6	3-4	1.34	0.16	0.12	9.7	-19.1	6.4	16.2
EHS6	4-5	1.26	0.18	0.17	8.2	-19.0	6.8	17.8
EHS6	5-6	1.29	0.16	0.16	9.4	-17.2	6.5	17.4
EHS6	6-7	1.27	0.15	0.18	9.7	-19.5	8.1	17.3
EHS6	7-8	1.30	0.18	0.18	8.6	-19.1	6.8	17.5
EHS6	8-9	1.30	0.17	0.18	9.0	-19.1	6.4	16.6
EHS6	9-10	1.26	0.16	0.15	9.0	-19.5	6.8	16.3
EHS6	10-12	1.24	0.16	0.20	9.0	-19.5	7.7	16.4
EHS12	0-1	0.67	0.15	0.24	5.3	-20.0	6.0	18.8
EHS12	1-2	0.66	0.13	0.22	6.0	-20.3	9.4	19.6
EHS12	2-3	0.73	0.12	0.13	6.9	-19.7	6.8	18.8
EHS12	3-4	0.74	0.12	0.09	7.1	-19.2	5.7	18.0
EHS12	4-5	0.72	0.12	0.08	7.2	-20.1	6.9	16.5
EHS12	5-6	0.75	0.11	0.06	7.8	-21.8	4.4	16.0
EHS12	6-7	0.74	0.11	0.05	8.0	-21.8	6.2	16.3
EHS12	7-8	0.80	0.11	0.07	8.4	-21.8	4.0	15.6
EHS12	8-9	0.75	0.11	0.07	8.3	-23.7	4.5	16.0
EHS12	9-10	0.87	0.12	0.06	8.5	-23.3	5.2	17.3
EHS12	10-12	0.89	0.12	0.07	8.7	-21.6	3.1	16.0
EHS12	12-14	0.85	0.11	0.06	8.7	-22.3	4.6	14.2
EHS12	14-16	0.90	0.12	0.07	9.0	-20.8	4.3	15.8
EHS12	16-18	0.97	0.12	0.07	9.3	-19.6	4.7	13.7
EHS12	18-20	0.92	0.13	0.11	8.2	-19.8	4.1	15.1
EHS12	20-22	1.06	0.12	0.05	10.4	-18.8	3.7	10.9
EHS12	22-24	1.10	0.12	0.06	10.5	-20.4	4.0	13.0
EHS12	24-26	1.11	0.12	0.07	10.8	-20.9	1.3	10.4
EHS12	26-28	1.13	0.12	0.20	11.0	-22.3	5.3	12.1
EHS12	28-30	0.96	0.10	0.13	10.8	-20.2	2.1	15.1
WHS12	0-1	0.93	0.15	0.10	7.2	-19.2	7.6	7.7
WHS12	1-2	0.84	0.12	0.14	7.9	-17.8	4.3	15.7
WHS12	2-3	0.73	0.11	0.09	8.1	-20.2	5.5	17.1
WHS12	3-4	0.68	0.10	0.07	7.7	-19.7	5.5	17.5
WHS12	4-5	0.61	0.10	0.32	7.0	-19.7	2.6	12.1
WHS12	5-6	0.55	0.08	0.06	8.1	-20.7	3.7	14.9
WHS12	6-7	0.50	0.09	0.05	6.5	-20.8	5.3	16.5
WHS12	7-8	0.48	0.10	0.07	5.8	-19.4	2.8	16.4
WHS12	8-9	0.52	0.07	0.04	8.2	-20.1	1.8	16.3
WHS12	9-10	0.54	0.07	0.05	8.6	-21.5	5.7	16.3
WHS12	10-12	0.42	0.09	0.09	5.5	-22.6	4.1	15.2
WHS12	12-14	0.45	0.07	0.08	7.5	-21.2	3.9	12.4
WHS12	14-16	0.35	0.05	0.05	8.5	-22.7	2.7	14.0
WHS12	16-18	0.32	0.04	0.05	10.3	-21.0	1.3	16.4
WHS12	18-20	0.22	0.03	0.06	10.0	-21.3	2.8	13.8
WHS12	20-22	0.14	0.04	0.05	3.9	-21.9	3.1	11.8
WHS12	22-24	0.11	0.04	0.06	3.4	-23.5	2.9	13.5

Table 3: Bulk %TOC, %TN, %S, C:N, δ^{13}C, δ^{15}N, δ^{34}S compositions for the core samples

Chapter 4: A Holocene record of organic carbon

Introduction

The Arctic is presently experiencing profound changes in climate that are affecting sea level, sea ice cover, ecosystems, coastal erosion and much more besides (Thomas and Dieckmann, 2003). Sea ice, a vital part of the Arctic system, is currently undergoing a massive decline. The extent of Arctic sea ice has fallen by 30% since satellite records began. If sea ice extent continues to fall, some researchers fear that a transition to a seasonally ice free Arctic may occur (e.g. Stroeve et al., 2012), perhaps as soon as mid-century (Massonnet et al., 2012).

These changes could also have important consequences for the organic carbon cycle in the Arctic Ocean. The extent of sea ice cover and the timing of its melting are an important control on sea ice productivity as well as the productivity of the subsequent spring bloom in open water (Arrigo et al., 2008). Sea ice cover controls light availability (Fortier), stratification and nutrient supply (Vancoppenolle et al., 2013). Even as sea ice breaks up in spring, it affects pelagic biogeochemistry and food webs by seeding the spring bloom in the marginal ice zone and by providing important early food supplies to both pelagic zooplankton (Thomas and Dieckmann, 2003) and the rich benthic fauna that inhabits the shallow shelves of the Chukchi Sea (Grebmeier, 2012). Sea ice cover also plays an important role in the transfer of terrestrial material to ocean sediments, by transporting terrestrial material to away from coastal regions, and by restricting coastal erosion (Are et al., 2008; Reimnitz and Are, 2000). As sea ice volume and extent continues its rapid decline, the effect that this will have on Arctic marine biogeochemistry is not yet well understood.

However, the present is not the only recent time of great change in the Arctic. As the last ice age drew to a close, the Arctic experienced massive changes including sea level

rise, coastal retreat and the re-establishment of a connection with the Pacific Ocean through the Bering Strait. The Chukchi shelf and Bering Land Bridge were flooded by rising sea levels approximately 11-12000 years BP (Keigwin et al., 2006). As sea level rose and the coastline retreated, the Chukchi slope and basin no longer received direct inputs from the numerous small rivers along the Chukchi coastal plain (Hill et al., 2007; Keigwin et al., 2006; Rachold et al., 2004). And the opening of the Bering Strait reconnected the Chukchi Sea with fresher, nutrient and silicate rich North Pacific waters flowing through the Bering Strait (Ortiz et al., 2009). There is also evidence for highly variable sea ice cover during the Holocene (McKay et al., 2008).

Although recent sediment studies (e.g. Belicka and Harvey, 2009; Goñi et al., 2005; Naidu, 2000; Schreiner et al., 2013; Tolosa et al., 2013) of the Western Arctic Ocean have led to an improvement in our understanding of the present state of the carbon cycle, many of the samples taken were surface grabs or short cores. These records provide information about recent activity, but do not provide the kind of longer record that would be necessary to reconstruct the quaternary paleoenvironmental history of the Western Arctic Ocean. The absence of longer, high resolution, cores has also precluded study of longer term Holocene records of the carbon cycle. These are of particular interest given the significant, and continuing, changes that have affected the Western Arctic Ocean since the last glacial maximum ca. 20000 years BP (Stein and Macdonald, 2004). A better grasp of past changes will surely illuminate the present, and lead to better predictions of how the Western Arctic Ocean may respond to future pressures.

In order to further our understanding of Holocene change in the Arctic, the Healy-Oden Transarctic Expedition (HOTRAX) obtained a series of 29 cores from across the Arctic Ocean (Darby et al., 2005; Dennis A. Darby et al., 2009). One of these cores, JPC-5, was taken from the Chukchi slope. This site is bounded on either side by sample sites from the earlier Shelf Basins Interactions expedition (see chapters 3 and 4).

Using %C, %N, $\delta^{13}C$, and $\delta^{15}N$, the JPC-5 core was analyzed with the Bayesian Isotope Mixing Model MixSIAR (Stock and Semmens, 2013). This model incorporate multiple end members and end member variability, enabling the calculation of probability distribution for source contributions (Parnell et al., 2013). These results will allow us to peer back through time as we seek to understand how, or if, the sources of organic carbon have changed during the Holocene at this Chukchi slope site.

Material and methods

Core HLY0501-JPC5 is a 16.7m long Jumbo Piston Core taken from the Chukchi slope (72° 41.4' N, 157° 31.2' W), at a water depth of 415m. A trigger core of 2.59m length was also taken and correlated to the piston core using radiocarbon dates and palynological assemblages (McKay et al., 2008), since piston cores disturb the uppermost sediments during barrel entry. The upper 12.4m of JPC5 and the trigger core consist of a sulfide-rich, olive-gray mud. In JPC5, this is underlain by a 4.33m ice rafted deposit of rich gray to gray brown sandy mud (McKay et al., 2008).

Radiocarbon dates for JPC5 were obtained using Accelerator Mass Spectrometry (AMS) on six bivalve shells from different core depths. Radiocarbon dates were then corrected for marine reservoir effects, and stable carbon isotope fluctuations with CALIB 5.0.2. McKay et al. (2008) used a regional reservoir correction (ΔR) of 0 years due to the young, overlying Atlantic water and the surface depth of the sample site, which is below the older Pacific water that lies between 30-200m. This age model suggested an average sedimentation rate of 156cm/ka.

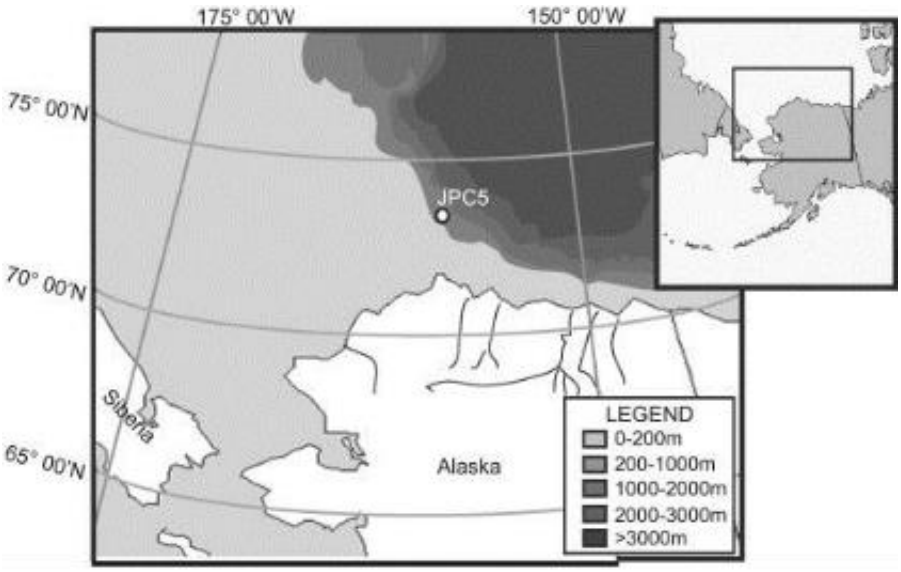

Figure 1: Core location map (image from Faux, 2009)

Darby et al. (2009) provides additional sedimentation rate estimates, based on age models of $\Delta R = 0$ years and $\Delta R = 460$ years, to account for uncertainty in the magnitude of the Arctic Ocean reservoir effect. Sedimentation rates for JPC5 were estimated to be between 159 and 161cm/ka with the two models. McKay et al. (2008) estimates the sedimentation rate for the trigger core to be 160.5cm/ka using ^{210}Pb dating. This would imply that the there is a 700 year gap between the bottom of the trigger core and the top of JPC5.

Results

The %OC in the core is remarkably consistent at around 1.1-1.2% (mean 1.16%) from the surface until the deepest sections of the core. Starting at 1080-1082cm, a sharp decrease in %OC to 0.6% is observed by 1240-1242cm. A similar trend is also present in %N. %N is consistently around 0.15% (mean 0.14%) until 1080-1082cm, where a decrease to 0.07% by 1240-1242cm is seen. However, the 1160-1162cm sample contains an unusually high %N at 0.17%; the decrease is not as consistent in %N as it is in %OC. These parallel trends in %OC and %N produce a fairly consistent pattern in C:N ratios, where no

trend is observed. Rather, C:N ranges from 8.40 to 11.46, with the single outlier (1200-1202cm) at 5.42.

Mean $\delta^{13}C$ was -23.2‰. A down core trend towards more depleted values was observed. Upper core samples were around -22‰ and $\delta^{13}C$ steadily decreases to around -26‰ in the deepest sections. There was no parallel trend in $\delta^{15}N$, rather, $\delta^{15}N$ varied between 4.8‰ and 10.1‰, with a mean value of 7.8‰.

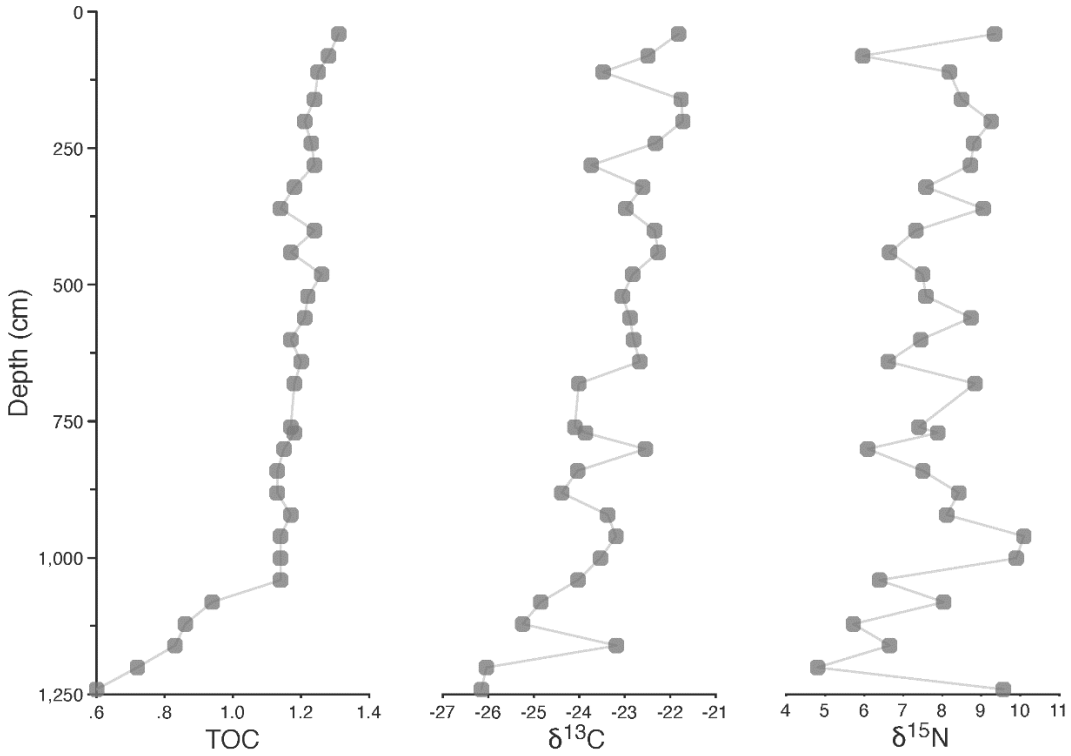

Figure 2: Down core %TOC, $\delta^{13}C$ and $\delta^{15}N$ for core HLY0501-JPC5

Discussion

In comparison with the sites sampled during the SBI campaign (Morris et al., 2015), core JPC-5 is more depleted in $\delta^{13}C$ and more enriched in $\delta^{15}N$. The %C, %N and C:N ratios match those sites pretty closely, with the deeper WHS 12 perhaps the closest analogue; both sites showing decreases in %OC and depletion in $\delta^{13}C$ with depth. In the EHS transect, the slope sites EHS4 and EHS6 also displayed similar patterns, although these were not observed in the basin site, EHS12. In EHS12, %OC and C:N increased with depth, but no clear trend in $\delta^{13}C$ was present.

The slight depletion in $\delta^{13}C$ might indicate a greater proportion of terrestrial material in this core than in the SBI sites. This would also fit with the higher C:N rations observed. However, the relatively enriched $\delta^{15}N$ is indicative of marine material; terrestrial material typically has a $\delta^{15}N$ around 1‰, whereas the mean value was 7.8‰. This is higher than typical marine values (around 5‰), which suggests that another source of enrichment is present. As the Chukchi slope, especially the area around Barrow Canyon, has been found to experience sediment advection (Bates et al., 2005; Moran et al., 2005) and supply from the highly productive southerly water of the Chukchi and Bering straits, it could be that the enrichment is caused by supply of substantially reworked marine material.

Model

Initially, a MixSIAR model was set up with the end members from Morris et al. (2015) (pelagic phytoplankton, ice algae, terrestrial). A ^{13}C vs ^{15}N biplot (Fig 3) was used to confirm the suitability of the model parameters (Phillips and Gregg, 2003; Phillips et al., 2014). A convex polygon bounded by all three sources was drawn (Smith et al., 2013); all of the Healy core data points plotted well outside the polygon. This implies a source

of carbon is missing from the model for the Healy core and the model ought to be rejected (Phillips and Gregg, 2003).

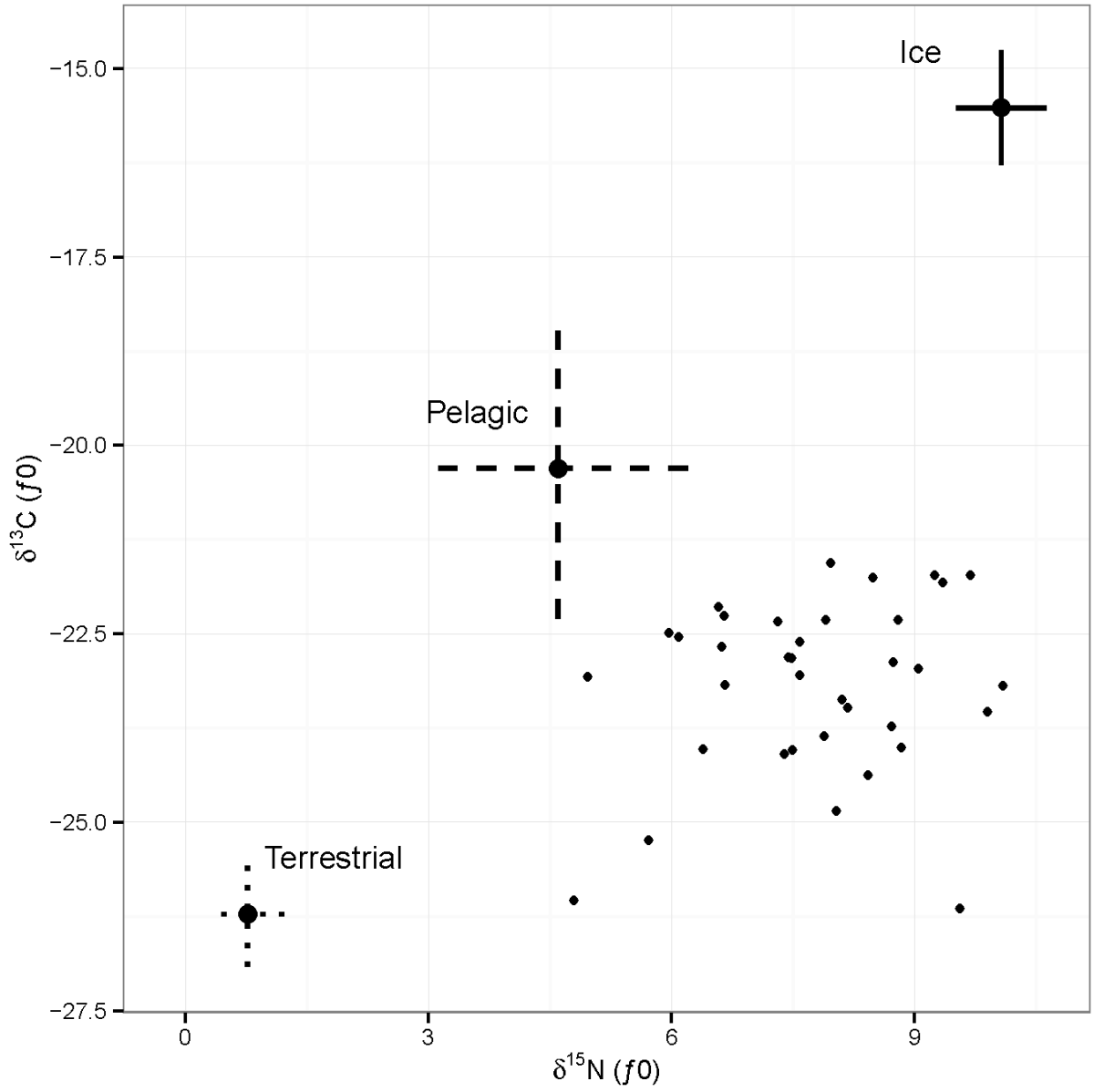

Figure 3: $\delta^{13}C$ vs $\delta^{15}N$ Isospace plot for core HLY0501-JPC5, using Morris et al. (2015) end members

Magen et al. (2010), proposed another set of end members, comprising terrestrial organic matter, fresh marine organic matter and recalcitrant organic matter, based upon data from the Mackenzie River, Chukchi sediments and sediment traps, respectively.

Using a ^{13}C vs ^{15}N biplot (Fig 4), all the Healy core samples were found to fit inside a polygon bounded by the end members.

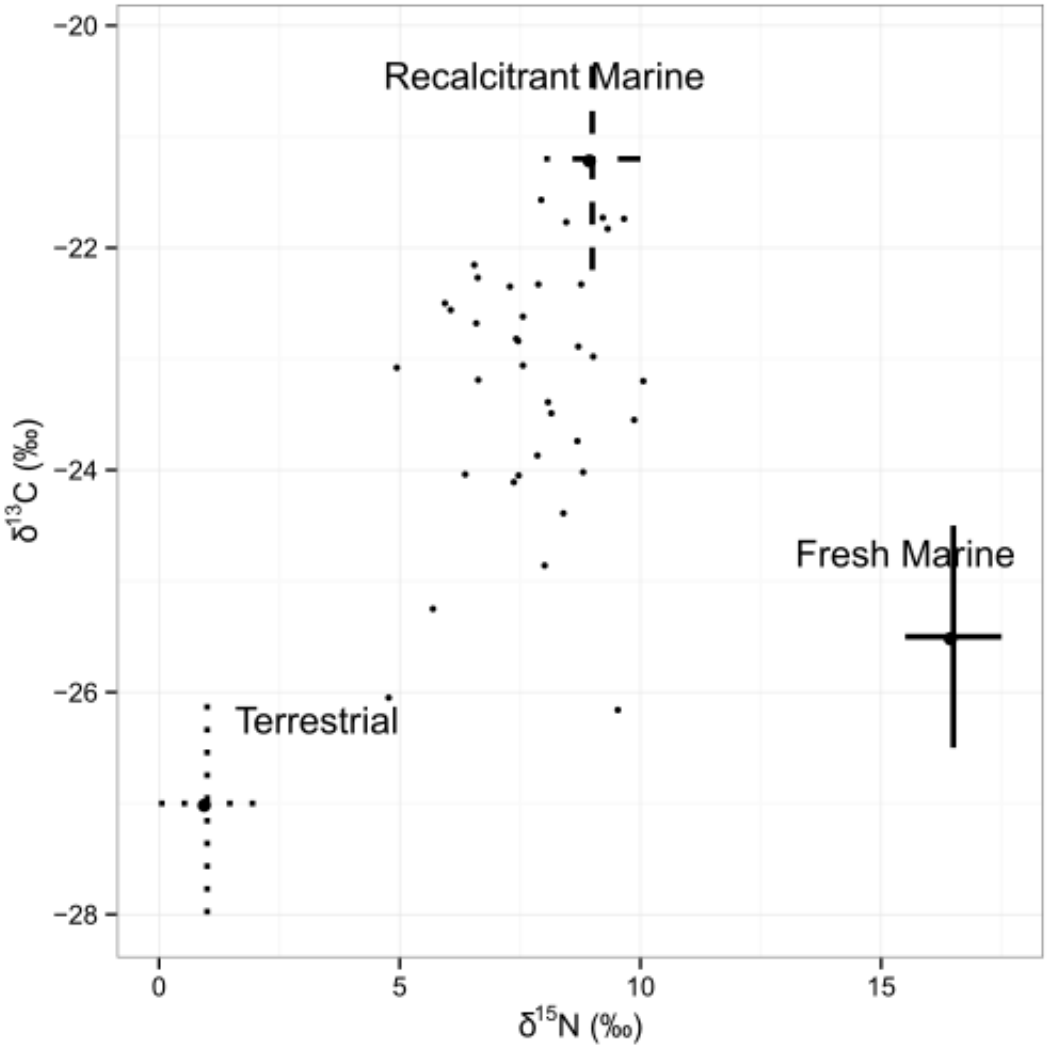

Figure 4: $\delta^{13}C$ vs $\delta^{15}N$ Isospace plot for HLY0501-JPC5 using end members from Magen et al. (2010)

Additionally, a Monte Carlo simulation (Smith et al., 2013) was performed to evaluate the proposed model (Fig 7). The samples all fell within the acceptable area of the mixing model, and no samples had to be excluded due to being outside the 95% mixing region proposed by the model. As the geometry of the model was now suitable, an analysis was performed using MixSIAR (Fig 5). The median values for the posterior density, a

measure of the probability distribution of each source, from the MixSIAR model were 6% (SD 2%) for fresh marine material, 71% (SD 3%) for recalcitrant marine and 22% (SD 2%) for terrestrial material.

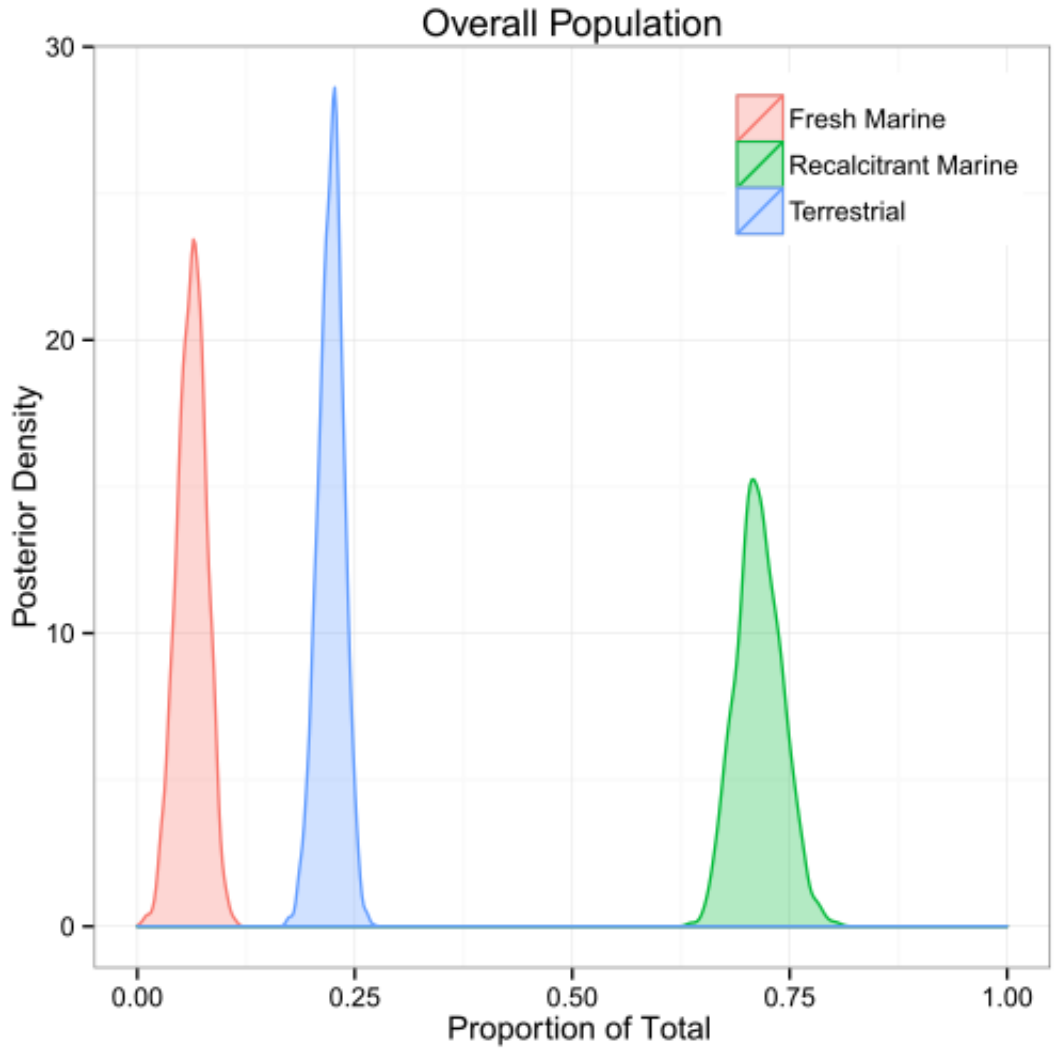

Figure 5: Posterior distributions for source contributions for core HLY0501-JPC5 using Magen et al. (2010) end members

This interpretation matches Faux et al. (2011) and McKay et al. (2008). Using dinocyst assemblages, pollen, spores and geochemical measurements, including ^{13}C, McKay et al. (2008) observed a shift from terrestrial to marine dominance over the course of the Holocene, which was evidenced by increasing $\delta^{13}C$, decreasing C:N and pollen counts.

Faux et al. (2011) also observed high concentrations of marine biomarkers in the core samples, suggesting that marine organic matter was dominant in the core, but with a substantial and consistent terrestrial component. Tolosa et al. (2013) also found evidence for a substantial refractory algal material contribution to sediments and suspended particulate matter on the Mackenzie slope and Amundsen Gulf, slightly to the East of our study area. This area receives substantially more terrestrial material via the Mackenzie River than sites in the Chukchi (Goñi et al., 2005). Our findings fit with the general trend to lower terrestrial contributions as the Mackenzie River influence decreases (Magen et al., 2010).

To study downcore trends, the MixSIAR model was repeated, but as a hierarchical model with the samples split into upper, middle and lower core sections. When run in this manner, a trend to increasing terrestrial material can be observed downcore. There is a transition from upper to middle to lower core visible in the C vs N biplot (Fig 6), with the upper core samples mostly clustered around the refractory marine end member, but the lower core samples situated somewhat more toward the terrestrial end member. The middle core samples were intermediate. The median values from the MixSIAR model for fresh marine, recalcitrant marine and terrestrial material were 5% (SD 3%), 79% (SD 6%) 16% (SD 4%) in the upper core (Fig 9), 8% (SD 3%), 68% (SD 6%), 23% (SD 4%) in the middle section (Fig 10), and 18% (SD 4%), 46% (SD 6%), 36% (SD 5%) for the lower section (Fig 11). None of the core sections were mostly terrestrial; even for the lower core samples, refractory and fresh marine material comprises the majority of the preserved organic matter. However, the deepest and oldest (possibly 9000 years BP (McKay et al., 2008)) core sections show a stronger terrestrial contribution (Fig 12). The decreased terrestrial contribution over the course of the Holocene concurs with the landward shift of terrestrial sediment sources such as rivers and eroding coastlines in the period between the flooding of the Chukchi Shelf (12000 years BP) and modern sea

levels (7000 years BP) The model also predicted an increase in the contribution of fresh marine material in the lower core sections. But the polyunsaturated fatty acid fraction, which is highly labile and can be used as an indicator of fresh marine inputs, relatively low throughout the core compared to adjacent SBI sites. As Faux et al. (2011) found high concentrations of many other marine biomarkers throughout the core, it seems more reasonable to interpret the contributions of marine material to the core as being mostly degraded.

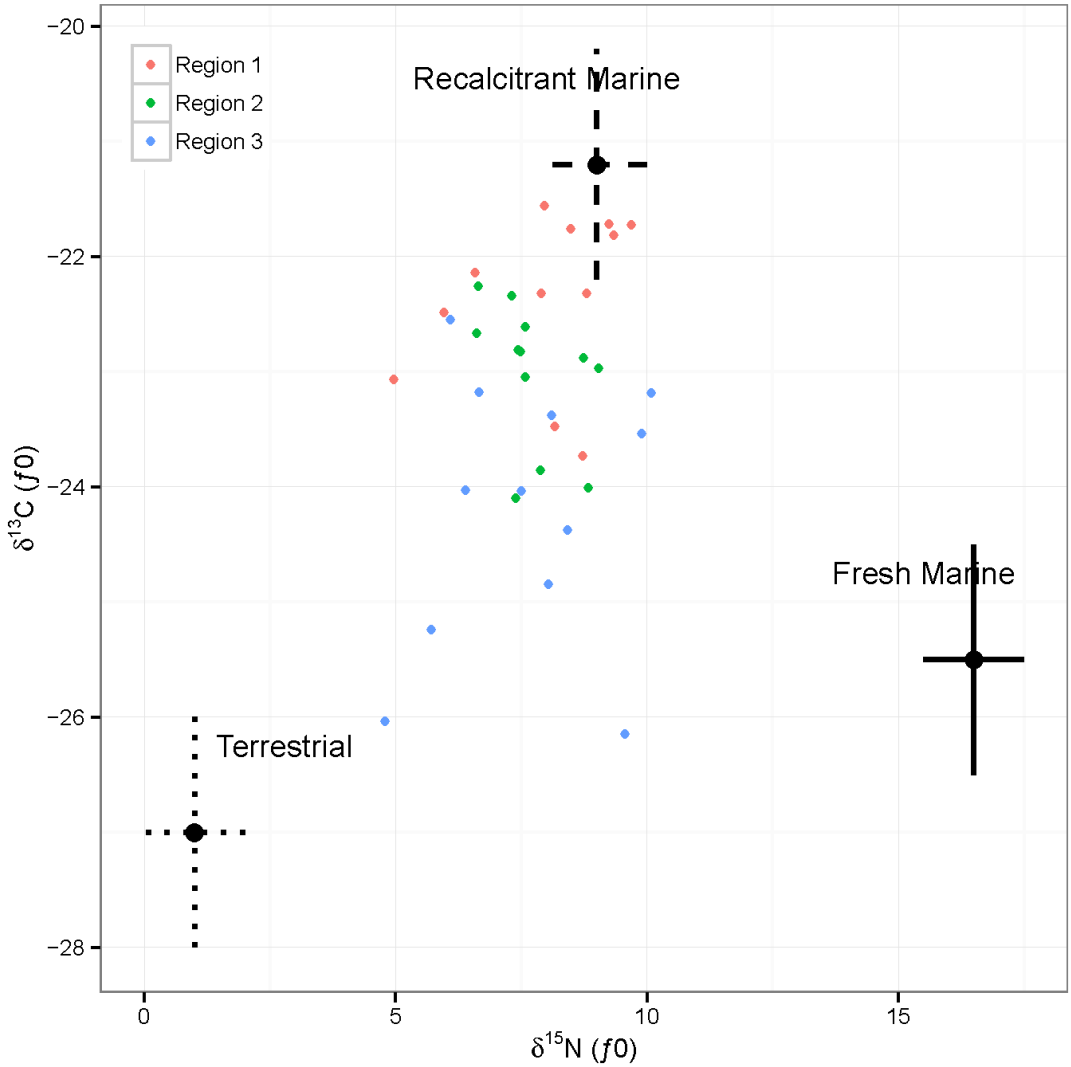

Figure 6: $\delta^{13}C$ vs $\delta^{15}N$ Isospace plot for core HLY0501-JPC5 using Magen et al. (2010) end members. Samples are grouped by position within the core Region 1 = upper core, region 2 = middle core, region 3 = lower core

Conclusions

This chapter presents some of the first ^{13}C isotopic data and the first ^{15}N data on a Holocene timescale from the Chukchi Sea. We found evidence of a strong and consistent marine signature, in conjunction with decreasing levels of terrestrial influence over the course of the Holocene. Most of the marine material appears to be degraded rather than fresh, suggesting that it is supplied and mixed by currents from other parts of the Arctic.

Bibliography

Are, F., Reimnitz, E., Grigoriev, M., Hubberten, H., Rachold, V., 2008. The Influence of Cryogenic Processes on the Erosional Arctic Shoreface. J. Coast. Res. 24, 110–121. doi:10.2112/05-0573.1

Arrigo, K.R., van Dijken, G., Pabi, S., 2008. Impact of a shrinking Arctic ice cover on marine primary production. Geophys. Res. Lett. 35, L19603. doi:10.1029/2008GL035028

Bates, N., Hansell, D., Bradleymoran, S., Codispoti, L., 2005. Seasonal and spatial distribution of particulate organic matter (POM) in the Chukchi and Beaufort Seas. Deep Sea Res. Part II Top. Stud. Oceanogr. 52, 3324–3343. doi:10.1016/j.dsr2.2005.10.003

Belicka, L.L., Harvey, H.R., 2009. The sequestration of terrestrial organic carbon in Arctic Ocean sediments: A comparison of methods and implications for regional carbon budgets. Geochim. Cosmochim. Acta 73, 6231–6248. doi:10.1016/j.gca.2009.07.020

Darby, D.A., Jakobsson, M., Polyak, L., 2005. Icebreaker Expedition Collects Key Arctic Seafloor and Ice Data. Eos (Washington. DC). 86, 549, 552.

Darby, D.A., Ortiz, J., Polyak, L., Lund, S., Jakobsson, M., Woodgate, R.A., 2009. The role of currents and sea ice in both slowly deposited central Arctic and rapidly deposited Chukchi–Alaskan margin sediments. Glob. Planet. Change 68, 58–72. doi:10.1016/j.gloplacha.2009.02.007

Darby, D.A., Polyak, L., Jakobsson, M., 2009. The 2005 HOTRAX Expedition to the Arctic Ocean. Glob. Planet. Change 68, 1–4. doi:10.1016/j.gloplacha.2009.04.005

Faux, J.F., Belicka, L.L., Harvey, H.R., 2011. Organic sources and carbon sequestration in

Holocene shelf sediments from the western Arctic Ocean. Cont. Shelf Res. 31, 1169–1179. doi:10.1016/j.csr.2011.04.001

Goñi, M.A., Yunker, M.B., MacDonald, R.W., Eglinton, T.I., 2005. The supply and preservation of ancient and modern components of organic carbon in the Canadian Beaufort Shelf of the Arctic Ocean. Mar. Chem. 93, 53 – 73. doi:10.1016/j.marchem.2004.08.001

Grebmeier, J.M., 2012. Shifting Patterns of Life in the Pacific Arctic and Sub-Arctic Seas. Ann. Rev. Mar. Sci. 4, 63–78. doi:10.1146/annurev-marine-120710-100926

Hill, J.C., Driscoll, N.W., Brigham-Grette, J., Donnelly, J.P., Gayes, P.T., Keigwin, L., 2007. New evidence for high discharge to the Chukchi shelf since the Last Glacial Maximum. Quat. Res. 68, 271–279. doi:10.1016/j.yqres.2007.04.004

Keigwin, L.D., Donnelly, J.P., Cook, M.S., Driscoll, N.W., Brigham-Grette, J., 2006. Rapid sea-level rise and Holocene climate in the Chukchi Sea. Geology 34, 861–864. doi:10.1130/G22712.1

Magen, C., Chaillou, G., Crowe, S.A., Mucci, A., Sundby, B., Gao, A., Makabe, R., Sasaki, H., 2010. Origin and fate of particulate organic matter in the southern Beaufort Sea – Amundsen Gulf region, Canadian Arctic. Estuar. Coast. Shelf Sci. 86, 31–41. doi:10.1016/j.ecss.2009.09.009

Massonnet, F., Fichefet, T., Goosse, H., Bitz, C.M., Philippon-Berthier, G., Holland, M.M., Barriat, P.-Y., 2012. Constraining projections of summer Arctic sea ice. Cryosph. 6, 1383–1394. doi:10.5194/tc-6-1383-2012

McKay, J.L., de Vernal, A., Hillaire-Marcel, C., Not, C., Polyak, L., Darby, D., 2008. Holocene fluctuations in Arctic sea-ice cover: dinocyst-based reconstructions for the eastern Chukchi SeaThis article is one of a series of papers published in this Special Issue on the theme Polar Climate Stability Network .GEOTOP Publication 2008-0023. Can. J. Earth Sci. 45, 1377–1397. doi:10.1139/E08-046

Moran, S.B., Kelly, R.P., Hagstrom, K., Smith, J.N., Grebmeier, J.M., Cooper, L.W., Cota, G.F., Walsh, J.J., Bates, N.R., Hansell, D.A., Maslowski, W., Nelson, R.P., Mulsow, S., 2005. Seasonal changes in POC export flux in the Chukchi Sea and implications for water column-benthic coupling in Arctic shelves. Deep Sea Res. Part II Top. Stud. Oceanogr. 52, 3427–3451. doi:10.1016/j.dsr2.2005.09.011

Morris, D.J., O'Connell, M.T., Macko, S.A., 2015. Assessing the importance of terrestrial organic carbon in the Chukchi and Beaufort seas. Estuar. Coast. Shelf Sci. 164, 28–38. doi:10.1016/j.ecss.2015.06.011

Naidu, A.S., 2000. Organic carbon isotope ratios ($\delta^{13}C$) of Arctic Amerasian continental

shelf sediments. Int. J. Earth Sci. 89, 522–532.

Ortiz, J.D., Polyak, L., Grebmeier, J.M., Darby, D., Eberl, D.D., Naidu, S., Nof, D., 2009. Provenance of Holocene sediment on the Chukchi-Alaskan margin based on combined diffuse spectral reflectance and quantitative X-Ray Diffraction analysis. Glob. Planet. Change 68, 73–84. doi:10.1016/j.gloplacha.2009.03.020

Parnell, A.C., Phillips, D.L., Bearhop, S., Semmens, B.X., Ward, E.J., Moore, J.W., Jackson, A.L., Grey, J., Kelly, D.J., Inger, R., 2013. Bayesian stable isotope mixing models. Environmetrics 24, 387–399. doi:10.1002/env.2221

Phillips, D.L., Gregg, J.W., 2003. Source partitioning using stable isotopes: coping with too many sources. Oecologia 136, 261–9. doi:10.1007/s00442-003-1218-3

Phillips, D.L., Inger, R., Bearhop, S., Jackson, A.L., Moore, J.W., Parnell, A.C., Semmens, B.X., Ward, E.J., 2014. Best practices for use of stable isotope mixing models in food-web studies. Can. J. Zool. 92, 823–835. doi:10.1139/cjz-2014-0127

Rachold, V., Eicken, H., Gordeev, V., Grigoriev, M., Hubberten, H., Lisitzin, A., Shevchenko, V., Schirmeister, L., 2004. Modern Terrigenous Organic Carbon Input to the Arctic Ocean, in: Stein, R., Macdonald, R.W. (Eds.), The Organic Carbon Cycle in the Arctic Ocean. Springer, pp. 33–56.

Reimnitz, E., Are, F.E., 2000. Coastal Bluff and Shoreface Comparison over 34 Years Indicates Large Supply of Erosion Products to Arctic Seas. Polarforschung 68, 231 – 235.

Schreiner, K.M., Bianchi, T.S., Eglinton, T.I., Allison, M.A., Hanna, A.J.M., 2013. Sources of terrigenous inputs to surface sediments of the Colville River Delta and Simpson's Lagoon, Beaufort Sea, Alaska. J. Geophys. Res. Biogeosciences 118, 808–824. doi:10.1002/jgrg.20065

Smith, J. a., Mazumder, D., Suthers, I.M., Taylor, M.D., 2013. To fit or not to fit: Evaluating stable isotope mixing models using simulated mixing polygons. Methods Ecol. Evol. 4, 612–618. doi:10.1111/2041-210X.12048

Stein, R., MacDonald, R.W., 2004. The organic carbon cycle in the Arctic Ocean. Springer.

Stock, B.C., Semmens, B.X., 2013. MixSIAR GUI User Manual, version 1.0.

Stroeve, J.C., Serreze, M.C., Holland, M.M., Kay, J.E., Malanik, J., Barrett, A.P., 2012. The Arctic's rapidly shrinking sea ice cover: A research synthesis. Clim. Change 110, 1005–1027. doi:10.1007/s10584-011-0101-1

Thomas, D.N., Dieckmann, G.S. (Eds.), 2003. Sea Ice. Blackwell Science Ltd, Oxford, UK.

doi:10.1002/9780470757161

Tolosa, I., Fiorini, S., Gasser, B., Martín, J., Miquel, J.C., 2013. Carbon sources in suspended particles and surface sediments from the Beaufort Sea revealed by molecular lipid biomarkers and compound-specific isotope analysis. Biogeosciences 10, 2061–2087. doi:10.5194/bg-10-2061-2013

Vancoppenolle, M., Meiners, K.M., Michel, C., Bopp, L., Brabant, F., Carnat, G., Delille, B., Lannuzel, D., Madec, G., Moreau, S., Tison, J.L., van der Merwe, P., 2013. Role of sea ice in global biogeochemical cycles: Emerging views and challenges. Quat. Sci. Rev. 79, 207–230. doi:10.1016/j.quascirev.2013.04.011

Additional images

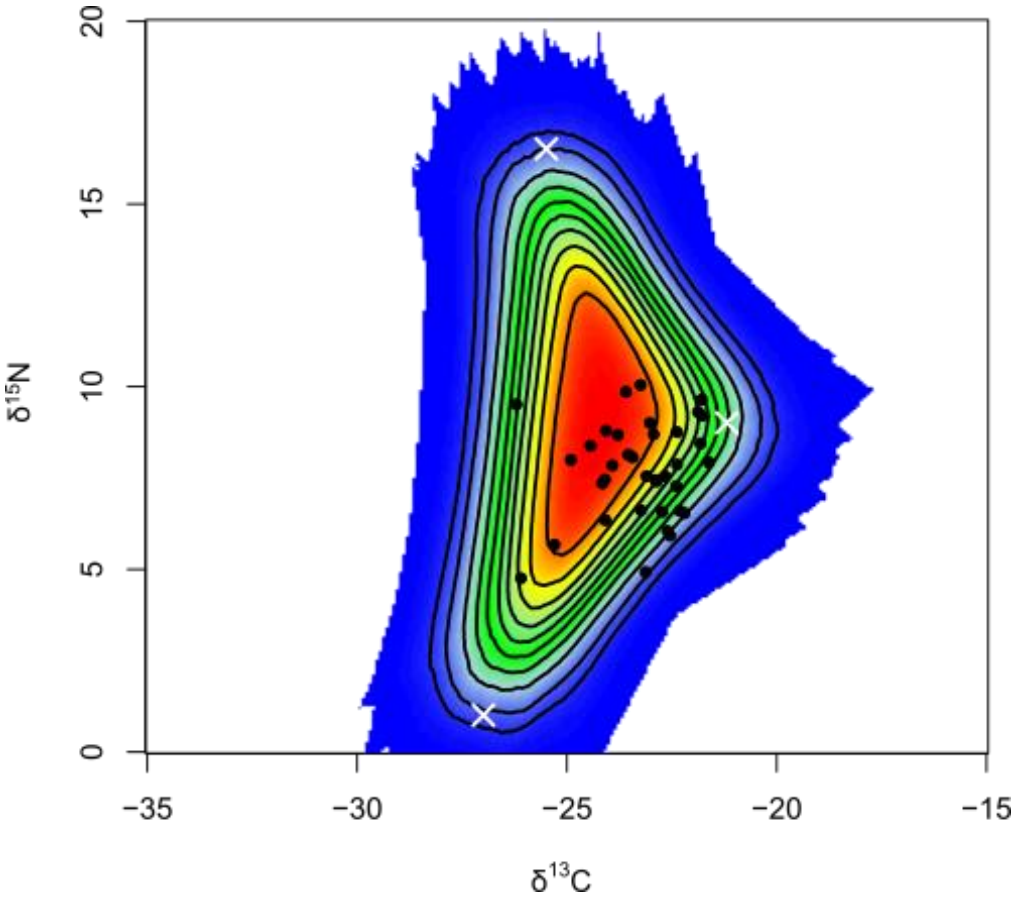

Figure 7: Mixing region for samples and end members using Magen et al. (2010) end members and model from Smith et al. (2013)

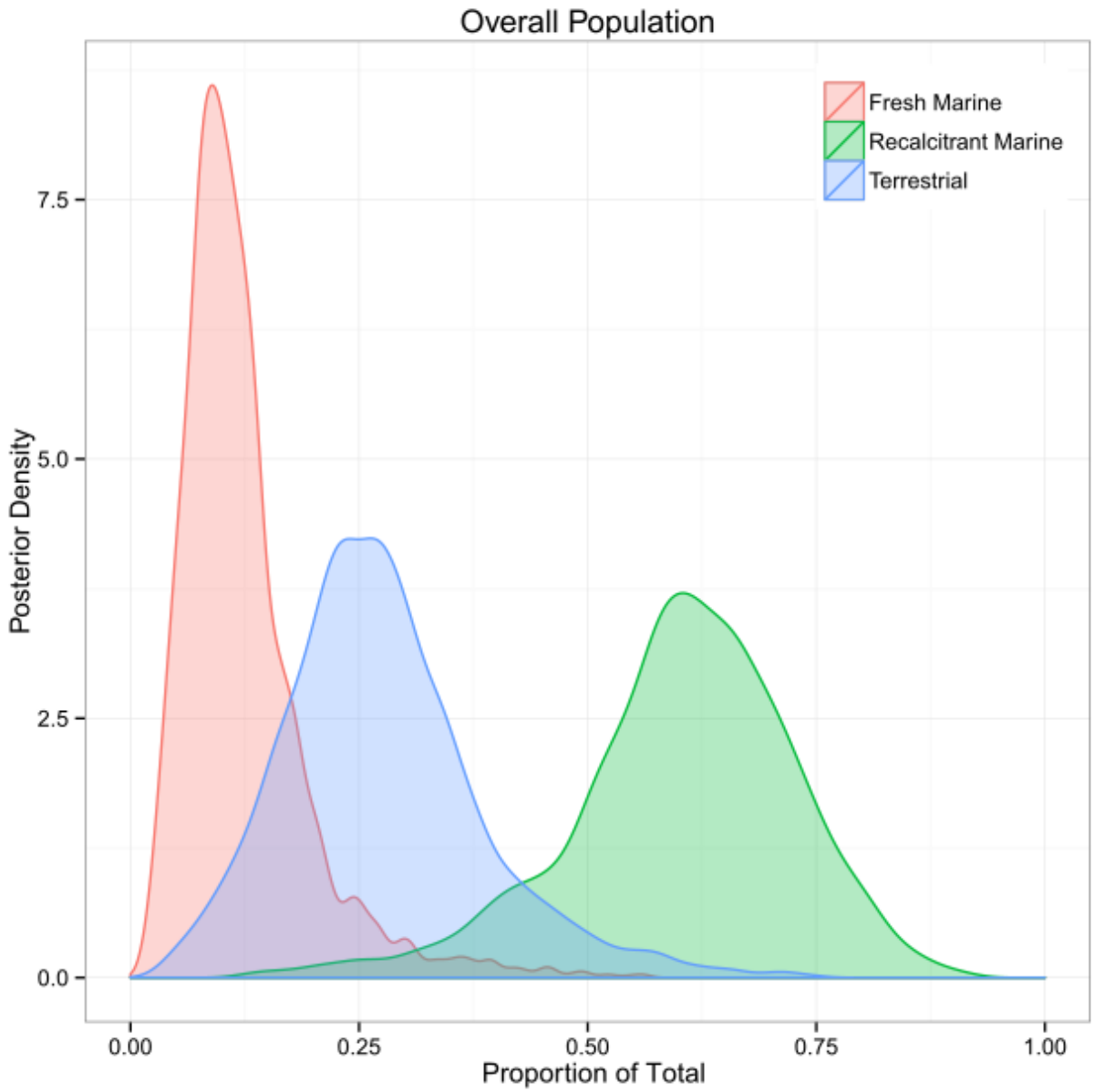

Figure 8: Overall posterior distributions for source contributions HLY0501-JPC5 when separated by region

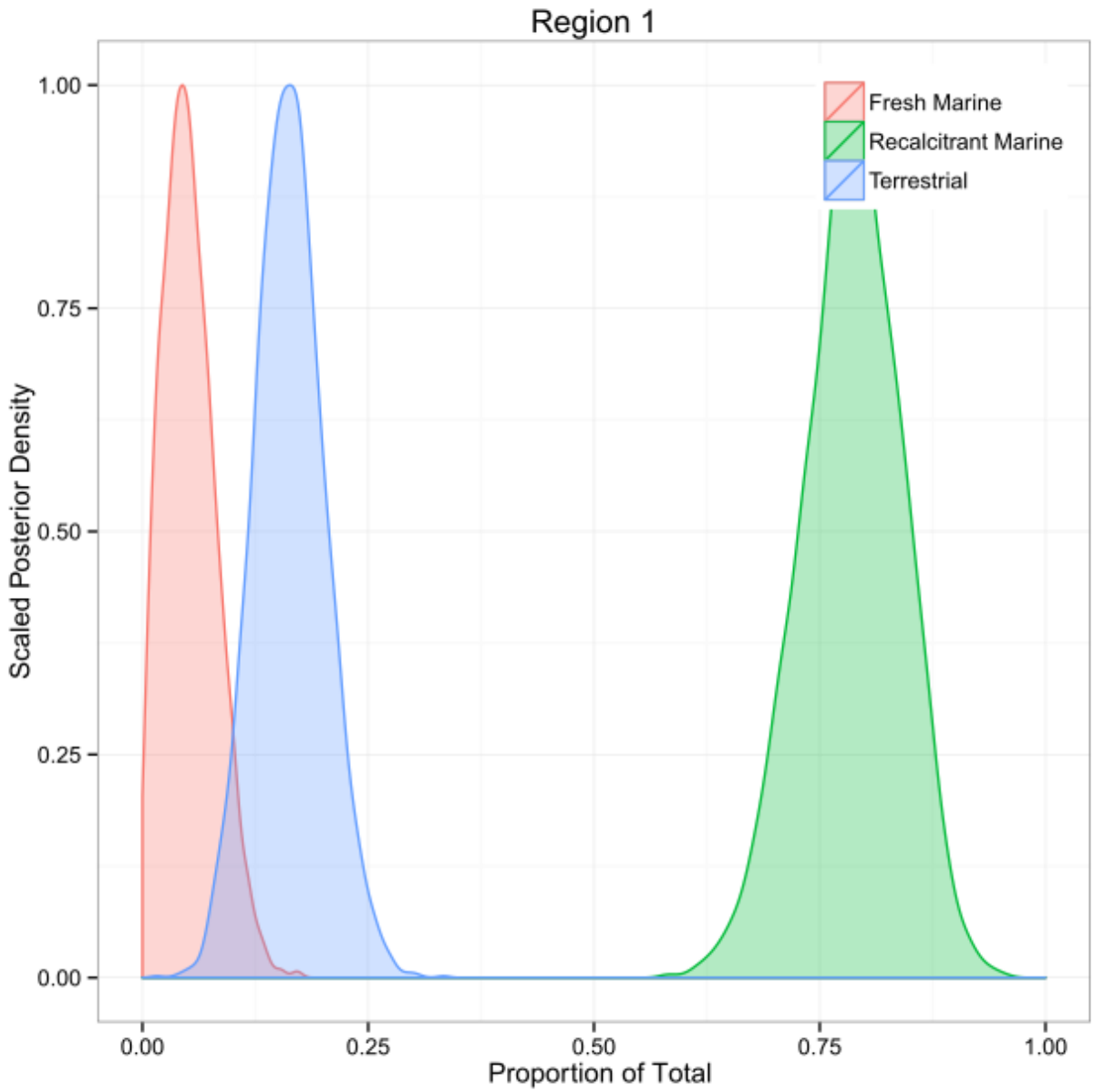

Figure 9: Posterior distributions for source contributions from the upper core of HLY0501-JPC5

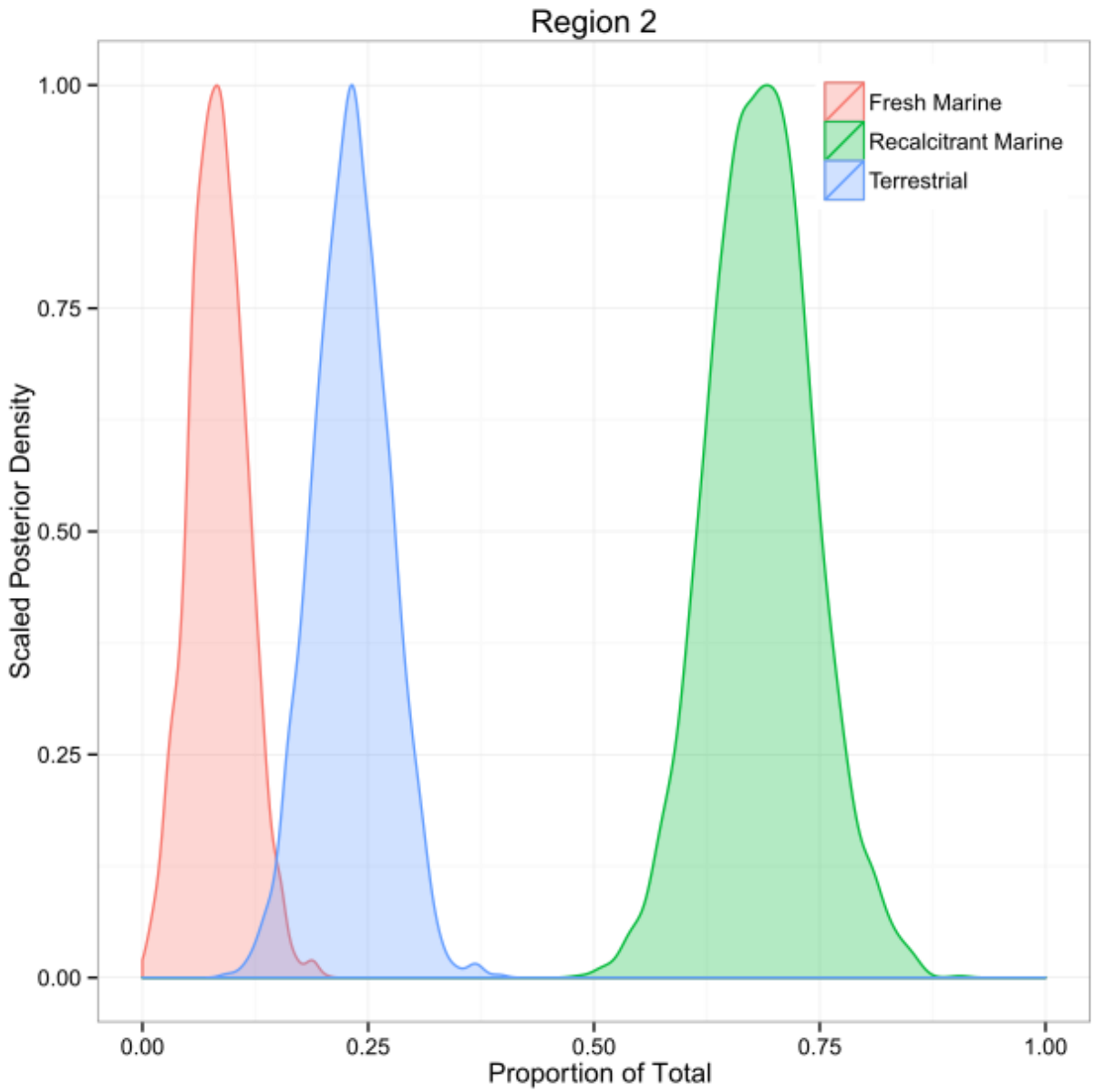

Figure 10: Posterior distributions for source contributions from the middle core of HLY0501-JPC5

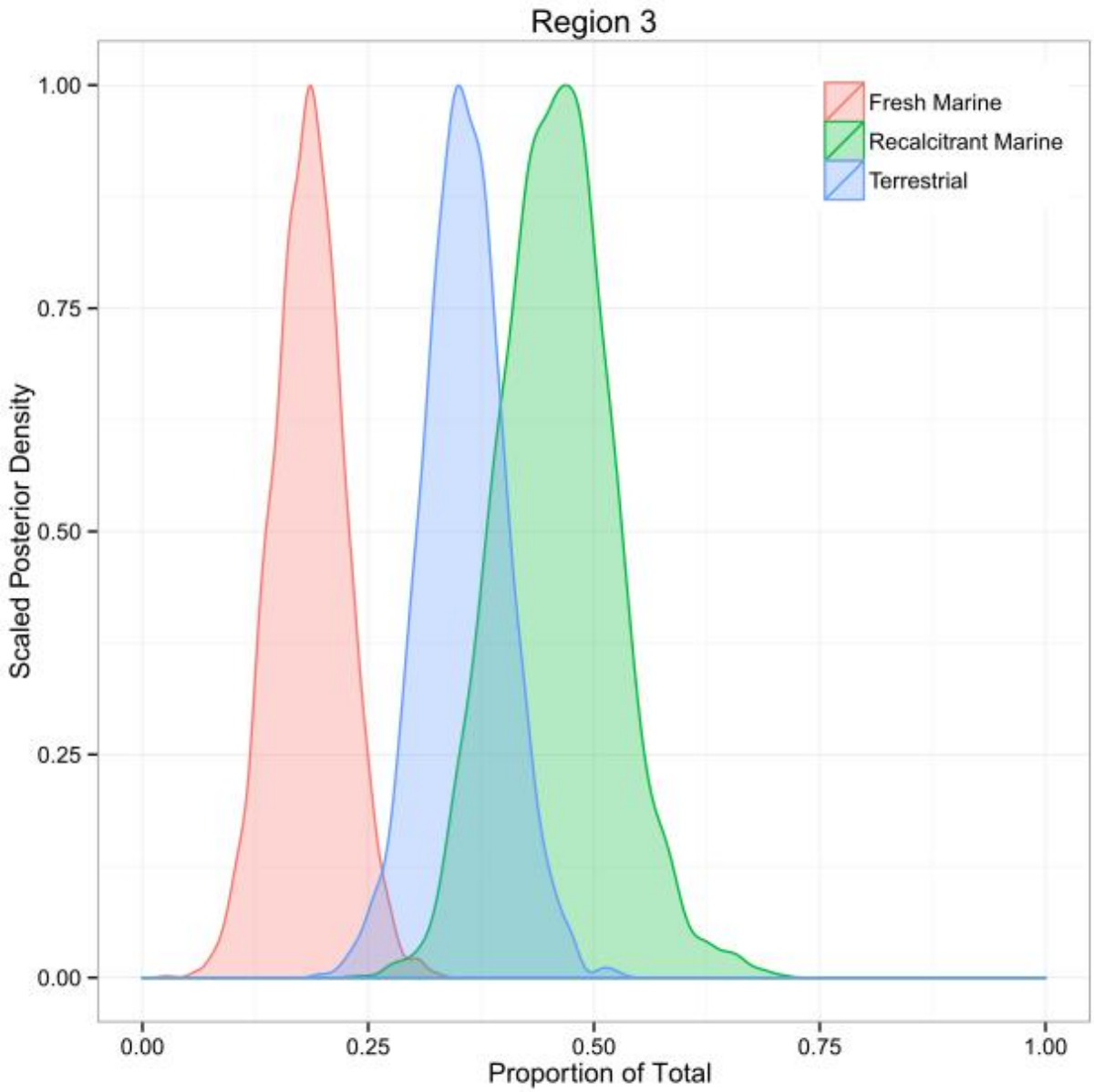

Figure 11: Posterior distributions for source contributions from the lower core of HLY0501-JPC5

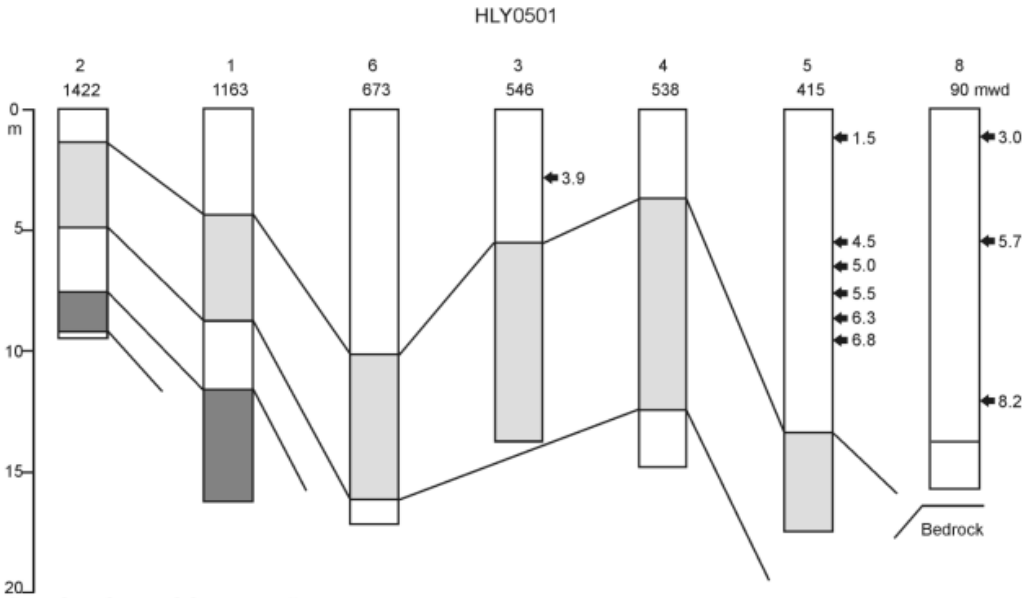

Samples obtained from core #5.

Water Depth - 415m

Holocene Sediments unshaded (age in thousands of years indicated by arrows)

Figure 12: Core correlation for HLY0501-JPC5 core

Core	Depth	%TOC	%TN	C:N	δ^{13}C	δ^{15}N
HLY0501JPC-1	0-2	1.26	0.16	9.44	-21.80	5.06
HLY0501TC	0-2	1.38	0.19	8.40	-20.40	9.73
	40-42	1.36	0.15	10.62	-20.84	6.05
	80-82	1.33	0.16	9.78	-20.97	7.42
	120-122	1.27	0.14	10.62	-21.13	7.95
HLY0501JPC	40-42	1.31	0.16	9.70	-21.24	9.01
	80-82	1.28	0.16	9.55	-21.92	5.90
	110-112	1.25	0.14	10.59	-22.21	8.38
	160-162	1.24	0.16	9.01	-20.56	7.93
	200-202	1.21	0.16	8.61	-20.56	8.51
	240-242	1.23	0.16	8.92	-21.05	9.18
	280-282	1.24	0.17	8.70	-22.42	7.82
	320-322	1.18	0.15	9.11	-21.60	7.37
	360-362	1.14	0.13	9.95	-21.82	9.35
	400-402	1.24	0.15	9.87	-21.76	6.70
	440-442	1.17	0.14	9.85	-21.14	7.21
	480-482	1.26	0.15	9.85	-21.64	7.56
	520-522	1.22	0.13	10.73	-21.75	7.25
	560-562	1.21	0.16	8.91	-21.60	7.99
	600-602	1.17	0.15	9.21	-21.53	8.05
	640-642	1.20	0.14	9.97	-21.48	6.81
	680-682	1.18	0.13	10.83	-22.93	9.58
	760-762	1.17	0.16	8.79	-22.21	6.72
	770-772	1.18	0.13	10.49	-22.75	8.44
	800-802	1.15	0.15	9.11	-21.27	6.13
	840-842	1.13	0.12	10.63	-22.95	8.18
	880-882	1.13	0.13	9.95	-23.06	8.96
	920-922	1.17	0.13	10.62	-22.79	7.76
	960-962	1.14	0.13	10.12	-22.61	9.61
	1000-1002	1.14	0.15	8.84	-22.24	9.62
	1040-1042	1.14	0.14	9.61	-23.46	6.18
	1080-1082	0.94	0.10	11.46	-23.56	7.89
	1120-1122	0.86	0.11	9.16	-23.82	5.60
	1160-1162	0.83	0.17	5.62	-22.78	7.00
	1200-1202	0.72	0.08	9.99	-24.93	5.42
	1240-1242	0.60	0.07	10.07	-24.92	9.35

Table 1: Bulk %TOC, %TN, %S, C:N, δ^{13}C, δ^{15}N compositions for the JPC0501-JPC5 core

Sample	Composite depth (cm)	Corrected depth (cm)	Sample type ^{13}C age (years)	Uncorrected (years BP) $\Delta R = 0$	Calendar age	CAMS no.
Section 1, 36-38 cm	36.0-38.0	112.0	Bivalve, Thyasira	1930 ± 45	1468	128414
Section 4, 76-78 cm	483.0-485.0	559.0	Bivalve, Yoldia	4465 ± 50	4572	128415
Section 5, 12-14 cm	568.5-570.5	644.5	Bivalve, Thyasira	4820 ± 70	5130	128416
Section 5, 132-134 cm	688.5-690.5	764.5	Bivalve, Yoldia	5220 ± 40	5593	128417
Section 6, 88-90 cm	799.0-801.0	875.0	Bivalve, Portlandia	5885 ± 40	6306	128418
Section 7, 18-20 cm	879.5-881.5	955.5	Bivalve, Portlandia and Thyasira	6395 ± 45	6867	128419

Table 2: Radiocarbon data for the HLY0501-JPC5 core. Data reproduced from McKay et al, 2008

Chapter 5: GC-IRMS of surface sediment alkanes

Introduction

Sea ice is a vital part of the Arctic system, but is currently in decline. Arctic sea ice extent has fallen by 30% since satellite records began in 1979 (Stroeve et al., 2012). Since 2002, a series of extreme September sea ice extent minima have occurred, with record minima being seen in 2002, 2005 and then 2007 (Stroeve et al., 2008). Some researchers (e.g. Stroeve et al., 2012) now fear that sea ice may reach a critical threshold at which a transition to a seasonally ice free Arctic occurs, perhaps as soon as mid-century (Massonnet et al., 2012). A better understanding of the present state of the Arctic system could lead to better predictions of how it will react to the rapid change it is presently experiencing.

Polar marine biogeochemistry is an important part of the Arctic system, and of the global carbon cycle. It is heavily influenced by ice, which plays a significant role in controlling light availability (Fortier et al., 2002), stratification and nutrient supply (Vancoppenolle et al., 2013). The importance of sea ice for the organic carbon cycle goes beyond the primary productivity of sea ice algae (1-2g$Cm^{-2}a^{-1}$ (Gradinger, 2009)); sea ice algae influences pelagic biogeochemistry and food webs once released from the ice, seeding the spring phytoplankton bloom, providing important early grazing material for zooplankton, and exporting organic matter to the benthos (Thomas and Dieckmann, 2003). The spring bloom starts under the ice, and then follows summer sea ice retreat (Perrette et al., 2011). Recent decreases in sea ice extent have been associated with increases in pelagic productivity (Arrigo et al., 2008, Tremblay et al., 2011) and marine ecosystem shifts are occurring in response to changes in sea ice extent (Grebmeier et al., 2006). These changes have already been observed, and other perturbations are likely; as sea ice volume and extent continues its rapid decline, the cumulative effect that these

alterations to the carbon cycle will have on Arctic marine biogeochemistry is not yet well understood.

In addition to autochthonous carbon from pelagic and sea ice algae, organic carbon is also supplied to the Arctic from terrestrial sources. High runoff (Shiklomanov, 1998) links the Arctic shelves to terrestrial sources of organic carbon. Major rivers supply as much as $6Mta^{-1}$ POC to the Arctic Ocean (Rachold et al., 2004). As rising temperatures accelerate the decay/breakdown of permafrost inland (Vonk et al., 2013) the river born terrestrial source is likely to increase in importance. Terrestrial carbon is also supplied by substantial coastal erosion of low lying peat bluffs (Grigoriev et al., 2004; Jorgenson and Brown, 2005), which may constitute the largest source of organic carbon in some parts of the Arctic (Vonk et al., 2012) and are vulnerable to warming. The extent of sea ice and the timing of its melting also affects these processes by protecting coastlines from erosion (Are et al., 2008) and by transporting terrestrially derived material far offshore (Eicken et al., 2005).

Our sample sites are located in the Eastern Chukchi Sea, one of the Arctic's marginal seas. Located to the North of the Bering Strait, the Chukchi separates Alaska from Kamchatka. The broad, shallow shelf of the Chukchi Sea supports high productivity during the summer (as high as $720\text{-}840gm^{-2}a^{-1}C$ (Springer and McRoy, 1993). This productivity is tightly coupled to the underlying sediments and supports a significant benthic ecosystem (Grebmeier and McRoy, 1989). Marine material is supplied by advection of material from adjacent the highly productive Bering Sea (Dunton et al., 2005). Terrestrial organic carbo is delivered to the Eastern Chukchi primarily via smaller rivers and the Yukon River, which exports $2.02Mta^{-1}$ TOC (Guo and Macdonald, 2006). Coastal erosion is also a factor; rates are not yet well constrained for the Chukchi coast of Alaska, but an input of $0.4Mta^{-1}$ TOC has been estimated (Grigoriev et al., 2004).

Bulk methods of organic matter characterization such as %C, %N, C:N and stable isotopes (e.g Morris et al., 2015) can be used to distinguish between different sources of OM to the ocean, if the potential sources are sufficiently different atomically or isotopically that they can be distinguished. But with the use of GC and GC-IRMS, compounds preserved in sediments can be characterized. These molecular fossils, or biomarkers, have the potential to provide detailed information about the sources, and transformation, of organic material to ocean sediments, particularly if the compounds can be closely identified with a specific source (e.g. Bianchi and Canuel, 2011), supplementing what can be gleaned from bulk analysis.

One such class of biomarkers is the normal alkanes (n-alkanes), which are straight chain hydrocarbons. Algal material typically contains short chain alkanes (C_{15}-C_{19}) (Blumer et al., 1971; Cranwell, 1982). Marine plants and macroalgae typically produce alkanes with an intermediate chain length (C_{21}-C_{25}) (Ficken et al., 2000). Terrestrial plants typically produce longer chain alkanes (C_{25}-C_{33}) with a distinctive distribution caused by predominance of odd to even homologues (Eglinton and Hamilton, 1967; Rielley et al., 1991). Higher plant material also frequently has a maximum contribution around C_{27}/C_{29}. Petrogenic deposits also supply alkanes which are frequently distinguished by a homologous series of alkanes with little to no odd to even predominance (OEP) and an elevated background level caused by unresolved complex mixture (UCM). These differences enable n-alkanes to be used to distinguish between sources of organic carbon; samples with abundant short chain n-alkanes probably contain much marine material, samples with abundant longer chain alkanes most likely contain terrestrial material if a strong OEP is observed, or petrogenic material if abundances of odd and even chained homologues are approximately equal and UCM is present. A number of studies have used alkane biomarkers, sometimes in conjunction with other compound classes, to investigate the sources of organic material to the Chukchi and Beaufort Seas

(e.g. Belicka et al., 2004, 2002; Goñi, 2000; Shaw et al., 1979; Yunker, 2002; Yunker et al., 2005, 1993, 1991).

Combining abundance patterns and chain lengths of n-alkanes with compound specific isotope analysis via gas chromatography – isotope ratio mass spectrometry (GC-IRMS) provides an extra layer of information about the sources of the individual compounds (Eglinton and Eglinton, 2008; Sessions, 2006). The $\delta^{13}C$ of the individual compounds can be linked to the original source material if the source $\delta^{13}C$ is known, because lipids such as hydrocarbons are typically 5-8‰ more depleted than the source (Hoefs, 2009). Recent examples of the use of this technique in the Arctic include Goñi et al. (2005), Drenzek et al. (2007) and Tolosa et al. (2013), who looked at terrestrial and petrogenic sources of biomarkers on the Mackenzie Shelf. Budge et al. (2008) and Wang et al. (2014) used GC-IRMS to trace fatty acids associated with sea ice algae and diatoms through the

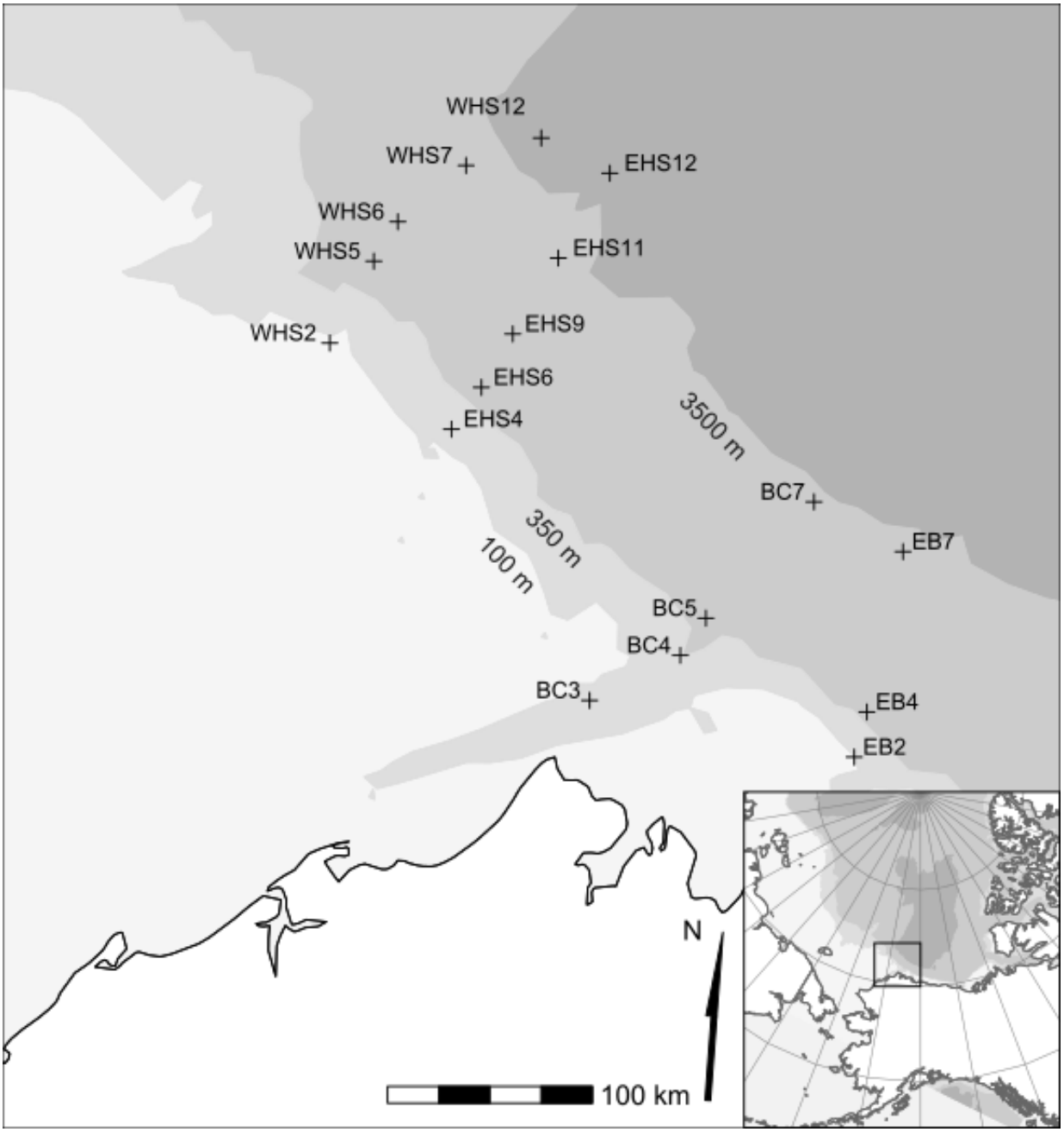

Figure 1: Location chart showing the position of the sample locations. Inset shows location within the wider Western Arctic region. EB: East Barrow; BC: Barrow Canyon; EHS: East Hanna Shoal; WHS: West Hanna Shoal

Bering food chain. Belt et al. (2008) used GC-IRMS to confirm that the isoprenoid hydrocarbon IP-25 had sea ice algae as its source. In this chapter, the $\delta^{13}C$ of individual alkanes from 7 surface core sites from the Chukchi Sea were analyzed. To our

knowledge, this is the first report of compound specific isotope analysis of n-alkanes from the Chukchi Sea.

Methods

Sediment sampling

The study area is composed of portions of the continental shelf, slope and basin of the NE Chukchi Sea and W Beaufort Sea. As part of the Shelf Basins Interactions Program (SBI) (Grebmeier and Rodger Harvey, 2005; Grebmeier et al., 2009), samples were selected from two shelf-to-basin transects. Samples from East of Barrow Canyon (EB2, EB4, EB7) were collected between July and August 2002. Those from East of Hanna Shoal (EHS6, EHS 11) were collected during May and June 2002, with the exception of EHS-12, which was collected in July and August 2004. The sediment cores were taken with a Pouliot box corer with an area of 0.06m^2. The outer edges of the cores were then discarded and the remaining portion was sectioned by 1cm intervals for the first 10cm, and every 2cm thereafter. The subsamples were then stored at -20^oC in pre-cleaned plastic or glass I-Chem jars with Teflon lined lids aboard ship until further processing on shore.

Sediment extraction

A 1:1 mixture of dichloromethane and methanol was used to extract sediment samples. This was performed in glass tubes with Teflon lined caps. The samples were sonicated for 2 minutes at the beginning of the extraction, before being stored overnight at 4^oC. Following the extraction, the organic phase was partitioned by the addition of nanopure water and then centrifuged at 1200rpm for 5 minutes. This was repeated 3 times, and all the organic phases were combined and dried by rotary evaporation.

The extracts were spiked with the internal standard, 5a-Cholestane and then saponified with 0.5M KOH in methanol at 30°C for five minutes. The polar and neutral phases were separated by the addition of water and subsequent extraction with a 9:1 mixture of hexane:diethyl ether. The neutral lipids were then derivatized with a 3:1 bis(trimethylsilyl)trifluoroacetemide:pyridine mixture at 50°C for 15 minutes.

High Performance Liquid Chromatography Separation

Following the derivatization, samples were separated by high performance liquid chromatography (HPLC). A Phenomenex Luna 5µm silica 250x4.60mm column was used with Phenomenex silica security guard column (4mm long with an internal diameter of 3.0mm). Samples were eluted with hexane, dichloromethane and methanol at a flow rate of 0.5ml/minute; after an initial isocratic hold of 100% hexane for 10 minutes, the dichloromethane concentration was increased to 20% over 5 minutes. This was followed by a 5 minute gradient to 100% dichloromethane. After this, the percentage of methanol was increased from 0-5% over five minutes and then held at 5% for 23 minutes. The column was then pumped for 10 minutes with 100% hexane in preparation for the next sample at a flow rate of 1ml/min (Tolosa and de Mora, 2004).

Gas Chromatography Isotope Ratio Mass Spectrometry

GC-IRMS was performed using an HP 5890 II GC with a 60m x 3.20mm (0.25um internal diameter) DB5 column (J+W Scientific) connected to a GV Instruments Isoprime mass spectrometer. Helium at a flow rate of 1ml/min was used as the carrier gas. Samples were injected splitless, with the entire sample directed into a narrow bore glass inlet sleeve at 275°C. The oven was at initial temperature of 60°C. After being held at 60°C for one minute, the temperature was increase to 120°C at a rate of 15°C/min. Upon reaching 120°C, a second ramp to 300°C at 40°C/min. The oven was then held at 300°C for 40 minutes, giving a total run time of 90 minutes. A heart-split valve was used to

vent the solvent to the flame ionization detector before being switched to direct gas flow through a CuO filled glass combustion furnace at 850°C. Flow from the furnace was supplemented by additional He to carry the GC effluent gases to the IRMS and to provide back pressure for the heart split valve. A cryogenic water trap held at -70°C removed water from the gas flow before introduction to the mass spectrometer. Three pulses of calibrated reference CO_2 were analyzed at the beginning and end of each sample run to enable calculation of isotope ratios relative to the standard and to control signal stability. Additionally, a deuterated naphthalene standard of known isotope composition was analyzed daily to monitor instrumental performance.

Isotope compositions are reported in δ notation as deviations from the standard, given in parts per thousand (per mill, ‰):

$$\delta^{13}C\ (‰) = (R_{sample}/R_{standard}) - 1) \times 1000$$

R is the abundance ratio of the heavy to light isotopes ($^{13}C/^{12}C$). Samples are measured against carbon dioxide which has been calibrated against the NBS22 standard. Carbon values were corrected for mass overlap with isotopes of oxygen. Measurement reproducibility is typically better than ±0.2‰.

Results

Overall, the mean value for the alkanes tested was -31.6‰ (Fig 2), with very slight tendency to depletion in the odd alkanes versus the even alkanes. In general, the samples had a strong OEP with low concentrations of shorter chain alkanes. Only small differences between odd and even alkanes were observed.

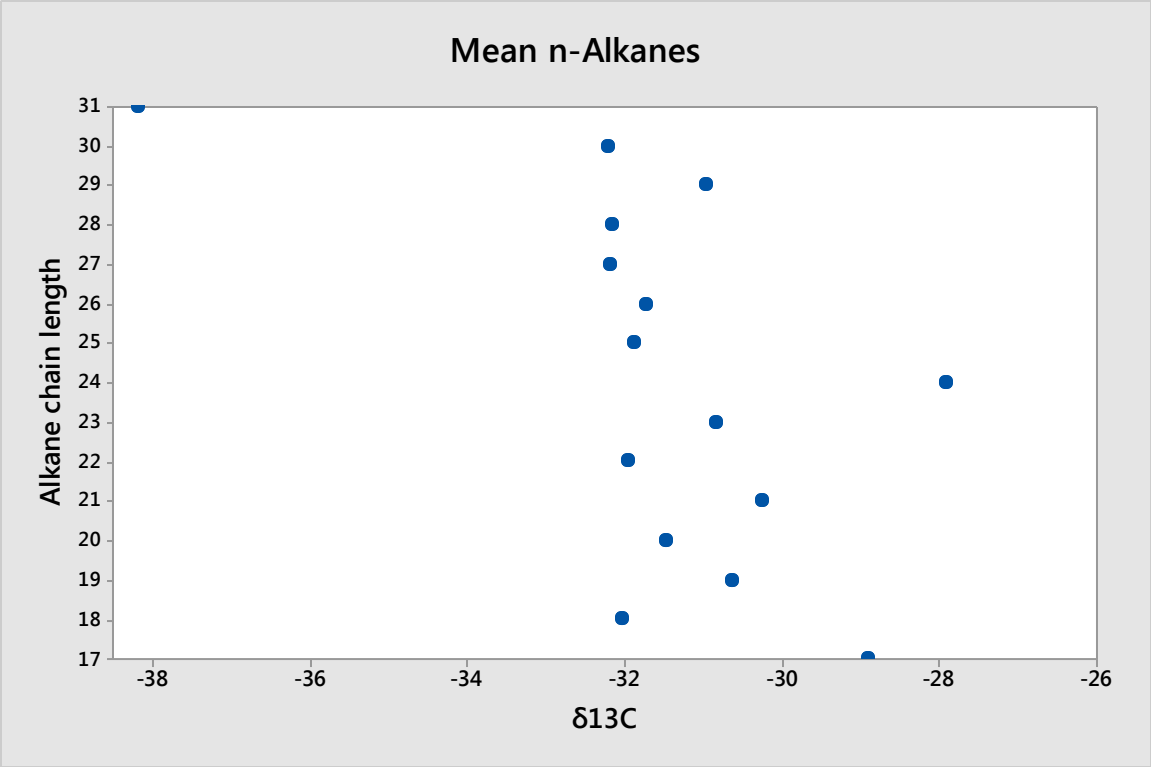

Figure 2 Mean n-Alkanes for all samples

The Chukchi shelf stations (STN1 and STN2) had mean $\delta^{13}C$ of -31.5‰ and -29.5‰, respectively. STN1 (Fig 3) included a more enriched value (-28.9‰) for the short chain alkane C_{17}, while the longer chain C_{22}-C_{28} alkanes ranged from -30.9‰ to -33.1‰. STN2 0-1 cm yielded $\delta^{13}C$ for C_{22}-C_{31} (except C_{28}) with a mean value of -29.9‰. The C_{22} and C_{24} alkanes were enriched compared to the average n-alkane $\delta^{13}C$ for the sample, at -26.4‰ and -15.4‰ respectively (Fig 4).

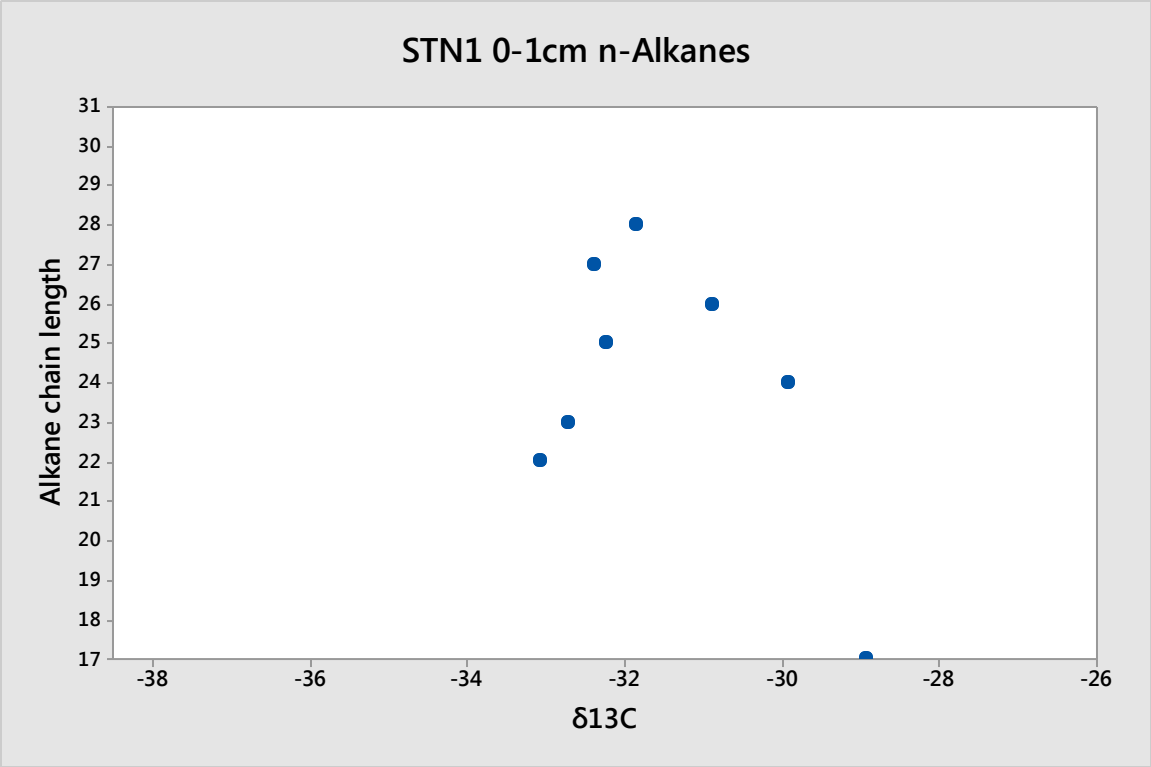

Figure 3 STN1 0-1 cm n-Alkanes

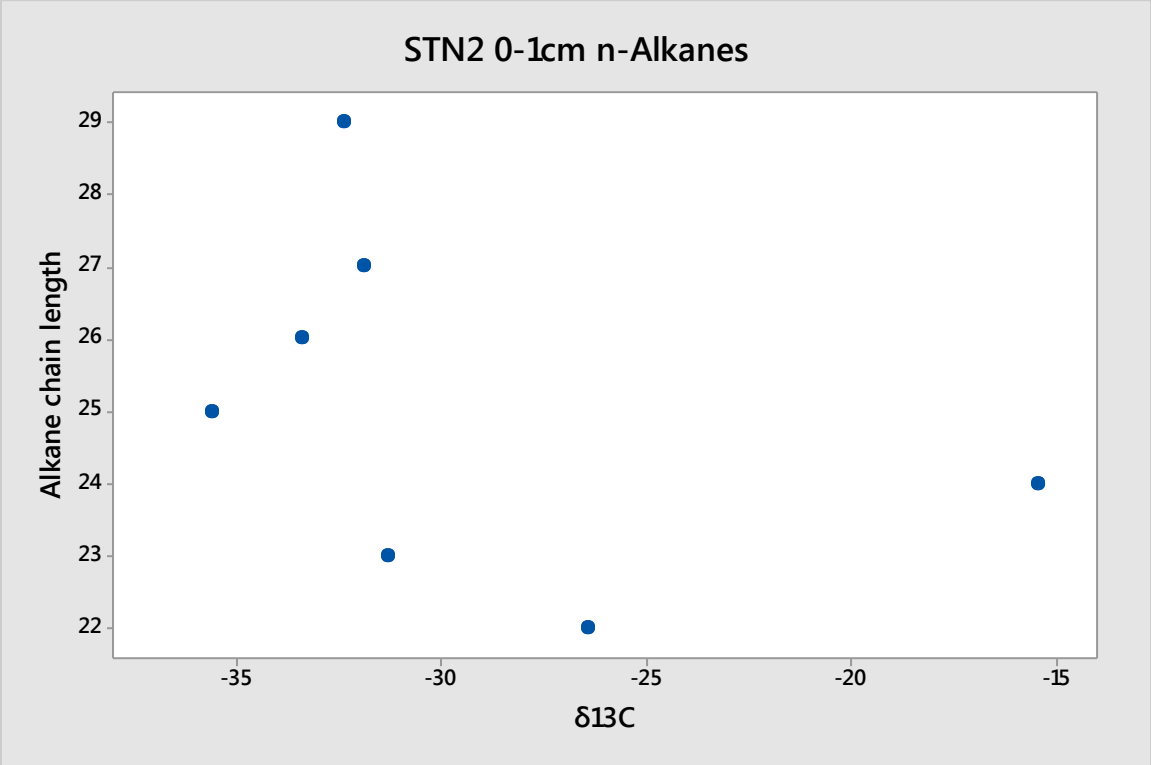

Figure 4 STN2 0-1 cm n-Alkanes

From the East Hanna Shoal transect, EHS11 (Fig 5) and EHS 12 (Fig 6) had mean $\delta^{13}C$ of -29.4‰ and -31.5‰ respectively. These basin sites had the most complete series of n-alkanes of any of the samples. In both samples, the short chain alkanes were slightly enriched compared to the long chain alkanes >C_{23} (by 2.0‰ and 0.3‰ respectively). For EHS11, the C_{26} and C_{28} alkanes were slightly depleted compared to the odd alkanes (except C_{29}). EHS11 and EHS12 both contained the algal alkanes C_{17} and C_{19}. The $\delta^{13}C$ for these alkanes were similar to the means for each site with the exception of C_{17} for EHS12, which was slightly enriched at -26.2‰.

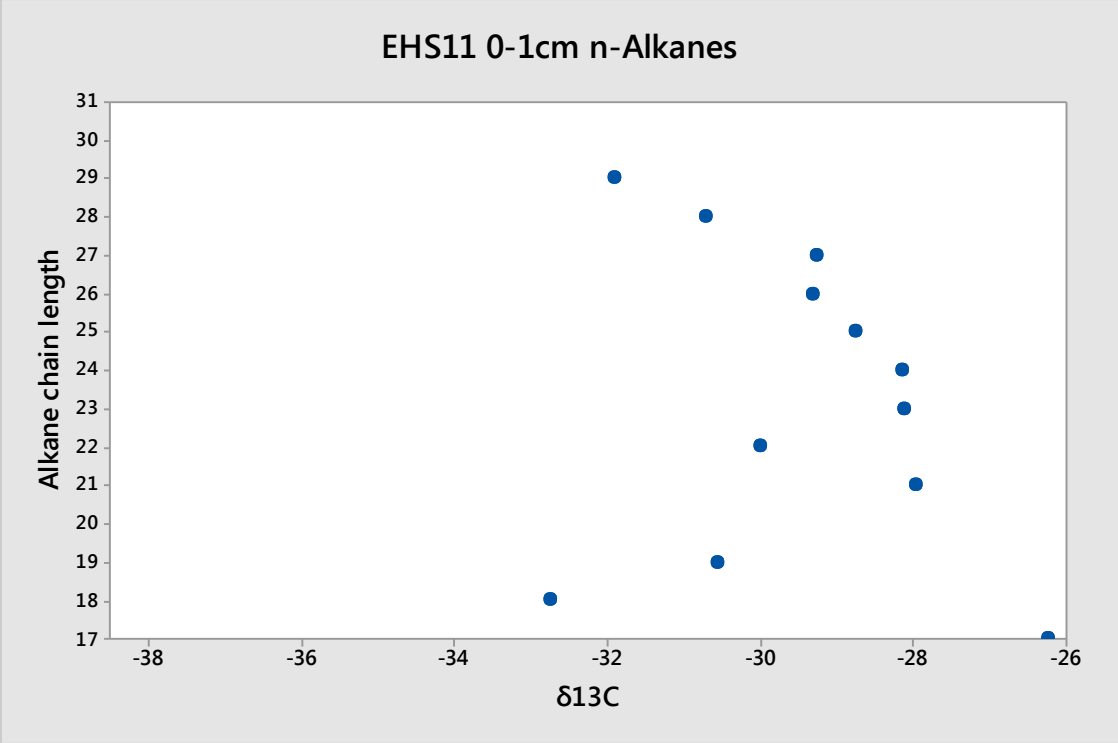

Figure 5 EHS11 0-1 cm n-Alkanes

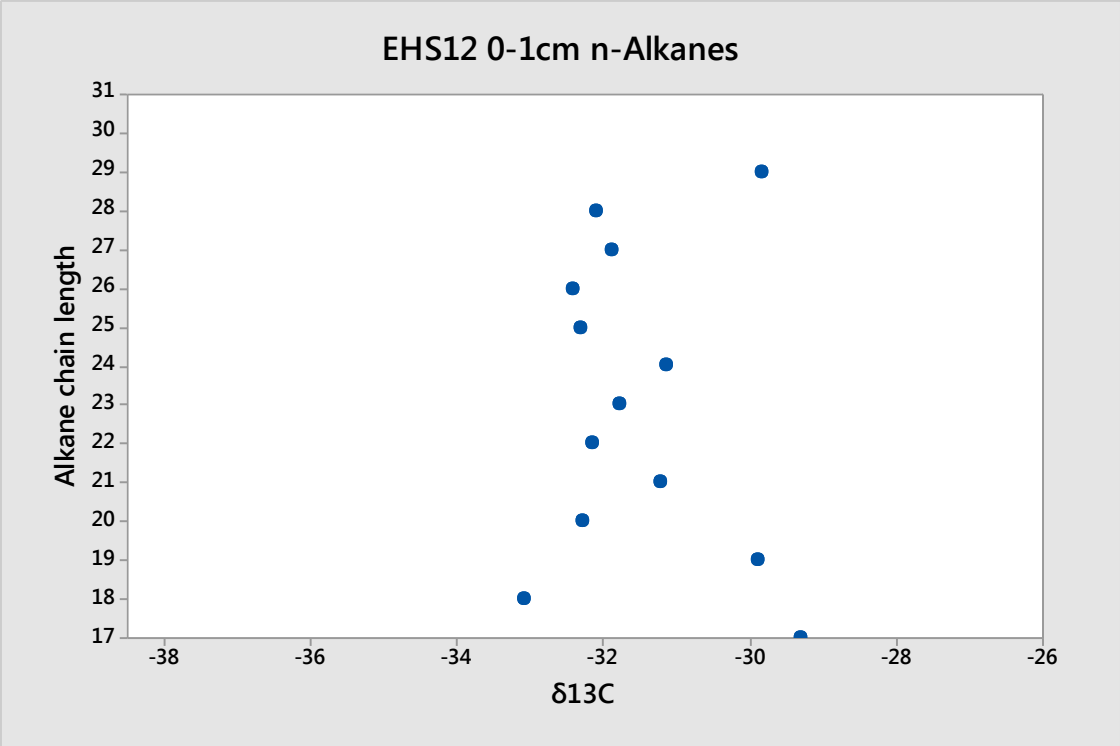

Figure 6 EHS12 0-1 cm n-Alkanes

Samples EB4 (Fig 7) and EB7 (Fig 8) were the most depleted samples overall. EB4 had a mean $\delta^{13}C$ of -32.9‰, while EB7 had a mean $\delta^{13}C$ of -32.0‰. EB4 also had the second highest concentration of n-alkanes. For EB4, the $\delta^{13}C$ of the odd n-alkanes were 1.2‰ more depleted than the even homologues. For EB7, the even n-alkanes were 1.0‰ more depleted than the odd n-alkanes. C_{23}, C_{24} and C_{25} were relatively enriched compared to the rest of the sample.

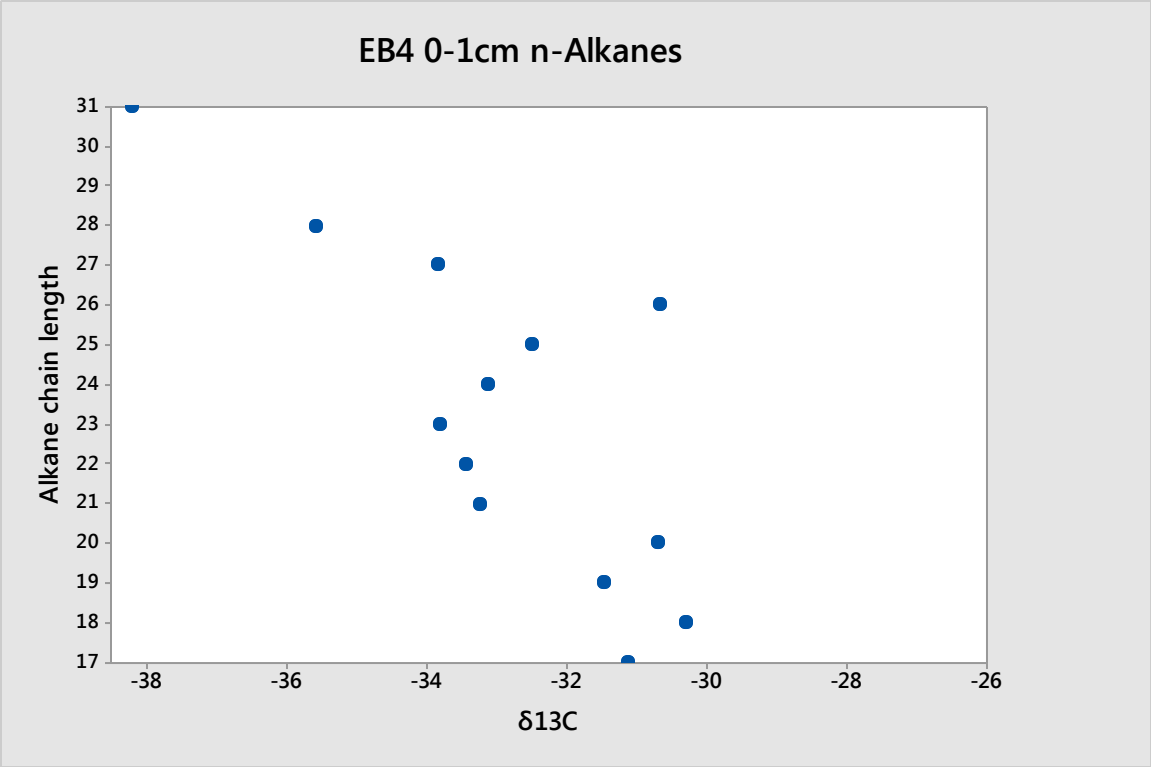

Figure 7 EB4 0-1 cm n-Alkanes

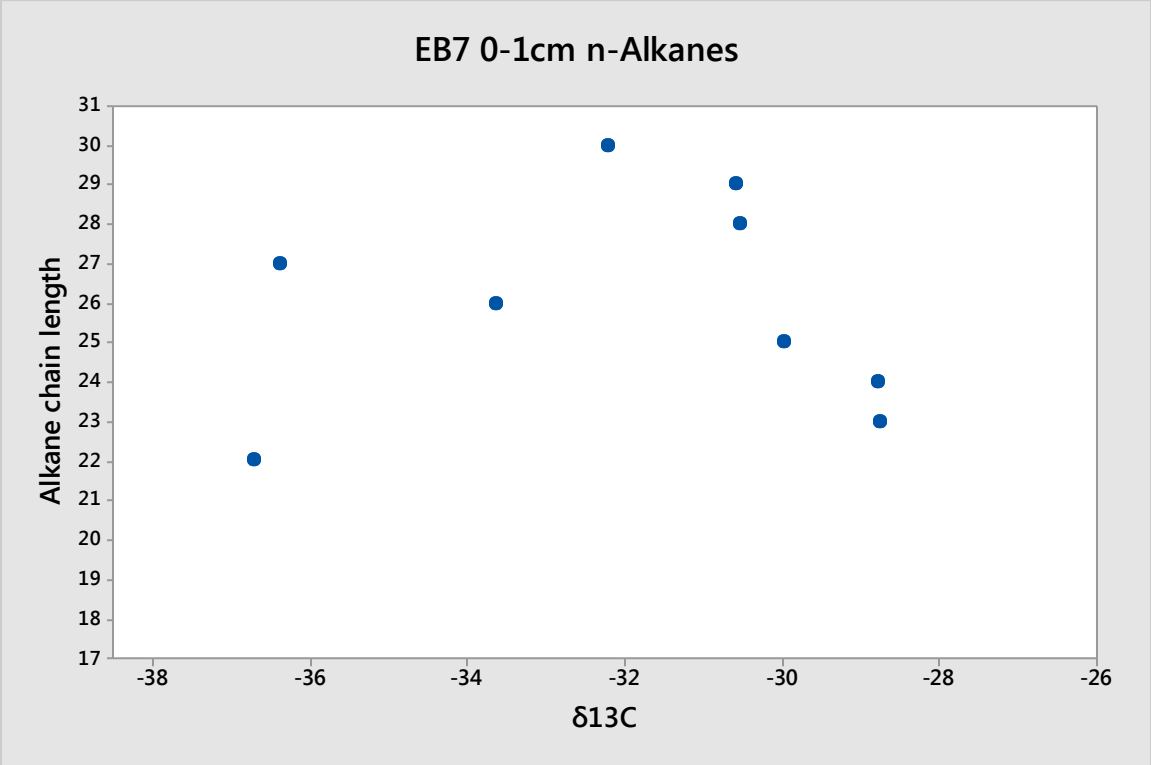

Figure 8 EB7 0-1 cm n-Alkanes

Discussion

The strong OEP and relatively high concentrations of long chain n-alkanes found in most sample sites are strongly indicative of a terrestrial higher plant contribution. Terrestrial plants synthesize waxes to protect their leaves, and the long chain alkanes are thought to be the degradation product. Terrestrial plants have a bulk carbon $\delta^{13}C$ around -27‰ (Hoefs, 2009), so it would be expected that their alkanes, being found in the depleted lipids fraction, would have a $\delta^{13}C$ around -32‰. This is consistent with our overall mean of -31.6‰, which provides an additional confirmation that these alkanes are indeed terrestrial in origin. A substantial $\delta^{13}C$ difference between the odd and even n-alkanes was not observed, which would suggest that they have a similar source (i.e. terrestrial plants) (Tolosa et al., 2013). An alternative source could be petrogenic, either from contamination or transport of terrestrial deposits rich in petrogenic material. The Mackenzie River contributes 2.1 x 10^9kg POC and 1.3x10^9kg dissolved OC from shale outcrops to the Mackenzie delta (Macdonald et al., 1998). The Colville River also drains some possible sources of petrogenic alkanes (Yunker et al., 1993). However, petrogenic alkanes typically display a very low OEP, and have a distinctive unresolved complex mixture in the chromatogram. Neither of these petrogenic indicators was observed.

Algal n-alkanes are typically in the range of C_{15}-C_{19} (Cranwell, 1982). These short chain alkanes were not found in great abundance, indicating that algae were not making a significant contribution to the alkanes. Isotopically, the n-alkane range of -26.2‰ to -33.1‰ indicates a source in the range of -21‰ to -28‰. While this value is somewhat more depleted than other estimates for phytoplankton isotope composition (e.g. Belicka and Harvey, 2009; Morris et al., 2015), it does fit within the very broad $\delta^{13}C$ range for arctic phytoplankton (from -16‰ to -30‰ (Stein and Macdonald, 2004)). The depleted

$\delta^{13}C$ values for the short chain n-alkanes suggest that sea ice algae are not a significant part of the C_{15}-C_{19} n-alkanes. Sea ice algae can vary between -8‰ to -26‰ (Tremblay et al., 2006), but a more typical value for sea ice algae is around -14‰ (Gradinger, 2009), which would result in a lipid isotope composition close to -19‰. In contrast, the observed range of -26.2‰ to -33.1‰ is too depleted to have a significant sea ice algal component. Furthermore, the sea ice biomarker IP-25 was not observed in any samples. While absence of a biomarker does not prove that a sea ice algal contribution was made, there is insufficient evidence to suggest that a very strong sea ice algal contribution is possible in this area.

Conclusions

For alkanes in the Chukchi, the major source appears to be terrestrial plants (Belicka et al., 2004). While the concentration of short chain n-alkanes linked to marine algae was quite low, their $\delta^{13}C$ pointed to a pelagic phytoplankton source. There is no evidence of significant sea ice algal contributions to the $\delta^{13}C$ of short chain algal n-alkanes, nor is there biomarker evidence for their presence. The lack of UCM, high OEP and $\delta^{13}C$ of long-chain alkanes indicates that petrogenic alkanes are also not a significant source of organic material to the Chukchi Sea.

Bibliography

Are, F., Reimnitz, E., Grigoriev, M., Hubberten, H., Rachold, V., 2008. The Influence of Cryogenic Processes on the Erosional Arctic Shoreface. J. Coast. Res. 24, 110–121. doi:10.2112/05-0573.1

Arrigo, K.R., van Dijken, G., Pabi, S., 2008. Impact of a shrinking Arctic ice cover on marine primary production. Geophys. Res. Lett. 35, L19603. doi:10.1029/2008GL035028

Belicka, L.L., Harvey, H.R., 2009. The sequestration of terrestrial organic carbon in Arctic Ocean sediments: A comparison of methods and implications for regional carbon budgets. Geochim. Cosmochim. Acta 73, 6231–6248.

doi:10.1016/j.gca.2009.07.020

Belicka, L.L., MacDonald, R.W., Harvey, H.R., 2002. Sources and transport of organic carbon to shelf, slope, and basin surface sediments of the Arctic Ocean. Deep. Res. 49, 1463–1483.

Belicka, L.L., MacDonald, R.W., Yunker, M.B., Harvey, H.R., 2004. The role of depositional regime on carbon transport and preservation in Arctic Ocean sediments. Mar. Chem. 86, 65–88.

Belt, S.T., Massé, G., Vare, L.L., Rowland, S.J., Poulin, M., Sicre, M., Sampei, M., Fortier, L., 2008. Distinctive ^{13}C isotopic signature distinguishes a novel sea ice biomarker in Arctic sediments and sediment traps. Mar. Chem. 112, 158–167. doi:10.1016/j.marchem.2008.09.002

Bianchi, T.S., Canuel, E.A., 2011. Chemical Biomarkers in Aquatic Ecosystems, 1st ed. Princeton University Press, Princeton, NJ.

Blumer, M., Guillard, R.R.L., Chase, T., 1971. Hydrocarbons of marine phytoplankton. Mar. Biol. 8, 183–189. doi:10.1007/BF00355214

Budge, S.M., Wooller, M.J., Springer, A.M., Iverson, S.J., McRoy, C.P., Divoky, G.J., 2008. Tracing carbon flow in an arctic marine food web using fatty acid-stable isotope analysis. Oecologia 157, 117–29. doi:10.1007/s00442-008-1053-7

Cranwell, P., 1982. Lipids of aquatic sediments and sedimenting particulates. Prog. Lipid Res. 21, 271–308. doi:10.1016/0163-7827(82)90012-1

Drenzek, N.J., Montluçon, D.B., Yunker, M.B., Macdonald, R.W., Eglinton, T.I., 2007. Constraints on the origin of sedimentary organic carbon in the Beaufort Sea from coupled molecular 13C and 14C measurements. Mar. Chem. 103, 146 – 162. doi:10.1016/j.marchem.2006.06.017

Dunton, K.H., Goodall, J.L., Schonberg, S. V., Grebmeier, J.M., Maidment, D.R., 2005. Multi-decadal synthesis of benthic–pelagic coupling in the western arctic: Role of cross-shelf advective processes. Deep Sea Res. Part II Top. Stud. Oceanogr. 52, 3462–3477. doi:10.1016/j.dsr2.2005.09.007

Eglinton, G., Hamilton, R.J., 1967. Leaf Epicuticular Waxes. Science (80-.). 156, 1322–1335. doi:10.1126/science.156.3780.1322

Eglinton, T.I., Eglinton, G., 2008. Molecular proxies for paleoclimatology. Earth Planet. Sci. Lett. 275, 1–16. doi:10.1016/j.epsl.2008.07.012

Eicken, H., Gradinger, R., Gaylord, A., Mahoney, A., Rigor, I., Melling, H., 2005. Sediment transport by sea ice in the Chukchi and Beaufort Seas: Increasing

importance due to changing ice conditions? Deep. Res. 52, 3281–3302. doi:10.1016/j.dsr2.2005.10.006

Ficken, K.., Li, B., Swain, D.., Eglinton, G., 2000. An n-alkane proxy for the sedimentary input of submerged/floating freshwater aquatic macrophytes. Org. Geochem. 31, 745–749. doi:10.1016/S0146-6380(00)00081-4

Fortier, M., Fortier, L., Michel, C., Legendre, L., 2002. Climatic and biological forcing of the vertical flux of biogenic particles under seasonal Arctic sea ice. Mar. Ecol. Prog. Ser. 225, 1–16.

Goñi, M., 2000. Distribution and sources of organic biomarkers in arctic sediments from the Mackenzie River and Beaufort Shelf. Mar. Chem. 71, 23–51. doi:10.1016/S0304-4203(00)00037-2

Goñi, M.A., Yunker, M.B., MacDonald, R.W., Eglinton, T.I., 2005. The supply and preservation of ancient and modern components of organic carbon in the Canadian Beaufort Shelf of the Arctic Ocean. Mar. Chem. 93, 53 – 73. doi:10.1016/j.marchem.2004.08.001

Gradinger, R., 2008. Deep-Sea Research II Sea-ice algae : Major contributors to primary production and algal biomass in the Chukchi and Beaufort Seas during May / June 2002. Deep. Res. doi:10.1016/j.dsr2.2008.10.016

Gradinger, R., 2009. Sea-ice algae: Major contributors to primary production and algal biomass in the Chukchi and Beaufort Seas during May/June 2002. Deep Sea Res. Part II Top. Stud. Oceanogr. 56, 1201–1212. doi:10.1016/j.dsr2.2008.10.016

Grebmeier, J.M., Harvey, H.R., Stockwell, D.A., 2009. The Western Arctic Shelf–Basin Interactions (SBI) project, volume II: An overview. Deep Sea Res. Part II Top. Stud. Oceanogr. 56, 1137–1143. doi:10.1016/j.dsr2.2009.03.001

Grebmeier, J.M., McRoy, C.P., 1989. Pelagic-benthic coupling on the shelf of the northern Bering and Chukchi Seas. III. Benthic food supply and carbon cycling. Mar. Ecol. Prog. Ser. 53, 79–91.

Grebmeier, J.M., Overland, J.E., Moore, S.E., Farley, E. V, Carmack, E.C., Cooper, L.W., Frey, K.E., Helle, J.H., McLaughlin, F.A., McNutt, S.L., 2006. A major ecosystem shift in the northern Bering Sea. Science 311, 1461–4. doi:10.1126/science.1121365

Grebmeier, J.M., Rodger Harvey, H., 2005. The Western Arctic Shelf–Basin Interactions (SBI) project: An overview. Deep Sea Res. Part II Top. Stud. Oceanogr. 52, 3109–3115. doi:10.1016/j.dsr2.2005.10.004

Grigoriev, M.N., Rachold, V., Hubberten, H.W., Schirrmeister, L., 2004. Organic carbon input to the Arctic Seas through coastal erosion, in: Stein, R., Macdonald, R. (Eds.),

The Organic Carbon Cycle in the Arctic Ocean. Springer, Heidelberg, pp. 41–45.

Guo, L., MacDonald, R.W., 2006. Source and transport of terrigenous organic matter in the upper Yukon River: Evidence from isotope (δ 13 C, Δ 14 C, and δ 15 N) composition of dissolved, colloidal, and particulate phases. Global Biogeochem. Cycles 20, n/a–n/a. doi:10.1029/2005GB002593

Hoefs, J., 2009. Stable Isotope Geochemistry, Sixth. ed. Springer, Heidelberg.

Jorgenson, M., Brown, J., 2005. Classification of the Alaskan Beaufort Sea Coast and estimation of carbon and sediment inputs from coastal erosion. Geo-Marine Lett. 25, 69–80. doi:10.1007/s00367-004-0188-8

MacDonald, R.W., Solomon, S.M., Cranston, R.E., Welch, H.E., Yunker, M.B., Gobeil, C., 1998. A sediment and organic carbon budget for the Canadian Beaufort Shelf. Mar. Geol. 144, 255–273.

Massonnet, F., Fichefet, T., Goosse, H., Bitz, C.M., Philippon-Berthier, G., Holland, M.M., Barriat, P.-Y., 2012. Constraining projections of summer Arctic sea ice. Cryosph. 6, 1383–1394. doi:10.5194/tc-6-1383-2012

Morris, D.J., O'Connell, M.T., Macko, S.A., 2015. Assessing the importance of terrestrial organic carbon in the Chukchi and Beaufort seas. Estuar. Coast. Shelf Sci. 164, 28–38. doi:10.1016/j.ecss.2015.06.011

Perrette, M., Yool, A., Quartly, G.D., Popova, E.E., 2011. Near-ubiquity of ice-edge blooms in the Arctic. Biogeosciences 8, 515–524. doi:10.5194/bg-8-515-2011

Rachold, V., Eicken, H., Gordeev, V., Grigoriev, M., Hubberten, H., Lisitzin, A., Shevchenko, V., Schirmeister, L., 2004. Modern Terrigenous Organic Carbon Input to the Arctic Ocean, in: Stein, R., MacDonald, R.W. (Eds.), The Organic Carbon Cycle in the Arctic Ocean. Springer, pp. 33–56.

Rielley, G., Collier, R.J., Jones, D.M., Eglinton, G., 1991. The biogeochemistry of Ellesmere Lake, U.K.—I: source correlation of leaf wax inputs to the sedimentary lipid record. Org. Geochem. 17, 901–912. doi:10.1016/0146-6380(91)90031-E

Sessions, A.L., 2006. Isotope-ratio detection for gas chromatography. J. Sep. Sci. 29, 1946–1961. doi:10.1002/jssc.200600002

Shaw, D.G., McIntosh, D.J., Smith, E.R., 1979. Arene and alkane hydrocarbons in nearshore Beaufort Sea sediments. Estuar. Coast. Mar. Sci. 9, 435–449. doi:10.1016/0302-3524(79)90016-1

Shiklomanov, I.A., 1998. Comprehensive Assessment of the Freshwater Resources of the World: Assessment of Water Reources and Water Availability in the World.

Geneva.

Springer, A., McRoy, C., 1993. The paradox of pelagic food webs in the northern Bering Sea—III. Patterns of primary production. Cont. Shelf Res. 13, 575–599. doi:10.1016/0278-4343(93)90095-F

Stein, R., MacDonald, R.W., 2004. The organic carbon cycle in the Arctic Ocean. Springer.

Stroeve, J., Serreze, M., Drobot, S., Gearheard, S., Holland, M., Maslanik, J., Meier, W., Scambos, T., 2008. Arctic Sea Ice Extent Plummets in 2007. Eos, Trans. Am. Geophys. Union 89, 13. doi:10.1029/2008EO020001

Stroeve, J.C., Serreze, M.C., Holland, M.M., Kay, J.E., Malanik, J., Barrett, A.P., 2012. The Arctic's rapidly shrinking sea ice cover: A research synthesis. Clim. Change 110, 1005–1027. doi:10.1007/s10584-011-0101-1

Thomas, D.N., Dieckmann, G.S. (Eds.), 2003. Sea Ice. Blackwell Science Ltd, Oxford, UK. doi:10.1002/9780470757161

Tolosa, I., de Mora, S., 2004. Isolation of neutral and acidic lipid biomarker classes for compound-specific-carbon isotope analysis by means of solvent extraction and normal-phase high-performance liquid chromatography. J. Chromatogr. A 1045, 71–84. doi:10.1016/j.chroma.2004.06.037

Tolosa, I., Fiorini, S., Gasser, B., Martín, J., Miquel, J.C., 2013. Carbon sources in suspended particles and surface sediments from the Beaufort Sea revealed by molecular lipid biomarkers and compound-specific isotope analysis. Biogeosciences 10, 2061–2087. doi:10.5194/bg-10-2061-2013

Tremblay, J.-É., Bélanger, S., Barber, D.G., Asplin, M., Martin, J., Darnis, G., Fortier, L., Gratton, Y., Link, H., Archambault, P., Sallon, A., Michel, C., Williams, W.J., Philippe, B., Gosselin, M., 2011. Climate forcing multiplies biological productivity in the coastal Arctic Ocean. Geophys. Res. Lett. 38, n/a–n/a. doi:10.1029/2011GL048825

Tremblay, J.-E., Michel, C., Hobson, K.A., Gosselin, M., Price, N.M., 2006. Bloom dynamics in early opening waters of the Arctic Ocean. Limnol. Oceanogr. 51, 900–912.

Vancoppenolle, M., Meiners, K.M., Michel, C., Bopp, L., Brabant, F., Carnat, G., Delille, B., Lannuzel, D., Madec, G., Moreau, S., Tison, J.L., van der Merwe, P., 2013. Role of sea ice in global biogeochemical cycles: Emerging views and challenges. Quat. Sci. Rev. 79, 207–230. doi:10.1016/j.quascirev.2013.04.011

Vonk, J.E., Mann, P.J., Davydov, S., Davydova, A., Spencer, R.G.M., Schade, J., Sobczak,

W. V., Zimov, N., Zimov, S., Bulygina, E., Eglinton, T.I., Holmes, R.M., 2013. High biolability of ancient permafrost carbon upon thaw. Geophys. Res. Lett. 40, 2689–2693. doi:10.1002/grl.50348

Vonk, J.E., Sánchez-García, L., van Dongen, B.E., Alling, V., Kosmach, D., Charkin, A., Semiletov, I.P., Dudarev, O. V, Shakhova, N., Roos, P., Eglinton, T.I., Andersson, A., Gustafsson, Ö., 2012. Activation of old carbon by erosion of coastal and subsea permafrost in Arctic Siberia. Nature 489, 137–140. doi:10.1038/nature11392

Wang, S.W., Budge, S.M., Gradinger, R.R., Iken, K., Wooller, M.J., 2014. Fatty acid and stable isotope characteristics of sea ice and pelagic particulate organic matter in the Bering Sea: tools for estimating sea ice algal contribution to Arctic food web production. Oecologia 174, 699–712. doi:10.1007/s00442-013-2832-3

Yunker, M., 2002. Sources and Significance of Alkane and PAH Hydrocarbons in Canadian Arctic Rivers. Estuar. Coast. Shelf Sci. 55, 1–31. doi:10.1006/ecss.2001.0880

Yunker, M.B., Belicka, L.L., Harvey, H.R., MacDonald, R.W., 2005. Tracing the inputs and fate of marine and terrigenous organic matter in Arctic Ocean sediments : A multivariate analysis of lipid biomarkers. Deep. Res. 52, 3478–3508. doi:10.1016/j.dsr2.2005.09.008

Yunker, M.B., Macdonald, R.W., Cretney, W.J., Fowler, B.R., McLaughlin, F.A., 1993. Alkane, terpene and polycyclic aromatic hydrocarbon geochemistry of the Mackenzie River and Mackenzie shelf: Riverine contributions to Beaufort Sea coastal sediment. Geochim. Cosmochim. Acta 57, 3041–3061. doi:10.1016/0016-7037(93)90292-5

Yunker, M.B., MacDonald, R.W., Fowler, B.R., Cretney, W.J., Dallimore, S.R., McLaughlin, F.A., 1991. Geochemistry and fluxes of hydrocarbons to the Beaufort Sea shelf: A multivariate comparison of fluvial inputs and coastal erosion of peat using principal components analysis. Geochim. Cosmochim. Acta 55, 255–273. doi:10.1016/0016-7037(91)90416-3

Compound	Sample									
	EB4 0-1	EB7 0-1	EHS6 0-1	EHS11 0-1	EHS12 0-1	STN1 0-1	STN2 0-1*	STN2 4-5*	Melosira*	Mean
C17 Alkane	-31.1			-26.2	-29.3	-28.9				-28.9
C18 Alkane	-30.3			-32.7	-33.1					-32.0
C19 Alkane	-31.4			-30.6	-29.9					-30.6
C20 Alkane	-30.7				-32.3					-31.5
C21 Alkane	-33.2			-28.0	-31.2				-28.6	-30.2
C22 Alkane	-33.4	-36.7		-30.0	-32.1	-33.1	-26.4	-34.2	-29.6	-32.0
C23 Alkane	-33.8	-28.7		-28.1	-31.8	-32.7	-31.3	-28.6	-31.6	-30.8
C24 Alkane	-33.1	-28.8	-34.0	-28.1	-31.1	-29.9	-15.4	-25.0	-31.7	-27.9
C25 Alkane	-32.5	-30.0		-28.8	-32.3	-32.2	-35.6			-31.9
C26 Alkane	-30.7	-33.6		-29.3	-32.4	-30.9	-33.4			-31.7
C27 Alkane	-33.8	-36.4		-29.3	-31.9	-32.4	-31.9	-29.6		-32.2
C28 Alkane	-35.6	-30.5		-30.7	-32.1	-31.9				-32.2
Cholestane	-26.9	-26.9	-26.9	-26.9	-26.9	-26.9	-26.9	-26.9	-26.9	-26.9
C29 Alkane		-30.6	-27.5	-31.1	-29.8		-32.4			-31.0
C30 Alkane		-32.2								-32.2
Taraxerene	-29.9	-36.3			-32.4					-32.9
C31	-38.2									-38.2

Table 1: GC-IRMS data for cores EB4, EB7, EHS6, EHS11, EHS12, STN1, STN2, Melosira, and Mean
tab:one

Conclusions

This dissertation has attempted to further our understanding of the carbon cycle in the Western Arctic Ocean through the use of stable isotopes and Bayesian Stable Isotope Mixing Models. In general, the majority of the material preserved in the sediments was most likely of marine origin. However, evidence of a distinct terrestrial input was also seen, as well as a significant contribution from sea ice algae.

In chapter 3, data from a series of core tops and short cores from the Eastern Chukchi and Western Beaufort Sea were compiled, and the source contributions were estimated using the Bayesian SIMM SIAR. The mean %TOC was 1.2±0.3%, mean C:N was 9.0±1.3 and $\delta^{13}C$ ranged from -22.1 to -16.7‰ (mean -19.4±1.3‰). Modelling results from SIAR estimated the proportion of OM contributed by marine OM was between 50% and 70%, while terrestrial OM contributed up to 15%, and sea ice algal OM responsible for the remaining 25-35%. This suggests that, at least for the recent past, terrestrial material was not nearly as significant a source of OM as open water productivity. If ice free conditions increase marine productivity, it is likely that a larger amount of OM will be sequestered in the sediments of the Western Arctic Ocean, although this is likely to amount to quite a small negative feedback when compared to the decrease in albedo caused by open water conditions.

In chapter 4, a Holocene jumbo piston core from the Chukchi Sea was analyzed. The Bayesian approach used in chapter 3 was further developed by applying Monte Carlo models to validate the Bayesian model, and the Bayesian SIMM MixSIAR to perform the data analysis. It was found that most of the material was sourced from pre-aged algal material that was likely supplied to the site by advection. Using the hierarchical model embedded in MixSIAR, the oldest parts of the core did indicate a higher terrestrial contribution consistent with the inundation of the Chukchi coastal plain and subsequent coastal retreat over the course of the Holocene.

GC-IRMS was used to glean an additional layer of information from the Chukchi core top samples. The distribution of the alkanes in these samples was in keeping with a terrestrial higher plant source, and this analysis was reinforced by isotopic values for n-alkanes that were mostly around the expected values for terrestrial organic matter (around -32‰), with a range in $\delta^{13}C$ values from -15.4‰ to -38.2‰.

Two of the major limits to this dissertation are the incomplete nature of the sampling and the uncertainty in the end members. Although the use of Bayesian SIMMs helps mitigate the problem, the wide range of the marine and sea ice algal end members is a concern. To address this issue, samples of sea ice and marine phytoplankton obtained at different times of year and from different locations (likely on an East to West transect) could be analyzed for elemental and isotopic make up. In this way, an appropriate end

member for local conditions (timing of the bloom, changes in regional isotopic values) could be determined and used in SIMM analysis.

In terms of geographic coverage, areas of the Western Chukchi Sea have not been sampled sufficiently to build a complete picture of the organic carbon cycle. A clear extension of this dissertation's work would be to fill in some of the geographic gaps in sample availability.